BNL-99142-2013-IR

Use of Covariances in a Consistent Data Assimilation for Improvement of Basic Nuclear Parameters in Nuclear Reactor Applications: From Meters to Femtometers

M. Herman1, S. Hoblit, G. P. A. Nobre, A. Palumbo, M. T. Pigni2
National Nuclear Data Center, Brookhaven National Laboratory, Upton, NY

G. Palmiotti3, H. Hiruta, M. Salvatores
Idaho National Laboratory, Idaho Falls, ID

January 3, 2013

National Nuclear Data Center
Brookhaven National Laboratory
P.O. Box 5000
Upton, NY 11973-5000
www.nndc.bnl.gov

1Principal Investigator, BNL
2Current address: Oak Ridge National Laboratory, Oak Ridge, TN
3Principal Investigator, INL

DISCLAIMER

This report was prepared as an account of work sponsored by an agency of the United States Government. Neither the United States Government nor any agency thereof, nor any of their employees, nor any of their contractors, subcontractors, or their employees, makes any warranty, express or implied, or assumes any legal liability or responsibility for the accuracy, completeness, or any third party's use or the results of such use of any information, apparatus, product, or process disclosed, or represents that its use would not infringe privately owned rights. Reference herein to any specific commercial product, process, or service by trade name, trademark, manufacturer, or otherwise, does not necessarily constitute or imply its endorsement, recommendation, or favoring by the United States Government or any agency thereof or its contractors or subcontractors. The views and opinions of authors expressed herein do not necessarily state or reflect those of the United States Government or any agency thereof..

Contents

Introduction

Recognition of the key role physics plays in innovative reactor design was already made clear by E. Wigner in his warning: "It has been a bit forgotten that in all really creative thinking in reactor design, a working knowledge of nuclear reaction theory is required." More recently, extensive sensitivity and uncertainty studies [1, 2] and the availability of new covariance data [3] have allowed preliminary quantification of the impact of current nuclear data uncertainties on the design parameters of the Generation-IV systems (both fast neutron and thermal neutron systems). Similar quantifications can be done for the parameters that characterize the associated innovative fuel cycle to insure sustainability, waste minimization and drastic reduction of the proliferation risks [4, 5].

In parallel, there has been a growing and very significant trend to develop a new generation of reactor simulation tools that rely more and more on first principles. It is safe to say that the next generation of innovative nuclear systems will be assessed with a completely new set of tools, more science based, in sharp contrast with what has been done in the past.

However, the studies mentioned above point out that the present uncertainties in nuclear data should be significantly reduced in order to fully benefit from advances in modeling and simulation. Only a parallel effort in advanced simulation and nuclear data improvement will be able to provide designers with more general and well validated calculational tools to meet new design target accuracies. One further consideration related to the development of new advanced simulation tools is that there should be a more explicit link with the more fundamental physics parameters underlying the models used to describe cross sections that would avoid the use of processed, application-oriented, data (like multigroup cross sections).

Finally, current methodologies for reducing uncertainties coming from nuclear data, which rely on the use of integral experiment information to perform statistical multigroup (i.e., energy spectrum weighted) cross section data assimilation should evolve to embrace new frontiers in advanced simulation. One of the drawbacks of the classical methodologies is related to the energy group structure and the type of neutron energy spectrum that are adopted in the assimilation (adjustment). In fact, after such an adjustment is performed, neutronic designers are then tied to this energy group structure and neutron energy spectrum when carrying out further calculations. In reality, this can be quite a

limiting factor in view of the complex spectral issues that are involved in most reactor physics.

This work combines novel, but proven, methodologies for overcoming these limitations. In fact, this is the first attempt to build up a link between the wealth of precise integral experiments and a basic theory of nuclear reactions. Essential ingredients of such a procedure, denominated here as assimilation, are covariances for model parameters and sensitivity matrices. The latter provide direct link between reaction theory and integral experiments. The result is a consistent data assimilation performed directly on the basic nuclear physics parameters that are being used in a variety of nuclear reaction mechanisms. The resulting improvement in their performance will consequently reduce related uncertainties when employed in reactor calculations. By using integral reactor physics experiments (meter scale), information is propagated back to the nuclear physics level (femtometers) covering a range of more than 13 orders of magnitude.

The assimilation procedure should result in more accurate and more reliable evaluated data files of universal validity rather than tailored to a particular application. In fact, after data assimilation is carried out, the basic nuclear data file can be processed by a dedicated code into any energy group structure that the reactor physicist deems to be useful. On the other hand, integral experiments used in the assimilation should provide additional, possibly quite strict, constraints on the parameters entering nuclear reaction modeling, as well as the reaction models themselves.

This report describes three years of combined research by Brookhaben National Lab (BNL) and Idaho National Lab (INL) on establishing viable assimilation methodology. The emphasis of this paper is on the EMPIRE code calculations to prepare the priors, sensitivity matrices and covariances for the model parameters. For completeness, we also include a short summary of the assimilation results produced by INL and reported earlier in annual reports [6], [7], [8].

Section 1

Methodology Outline

As discussed above, the classical "statistical adjustment" techniques [9, 10, 11] provide adjusted multigroup nuclear data for applications, together with new, improved covariance data and reduced uncertainties for the required design parameters, in order to meet target accuracies.

One should, however, set up a strategy to cope with the drawbacks of the methodology, which are related to the energy group structure and energy weighting functions adopted in the adjustment. The reported study overcomes these limitations and potential inconsistencies by developing advanced simulation and modeling tools. It represents a genuine and original attempt to use a first principle approach as it deals directly with the information coming from nuclear theory calculations used in the evaluation procedure.

In fact, the classical statistical adjustment method can be improved by 'adjusting' reaction model parameters rather than multigroup nuclear data. The objective is to associate uncertainties of certain model parameters (such as those determining neutron resonances, optical model potentials, level densities, strength functions, etc.) and the uncertainties of theoretical nuclear reaction models themselves (such as optical model, compound nucleus, pre-equilibrium and fission models) with eventual discrepancies between calculations and experimental values for a large number of existing integral experiments. These experiments should be clean (i.e., well documented with high QA standards) and high accuracy (i.e., with as low as possible experimental uncertainties and systematic errors), and carefully selected to provide complementary information on different features and phenomena, e.g., different average neutron spectrum energy, different adjoint flux shapes, different leakage components in the neutron balance, different isotopic mixtures and structural materials etc.

In the past, a few attempts were made [12, 13] to apply a consistent approach for improving basic nuclear data, in particular to inelastic discrete levels and evaporation temperatures data of ^{56}Fe for shielding applications, and to resolved resonance parameters of actinides (e.g., γ and total widths, peak positions etc.). Although these efforts demonstrated the validity of the approach, they clearly indicated that there were signif-

icant challenges to be overcome for its practical application. This was mainly related to the way of getting the sensitivity coefficients and to the need of reliable, science-based, covariance information.

In the present work we made an effort to overcome both difficulties, using the approach that involves the following steps:

- Selection of the appropriate reaction mechanisms along with the respective model parameters to reproduce adopted microscopic cross section measurements with the EMPIRE code calculations. Coupled channels, quantum-mechanical pre-equilibrium theories, and advanced statistical model accounting for width fluctuations and full gamma cascade were employed to ensure state of the art modeling of all relevant reaction mechanisms. This step is essentially a full evaluation of a given material with the additional constraint that no manual modifications of the calculated results be permitted. This task was performed at BNL and is covered in this report.

- Determination of covariances matrices for the set of nuclear reaction model parameters obtained in the previous step. This was achieved by combining initial estimates of parameter uncertainties from RIPL-3, with uncertainties/covariances for the adopted experimental data through the KALMAN code. This way, the resulting parameter covariances contain constraints imposed by nuclear reaction theory and differential experiments. Typically, about 100 or more parameters were considered in this exercise, including resonance parameters for a few dominating resonances, optical model parameters for neutrons, level density parameters for all nuclei involved in the reaction, parameters entering pre-equilibrium models, parameters determining gamma-strength functions, and fission specific parameters in case of actinides. This task was performed at BNL and is covered in this report.

- Sensitivity of cross sections to the perturbation of the above mentioned reaction model parameters has been calculated with the EMPIRE code. An appropriate energy-group structure was used to represent these sensitivity matrices. This task was performed at BNL and is covered in this report.

- Use the adjoint technique to evaluate sensitivity coefficients of integral reactor parameters to the cross section variations, as described in the previous step. To perform this task, the ERANOS code system [14] was employed. It uses the most advanced techniques to compute sensitivity coefficients based on generalized perturbation theory for almost all integral reactor parameters of interest (reactivity coefficients, critical mass, spectrum indexes, power distributions, delayed neutron fraction etc). This task was performed at INL and detailed in separate annual reports.

- Consistent data assimilation on basic nuclear parameters using integral experiment analysis with best methodology available to remove discrepancies between calcula-

tion and measured quantities. This task was performed by INL. Experiments included static quantities as well as results from irradiation programs (e.g. PROFIL, TRAPU) that provide valuable information about minor actinide isotopes. After selection, experiments were analyzed with Monte Carlo calculations and ENDF/B-VII.0 data files in order to evaluate the C/E's of the selected integral quantities. Once the C/E's were made available, they were used together with the sensitivity coefficients coming from the previous step in a data assimilation code that provided improved parameters for nuclear reaction theory. This task was performed at INL and documented in separate annual reports.

- Feedback and checking of the parameters obtained in the previous step. This task consisted in verifying the credibility of the calculated variation of the parameters, using expertise of nuclear data evaluators, general consistency of the parameters with physical constraints and systematics, as well as checking the performance of the modified parameters in EMPIRE calculations. This task was performed at BNL.

1.1 Evaluation of Nuclear Physics Parameter Covariances

As indicated in the outline of the methodology, the first step is to provide estimated range of variation of nuclear physics parameters, including their covariance data. To this end the code EMPIRE [15] coupled to the KALMAN code was used.

The KALMAN code is an implementation of the Kalman filter technique based on minimum variance estimation. It naturally combines covariances of model parameters, of experimental data and of cross sections. This universality is a major advantage of the method. KALMAN uses measurements along with their uncertainties to constrain covariances of the model parameters via the sensitivity matrix. Then, the final cross section covariances can be calculated from the updated covariances for model parameters. This procedure consistently accounts for the experimental uncertainties and the uncertainties of the nuclear physics parameters. We emphasize that under the term 'reaction model' we mean also the resonance region described by models such as the Multi-Level Breit-Wigner formalism.

EMPIRE is a nuclear reaction model code system for nuclear data evaluation developed by BNL with a host of external collaborators. It is a modular system, comprising various nuclear models and designed for neutron cross section calculations over a broad range of energies. The code was used extensively in recent neutron cross section evaluation work; more than 70 materials included in the new US library ENDF/B-VII.0 [16], released in 2006, and ENDF/B-VII.1 [3] released in 2011, were evaluated by using the EMPIRE code.

EMPIRE integrates exceptional power under a single roof that is blended into a unique tool, equipped with a powerful graphic user interface and easy to use. This power consists

of a full set of nuclear reaction model codes, several extensive support nuclear data libraries and a number of utility codes important for file management and reflecting considerable know-how of neutron cross section evaluations accumulated over years.

The code is supported by several important libraries and utilities. Probably the most important is the Reference Input Parameter Library, its latest version being RIPL-3 released in 2008. This library provides input to individual nuclear reaction model codes. The combined results of model calculations are validated by comparison to experimental data retrieved from the most recent version of the international library of experimental reaction data, EXFOR. Then, the code automatically produces an ENDF-6 formatted file and performs extensive file checking up to file processing.

EMPIRE can be used over the whole energy range of interest to advanced fuel cycle applications, from thermal energy up to 20 MeV. This makes the EMPIRE code system unique. The point is that nuclear reaction modeling in its usual definition is restricted to the fast neutron region, covering the keV range and higher energies. In contrast to few other available evaluation code systems EMPIRE is taking huge advantage of another unique BNL development - the Atlas of Neutron Resonances [17] that allows extension of EMPIRE down to the resolved resonance region and thermal energy range. This is taken care of by the recently developed EMPIRE resonance module that has full access to the electronic version of the Atlas of Neutron Resonances. The latest 3.1 release of EMPIRE features also updated treatment of the fission channel and more precise parameterization that allows to reproduce fission cross sections within a few percent. In 2012, features essential for the assimilation of actinides, such as capability of perturbing PFNS and mu-bar, have been implemented and used in the most recent assimilation attempts of the three major actinides.

With the above capabilities, EMPIRE can generate input files for nuclear applications. This can be done by propagating fundamental nuclear physics quantities (nuclear masses, neutron resonance parameters, level densities, optical model potentials, nuclear excited levels and decay schemes, nuclear deformations, fission barriers, etc.) into quantities used as input parameters for nuclear engineering calculations such as cross sections, energy spectra of emitted neutrons, mu-bars for neutron scattering and others. From the practical point of view, these should be close or identical with those included in the ENDF/B-VII.1 library.

The EMPIRE code has another unique capability, namely recently developed covariance modules both the fast neutron region as well as the resonance region. These modules make use of the fact that both RIPL-3 and Atlas 2006 provide estimates of uncertainties of fundamental nuclear physics quantities that describe interaction of neutrons with atomic nuclei. Although covariance modules are still being refined, they are already in a position to provide reasonable estimates for a variety of nuclear application parameters. This can be done by the following procedure:

- The initial uncertainties of the nuclear physics parameters can be obtained from the

Atlas of Neutron Resonances, which provides uncertainties of neutron-, radiative- and fission-widths in the resonance region. In the fast neutron region, one should utilize the RIPL-3 library, which contains uncertainty estimates for level densities, optical model potentials, and some other quantities. The remaining uncertainties should be based on previous experience and available systematics.

- Propagate uncertainties of the above fundamental nuclear physics parameters to the uncertainties of cross sections and angular distributions which are used as input for application oriented calculations. In doing so, the KALMAN code uses sensitivity matrices calculated with EMPIRE, initial uncertainties on the physics parameters, and covariances for the adopted microscopic measurements. The resulting covariances for the nuclear physics parameters encapsulate our knowledge of nuclear reaction theory and microscopic experiments. They still miss the link to integral experiments, which is incorporated in the subsequent stages of the assimilation process.

- The list of nuclear physics parameters considered in the covariance calculations includes as a minimum:

  - neutron- and radiative-widths as well as energies for the first (about 10) resonances including the bound ones (about 30 parameters; not used for the actinides since sensitivity of the considered integral experiments to the resolved resonance region was negligible),

  - optical model parameters for incident neutrons (5 parameters),
    * real volume depth,
    * imaginary volume and surface depth,
    * real and imaginary diffuseness,

  - dynamic deformations used in the Coupled Channel or Distorted Wave Born Approximation calculations (1-3 parameters),

  - level density parameters for the compound nucleus, target nucleus, (n,p), and (n,a) residues (4 parameters),

  - mean free path and single-particle level density parameters for neutrons and protons in the preequilibrium model (3 parameters),

  - field strength parameters in the Multistep Direct Model (2-3 parameters),

  - tuning parameter in the gamma-strength function (1 parameter),

  - tuning parameters taking into account intrinsic uncertainties in the nuclear reaction models (3-5 parameters).

This list, if necessary, might be extended by adding energy dependencies of the parameters and/or considering optical model parameters for the outgoing channels.

In general, however, one should keep the list of perturbed parameters as short as possible.

1.2 Evaluation of Sensitivity Coefficients for Integral Experiments

In order to evaluate the sensitivity coefficients of the nuclear parameters to the integral parameters measured in a reactor physics experiment, a folding procedure will be applied, where the sensitivity calculated by EMPIRE, with the methodology outlined in the previous step are folded with those calculated by ERANOS (i.e., multigroup cross section sensitivity coefficient to integral parameters).

Following this procedure, the sensitivities of integral experiments to nuclear parameters p_k are defined as:

$$\frac{\Delta R}{\Delta p_k} = \sum_j \frac{\Delta R}{\Delta \sigma_j} \frac{\Delta \sigma_j}{\Delta p_k} \tag{1.1}$$

Here, R is an integral reactor physics parameter (e.g., k_{eff}, reaction rates, reactivity coefficient, etc.), and σ_j the multi-group cross section (the j index accounts for isotope, cross section type and energy group). In general, to compute σ_j one can use EMPIRE with an appropriate set of parameters p_k to generate first an ENDF/B file for the specific isotope and, successively, use NJOY to obtain multi-group cross sections. As specified in the previous section, one can compute the variation of the cross sections $\Delta \sigma_j$ resulting from a variation of each parameter p_k variation.

Specifically, the procedure consisted in the generation of the $\Delta \sigma_j$ corresponding to fixed, well chosen, variations of each p_k taken separately and therefore generating the $\Delta \sigma_j / \Delta p_k$. Following each EMPIRE calculation, an ENDF/B file for the isotope under consideration was generated and a subsequent run of NJOY on this file generated multigroup, infinite dilution, cross sections in the same energy structure (e.g., the 33 group energy structure) that was used for the computation of the reactor physics integral parameters. The multigroup cross section variations associated with the individual model parameter that has been varied in the corresponding EMPIRE calculation were computed as a difference to the reference NJOY calculation obtained using EMPIRE results calculated with the central values of the parameters. These calculations covered the needs of a large number of adjustments, using several experimental configurations and several integral experiments (e.g., k_{eff}, spectral indexes, reactivity coefficients etc.) in each configuration. In parallel, the cross section sensitivity coefficients to integral parameter $R = \Delta R / \sigma_j$ were provided by reactor physics calculations, using the standard Generalized Perturbation Theory in the ERANOS code system. Folding the two contributions (from EMPIRE and ERANOS) we obtained the sensitivity coefficients of integral quantities to nuclear physics parameters (see Eq. 1.1).

1.3 Deterministic assimilation of integral experiments

Finally, for the consistent data adjustment (or data assimilation), the proposed techniques make use of:

- quantified, science-based uncertainties and associated variance-covariance data,

- well documented, high accuracy and representative integral experiments,

- sensitivity coefficients for a wide variety of different design parameters (core and fuel cycle).

If B_p is the "a priori" nuclear data covariance matrix, S_B the sensitivity matrix of the performance parameters $B_i(i = 1, I)$ to the J nuclear cross sections, the "a priori" covariance matrix of the performance parameters is given by:

$$B_B = S_B^T B_p S_B \tag{1.2}$$

It can be shown that, using a set of K integral experiments A, characterized by a sensitivity matrix S_A, besides a set of statistically adjusted cross-section data, a new ("a posteriori") covariance matrix can be obtained

$$
\begin{aligned}
\widetilde{B_B} &= S_B^T \widetilde{B_p} S_B \\
&= \{B_B - S_B^T B_p S_A (S_A^T B_p S_A + B_A)^{-1} S_A^T B_p S_B\} \\
&= B_B\{1 - (S_B^T B_p S_B)^{-1}(S_A^T B_p S_A + B_A)^{-1}(S_A^T B_p S_B)^2\}
\end{aligned}
\tag{1.3}
$$

where B_A is the integral experiment uncertainty matrix. The previous matrix can then be used to define a new ("a posteriori") covariance matrix for the performance parameters B. From this expression, it results that in order to reduce the performance parameter "a priori" uncertainties, the most effective integral experiments are those with "representative" sensitivity profiles ($S_A \sim S_B$) and small experimental uncertainties ($B_A \sim 0$). Moreover, one can use the same equation to understand the effectiveness of a data adjustment and its "extrapolability" to a set of different reference systems. For this purpose, one has to introduce in the previous equation the sensitivity matrix of the design parameters ($i = 1, \cdots, I; n = 1, \cdots, N$) of a set of N reference systems, to the J nuclear data as matrix S_B. The subsequent step goes back to the initial set of nuclear physics parameters, first to check if the modified parameters conform to the adopted physics of nuclear reactions, and then to produce the improved ENDF/B-VII data files.

1.4 Direct Monte-Carlo assimilation of integral experiments

An alternative method was developed at BNL. It uses ENDF files produced for each "plus" and "minus" variation of the p_k model parameters, as described above, directly in a Monte-Carlo MCNP simulation of a particular integral experiment. The results of the simulation are then used to directly determine the sensitivity of the result of an integral experiment (for example, k_{eff}) to the EMPIRE parameters p_k. This method begins the same as the above method, running EMPIRE jobs for each parameter varied up and down by the amount specified in the sensitivity input file. Then the EMPIRE output file for each varied parameter is converted to an ENDF file. But then instead of processing the ENDF files to produce average cross sections, each file is processed by NJOY to produce an ACE file, which is then used in a Monte-Carlo simulation of an integral experiment, replacing the standard ACE file with the modified version. This is done for each parameter varied, for both the parameter varied "up" and "down." Then the sensitivity to the result of the simulation is calculated for each parameter, and the results of the sensitivities are then used in a KALMAN fit, where there is usually only one experimental point - the result of the integral experiment (typically k_{eff}). Here, the sensitivity matrix is reduced to a simple vector of sensitivities to each EMPIRE parameter, and the integral experiment is then fit using the KALMAN code. In an attempt to modify the EMPIRE parameters in a way that preserves the agreement with the differential data, the output covariance matrix for the EMPIRE parameters from the differential KALMAN fit is used when fitting the integral data. The KALMAN code will then fit the integral experiment by varying the parameters in a way which minimizes the change in the differential measurements. The various input files for the KALMAN fitting code are prepared from the sensitivity input file and the results of the MCNP simulations for each varied parameter by the code kefkal.f90. It reads the sensitivity input file (*-inp.sen*) and then reads the MCNP output file for each EMPIRE parameter simulation, forming a sensitivity to each parameter. All the required input files are created, and upon successful completion the KALMAN code can be run and to produce a new fitted value for the result of the integral experiment, usually a value of 1.0 for k_{eff}. The resulting modified EMPIRE parameters should then be used in another cycle of EMPIRE to check for any non-linearities in the parameters.

Section 2

Data Assimilation

The mechanics of assimilation as described in Section 1 have been applied to a number of materials as described in the following sections of this chapter. A set of prior EMPIRE parameters, the resulting cross sections, the sensitivities of the cross sections to the parameters and the parameter covariances were prepared at the NNDC at BNL. The application of these priors to integral experiments was carried out at INL, which completes a single cycle of assimilation.

The first assimilations performed at BNL and INL were for the structural materials ^{23}Na and ^{56}Fe, as described in INL report INL/EXT-10-20094 [6]. While much was learned from the assimilation of these materials, the resulting evaluations were not considered an improvement over the the existing ENDF/B-VII.0 and were not used in ENDF/B-VII.1. A summary of the details for these assimilations is provided below. Another second set of assimilations were performed for ^{235}U and ^{239}Pu as described in INL report INL/EXT-11-23501 [7]. For both of these materials a first round of assimilation was completed, with limited success, and a second round of EMPIRE calculations has been completed using an improved version of EMPIRE. In addition, the testing of a 'direct' method of assimilation of the EMPIRE calculations to integral experiments using Monte-Carlo methods was tested at BNL for ^{239}Pu with encouraging results. See sections below on ^{235}U and ^{239}Pu for further details. A first round of assimilation was also performed for ^{242}Pu and ^{105}Pd, described in INL report INL/EXT-12-27127 [8]. The integral experiment PROFIL-1 was used for ^{105}Pd and was found to be sensitive to only a few EMPIRE parameters. In spite of this relatively simple adjustment, a good assimilation could only be found if the EMPIRE uncertainties were adjusted ad hoc, perhaps an indication of a discrepancy between the differential and integral data sets, especially capture. ^{242}Pu was assimilated using a number of irradiation experiments, with limited success, where some parameters required variations greater than 1σ to obtain reasonable values for C/E, again suggesting conflict between integral and differential data. Finally, ^{238}U, not originally considered for assimilation, was added due to its role as an important actinide. Here, the calculations were performed using a new version of EMPIRE with new potentials, with good results.

The cross sections, sensitivities and covariances of parameters were prepared but have not yet been assimilated with integral data. Below, each material assimilated is discussed and results shown.

2.1 Assimilation of ^{23}Na

^{23}Na was selected for the assimilation feasibility study in view of its importance as fast reactor coolant and availability of suitable integral measurements. The biggest challenge for evaluators is the need to address considerable fluctuations of ^{23}Na cross sections well into MeV range and to find adequate parametrization for their description. This applies primarily to the total, elastic and inelastic cross sections; other reactions being of less interest due either to high thresholds or low cross sections (e.g., capture). The ENDF/B-VII.0 evaluation served as the reference, to be either reproduced (fluctuating region) or improved whenever necessary (resonances and high-end of the fast energy region).

In the resonance region the multi-level Breit-Wigner model was used, with the recent parametrization [17] adopted as basis that was updated and extended to 985 keV using the resonance module of EMPIRE. The resonance region in ^{23}Na consists of a huge resonance at 2.8 keV and minor resonances up to 985 keV for which missing information, such a parameter uncertainty, has been supplied with estimates. We also took in consideration the impact of the scattering radius, $R' = 4.9 \pm 0.2$ fm, on the cross sections. The parameters and the related uncertainties of 38 resonances (including the bound state) were retrieved from the electronic version of the ATLAS of neutron resonances [17].

2.1.1 EMPIRE calculations

In the fast energy region the optical, statistical Hauser-Feshbach and preequilibrium exciton models were used. Parametrization for these models was based on RIPL-3 initial values that were suitably adjusted. Fluctuations were handled by introducing two energy-dependent tuning parameters for total and absorption cross sections. Overall, more than 100 parameters were needed to describe the entire evaluation. The quality of evaluation in the fluctuating region was checked against ENDF/B-VII.0 and agreement on the level of a few percent was achieved. Finally, sensitivities of group cross sections to the above mentioned parameters along with the estimates of parameter covariances were supplied to our collaborators at INL for further analysis.

In the optical model calculations we used the recent parametrization based on Koning and Delaroche's [18] extensive analysis of spherical (or nearly spherical) nuclei . The energy and mass dependencies of potential parameters that were employed by those authors are more flexible than those used previously. Although ^{23}Na is strongly deformed and a coupled-channel potential would likely be more suitable, the flexibility of this potential allows for a reasonable description of both total and elastic cross sections and the elastic angular distributions. We varied 19 optical-model parameters, two scaling parameters for the total and absorption cross sections, as well as parameters related to the Hauser-Feshbach and exciton models. The scaling parameters TOTRED and FUSRED were also used as energy-dependent parameters to reproduce the fluctuations of high-resolution measurements in the MeV region. In Fig. 2.1 the point-wise cross sections for ^{23}Na(n,tot)
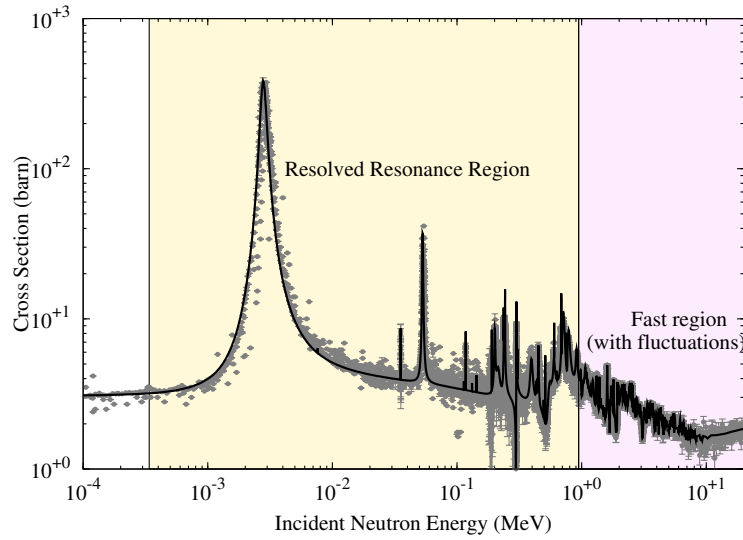
Figure 2.1: Calculated ^{23}Na(n,tot) point-wise cross sections in the resolved resonance region and fast neutron region along with experimental data.

are shown as an example. The resonance region is dominated by the resonance at 2.8 keV that is critical in the performance of the evaluation in integral testing. One notes that the fluctuating behavior extends into the MeV region where the cross sections were reproduced by applying an energy-dependent scaling to optical model calculations.

Figure 2.2: Calculated ^{23}Na(n,tot) point-wise cross sections (prior) in the fast neutron region along with experimental data (black line and grey points). KALMAN estimated uncertainties are shown in red.
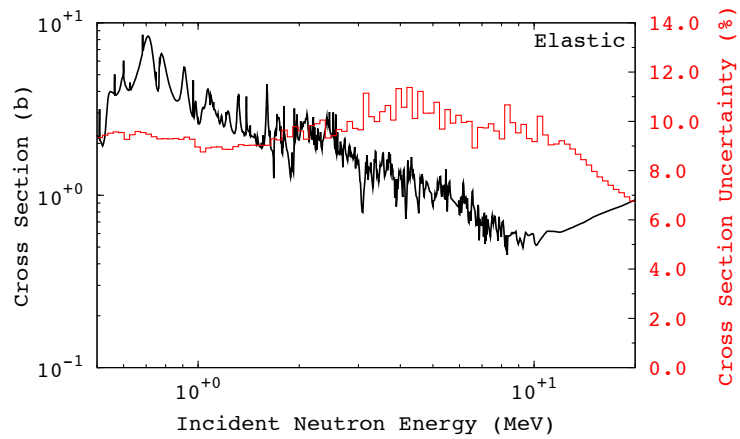
Figure 2.3: Calculated ^{23}Na(n,elastic) point-wise cross sections (prior) in the fast neutron region (black line). KALMAN estimated uncertainties are shown in red.
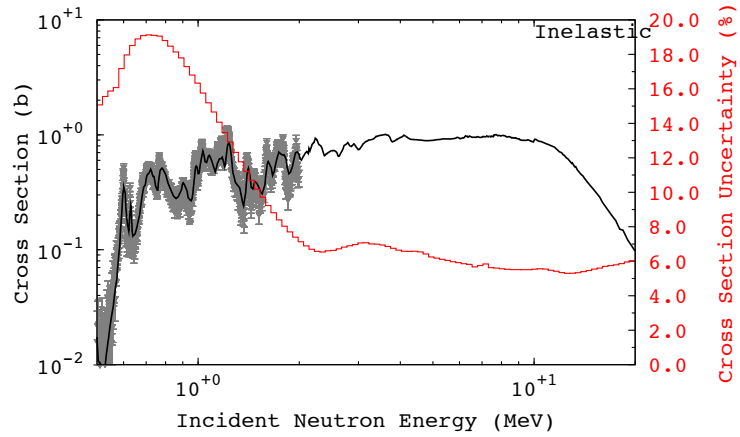
Figure 2.4: Calculated ^{23}Na(n,inel) point-wise cross sections (prior) in the fast neutron region along with experimental data (black line and grey points). KALMAN estimated uncertainties are shown in red.
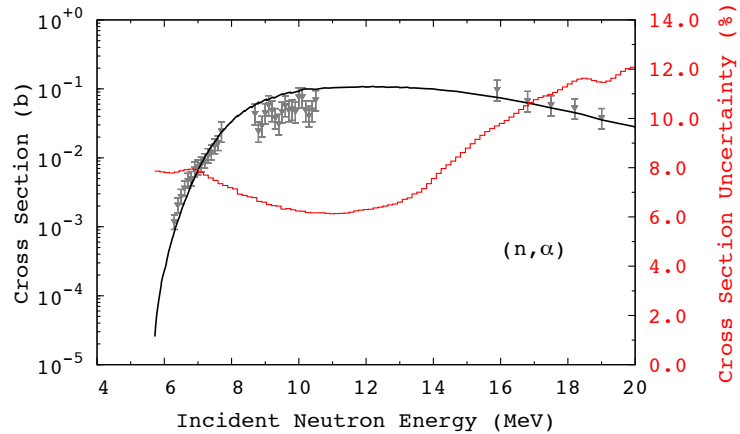
Figure 2.5: Calculated ^{23}Na(n,α) point-wise cross sections (prior) in the fast neutron region along with experimental data (black line and grey points). KALMAN estimated uncertainties are shown in red.

Figure 2.6: Calculated ^{23}Na(n,p) point-wise cross sections (prior) in the fast neutron region along with experimental data (black line and grey points). KALMAN estimated uncertainties are shown in red.
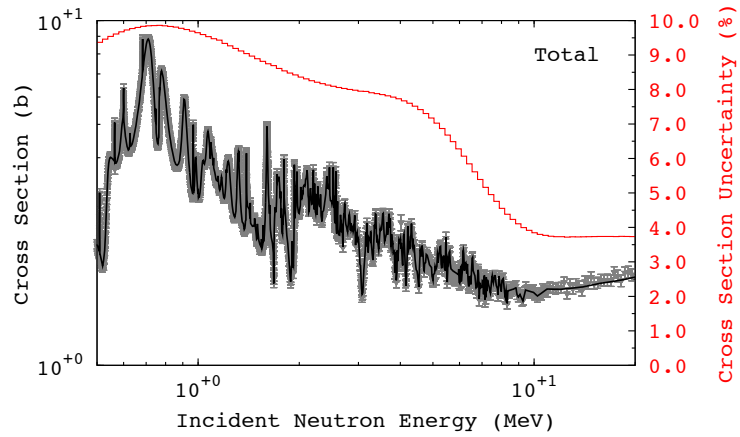

Figure 2.7: Calculated ^{23}Na(n,2n) point-wise cross sections (prior) in the fast neutron region along with experimental data (black line and grey points). KALMAN estimated uncertainties are shown in red.
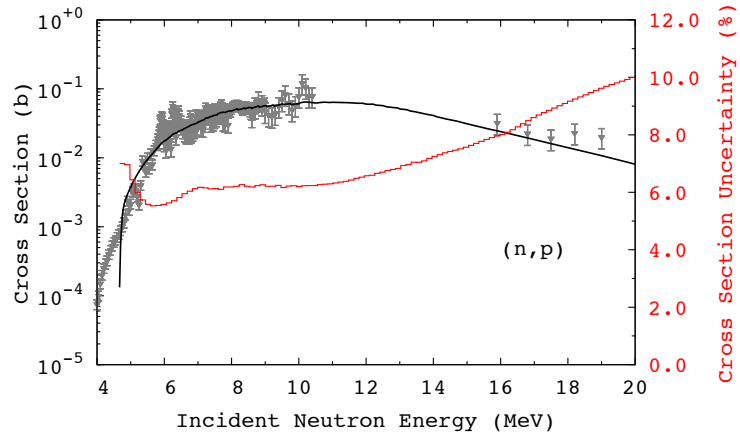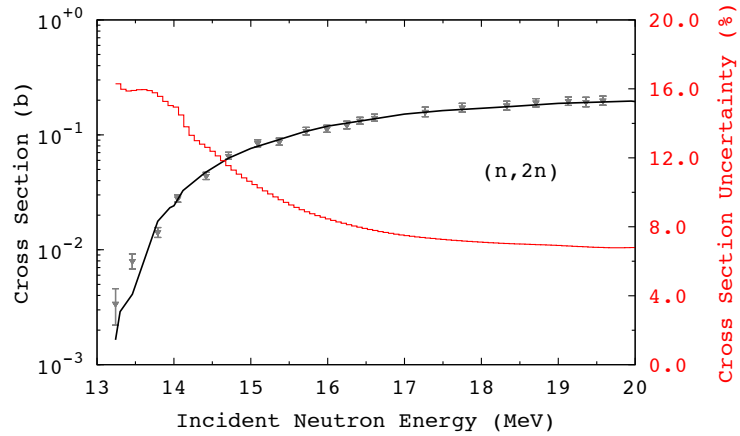
2.1.2 Results of assimilation

In order to perform the consistent data assimilation on the ^{23}Na a set of 136 nuclear parameters were selected and sensitivities to them in terms of multigroup cross section were calculated. The selected parameters include: scattering radius, bound level and 33 resonances (for each one: E$_n$ resonance peak energy, Γ_n neutron width, Γ_g radiative width, for a total of 102 parameters), 33 parameters in fast region (21 optical model parameters, 7 Hauser-Feshbach model parameters, and 5 preequilibrium Exciton model parameters).

For the assimilation INL used propagation experiments of neutrons in a medium dominated by ^{23}Na. These kinds of experiments were specifically intended for improving the data used in the shielding design of fast reactors. Thus, the analysis of these experiments can be effectively utilized for the sodium cross section improvement. Two experimental campaigns taken from the SINBAD database [6] have been used: the EURACOS campaign, and the JANUS-8 campaign. In these experiments measurements with activation detectors were carried out at various distances from the neutron source. A set of reaction rate slopes (one for each detector in the EURACOS and JANUS-8 experiment campaigns) was selected. The chosen slopes were the ratios of the fourth position to the first one for both detectors in the EURACOS experiment, while for the JANUS-8 experiment we selected the fourth to first position ratio for the ^{32}S and ^{197}Au detectors, fourth to second position for the ^{55}Mn, and third to first for the ^{103}Rh. The EMPIRE cross sections (prior) are quite consistent with those of ENDF/B-VII.0 and in some case are performing better. The results of the slope calculations using EMPIRE prior are listed in Tab. 2.1.

There is relatively little correlation among the selected slopes ensuring a good complementarity of information to be exploited in the data assimilation step. In spite of being close to diagonal, the correlation matrix for the selected integral experiments was included in the assimilation. A 41-group energy structure was adopted specifically to better describe the resonance structure of the ^{23}Na. The ERANOS code was used to calculate the multigroup sensitivity for the selected reaction rate slopes. The third column in Tab. 2.1 shows C/E values obtained as the result of assimilation. As it can be observed, except for the gold detectors that did already show good C/E agreement, a remarkable improvement is obtained after the adjustments.

The corresponding variations of the nuclear parameters that are needed for obtaining such improvement are shown in Tab. 2.2. Only the parameters that required at least 0.3% of variation are reported. All the variations are in less than 1σ of the initial uncertainties and, therefore, look acceptable. Some important parameters show a significant improvement in the *a posteriori* standard deviation (e.g., the scattering radius) that would translate in reduced uncertainties on design parameters when the *assimilated* cross sections are used. The only concern regards to the Γ_n of the resonance at 538 keV that requires a very large variation, almost corresponding to the initial standard deviation. More investigation is needed in order to see if this kind of variation is realistic.

We note, that assimilation of the resonance parameters along with the parameters

Table 2.1: Ratio of Calculation to Experiment (C/E) obtained for the integral experiments using prior data computed by EMPIRE and posterior data resulting from the assimilation.

Detector	prior C/E	posterior C/E
EURACOS ^{32}S	0.770 ± 0.085	0.997 ± 0.057
EURACOS ^{197}Au	0.954 ± 0.102	0.946 ± 0.010
JANUS-8 ^{32}S	0.538 ± 0.022	1.000 ± 0.022
JANUS-8 ^{197}Au	1.010 ± 0.033	0.959 ± 0.028
JANUS-8 ^{55}Mn	1.158 ± 0.025	1.028 ± 0.023
JANUS-8 ^{103}Rh	0.960 ± 0.106	0.976 ± 0.047

determining the fast neutron range, when combined with the integral experiments sensitive to both energy ranges introduces correlations among resonance and nuclear model parameters.

2.1.3 Conclusions

It has been noted in Ref. [6] that the improvement in C/E is the result of very large compensations after the parameters have been adjusted. The χ^2 test after adjustment provided a perfect value of 0.99 per degree of freedom. At first sight the assimilation of ^{23}Na exceeded all expectations, since relatively small adjustment of model parameters, totally within quoted uncertainties, lead to the practically perfect reproduction of the selected integral experiments - the very goal of the assimilation concept being achieved. However, subsequent analysis of the results showed that the final objective has not yet been fully satisfied.

Introduction of the assimilated model parameters in the EMPIRE code and recalculating the cross sections revealed that the latter differ from those which were predicted by the assimilation procedure. Therefore, their use in the direct calculation of the integral experiments resulted in discrepancies, which brought us back to the level of performance observed for the ENDF/B-VII.0 cross sections. There was an improvement in reproducing differential cross sections (e.g., much better reproduction of the (n,2n) reaction) but performance of the new file in calculating the integral experiments was mixed and did not appear to be unquestionably better. Our conclusion was that non-linearity effects were to be blamed for the difference between cross sections predicted by the basically linear assimilation procedure and actual model calculations, which are naturally non-linear. This effect could be minimized by an iterative assimilation starting with the reduced perturbation of the parameters. Unfortunately, this approach would be very time consuming due to the lengthy calculations of the integral experiments (over two days on the NNDC cluster). This was not possible within the scope of the current project but we are deter-

Table 2.2: Parameter variations and standard deviations obtained by data assimilation.

Parameter	Variation (%)	Prior stand. dev. (%)	Posterior stand. dev. (%)
Scat. Radius[a]	1.9	4.1	1.7
Γ_n Bound Level[b]	-6.4	8.0	6.4
Γ_n 2.8 keV[c]	0.6	1.9	1.9
Γ_γ 2.8 keV[c]	10.5	11.8	10.5
Γ_n 538 keV[c]	-57.2	65.9	58.4
Real Vol. Rad.[d]	-1.8	2.8	1.6
Real Surf. Diff.[e]	-0.8	5.0	4.7
Real Vol. Diff.[f]	-0.4	2.1	2.1
TOTRED[g]	-1.1	3.5	3.2
FUSRED[h]	-0.8	5.0	4.0

[a]Nuclear Scattering Radius

[b]Bound Level resonance

[c]Resonance Peak Energy

[d]Optical model real volume radius for target nucleus

[e]Optical model real surface diffuseness for target nucleus

[f]Optical model real volume diffuseness for target nucleus

[g]Optical model scaling of total cross sections due to intrinsic model uncertainty

[h]Optical model scaling of absorption cross sections due to intrinsic model uncertainty

mined to return to the issue when preparing new ^{23}Na evaluation for the next release of the ENDF/B library.

2.1.4   Lesson learned

- The results obtained in the assimilation procedure, even though apparently excellent, must be validated by feeding the new parameters back to the reaction code, recalculating cross sections, comparing them with the differential data and recalculating integral experiments.

- The non-linearity effects may distort the linear assimilation procedure and must be kept under control.

2.2   Assimilation of ^{56}Fe

Iron is an important structural material which has been extensively studied and thus many differential and integral experiments are available. It has also been observed that the ENDF/B-VII.0 evaluation for iron, in particular ^{56}Fe, is not a top performer. This, along with an abundance of measurements, makes iron a natural choice for assimilation. Similarly to ^{23}Na, iron presents a challenge due to the persistent (up to 10 MeV) fluctuations in the cross sections that cannot be predicted or even reproduced with any reaction theory modeling. Modulation of the total and absorption cross section as a function of incident energy, that was successfully applied in the sodium case, would be impractical for iron due to much finer energy structure in the fluctuations. Similar modulation in iron would require calculations at thousands of incident energies. Working with the smooth cross sections and ignoring fluctuations was therefore the only viable possibility of preserving adjustable theory predictions needed in the assimilation procedure.

2.2.1   EMPIRE calculations

In EMPIRE calculations for ^{56}Fe we used Coupled-Channels formalism for computation of the absorption cross sections, and direct inelastic scattering. We have adopted iron specific Coupled-Channel potential by Delaroche (RIPL-3 index 425) [19] coupling nine vibrational states as listed in Tab. 2.3. This potential should be valid from 0.1 MeV up to 14 MeV and was chosen because it provided better description of the cross sections than other optical model potentials available in RIPL-3.

Table 2.3: Collective levels used in direct calculations of ^{56}Fe.

N	E (MeV)	J^π	N_{ph}	Deformation
1	0.0000	0^+	0	0.000
2	0.8468	2^+	1	0.239
7	3.0762	3^-	1	0.197
4	2.6576	2^+	2	0.239
5	2.9415	0^+	2	0.239
3	2.0851	4^+	2	0.239
6	2.9599	2^+	2	0.050
9	3.1229	4^+	2	0.050
12	3.4453	3^+	2	0.050

Discrete levels were taken from the RIPL-3 level file and EMPIRE-specific level densities were used in the continuum region above. The pre-equilibrium emission of neutrons

was treated in terms of quantum-mechanical multistep models (TUL-MSD and Heidelberg MSC), while pre-equilibrium emission of protons was calculated with the classical exciton model (PCROSS). The Iwamoto-Harada model was invoked for computation of pre-equilibrium emission of alpha particles. Width fluctuations were considered within the HRTW approach up to 1 MeV. For incident neutron energies above 1 MeV Hauser-Feshbach model with full gamma cascade was used. The EGLO option was chosen for the E1 γ-strength function, since it turned out to provide the best results in default calculations.

The sensitivity calculations were performed for 37 model parameters in the fast neutron energy range. These were used in the KALMAN adjustment to differential cross sections measurement resulting in modification of several model parameters:

- Mean free path parameter in PCROSS set to 1.0 (default 1.5)

- Emission width of neutrons from ^{57}Fe multiplied by 1.008

- Emission width of protons from ^{57}Fe multiplied by 0.650

- Real volume OM potential diffuseness in ^{56}Fe scaled by 0.96

- Real volume OM potential depth in ^{56}Fe scaled by 1.01

- Imaginary surface OM potential radius in ^{56}Fe scaled by 1.01

- Imaginary surface OM potential depth in ^{56}Fe scaled by 1.04

Results of the calculations with the KALMAN adjusted parameters constitute our assimilation prior and are compared to the differential experimental data and ENDF/B-VII.1 evaluation in Figs. 2.8 - 2.12. One notes non-negligible differences between our prior and ENDF/B-VII.1 results. In particular, comparison of the total cross sections (see Fig.2.8) is only fair indicating that optical model used in our calculations might not be the optimal one apart from the neglect of fluctuations.

The elastic cross sections in our prior are lower than ENDF/B-VII.1 and do not account for a strong resonant structure, although above 5 MeV sparse experimental data seem to support EMPIRE calculations (Fig. 2.9).

The inelastic is likely to be one of the most important channels for integral validation. Comparison in Fig. 2.10 shows significant difference between our prior and ENDF/B-VII.1 below 10 MeV. Similar behavior is observed for the inelastic scattering to the first excited state in the target nucleus below 3 MeV, i.e., the region to which integral experiments are most sensitive. Again, lack of strong fluctuations below 3 MeV might be an obstacle in the assimilation process.

The (n,p) reaction, which is one of the prominent channels in the neutron interaction with ^{56}Fe is relatively well described below 5 MeV (Fig. 2.12) and, taking into account
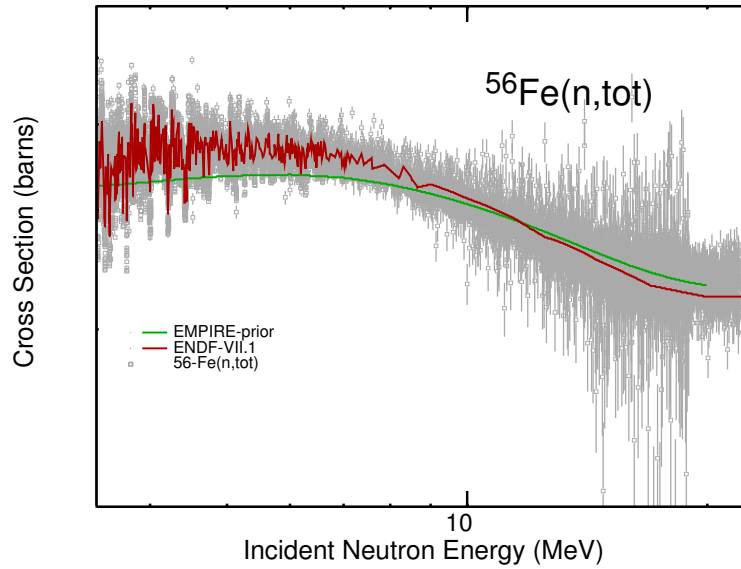
Figure 2.8: Total cross sections for neutrons interacting with ^{56}Fe. EMPIRE calculations are compared with experimental data and ENDF/B-VII.1 evaluation.
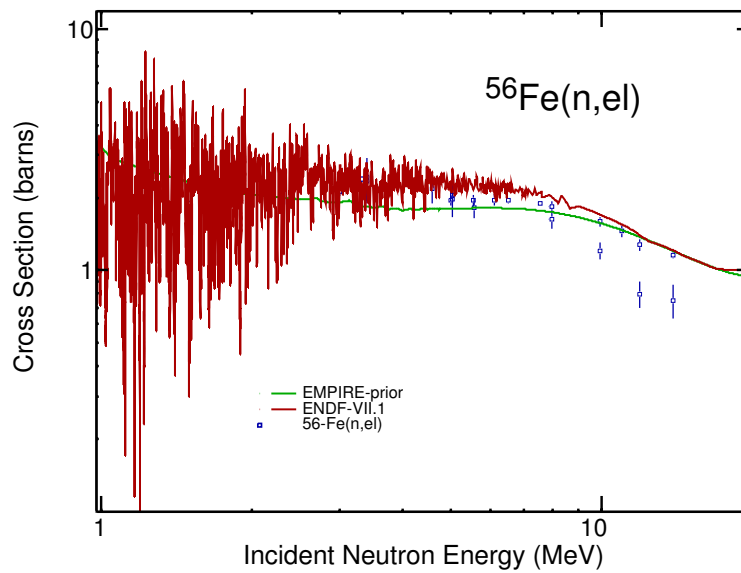
Figure 2.9: Elastic cross sections for neutrons scattered from ^{56}Fe. EMPIRE calculations are compared with experimental data and ENDF/B-VII.1 evaluation.
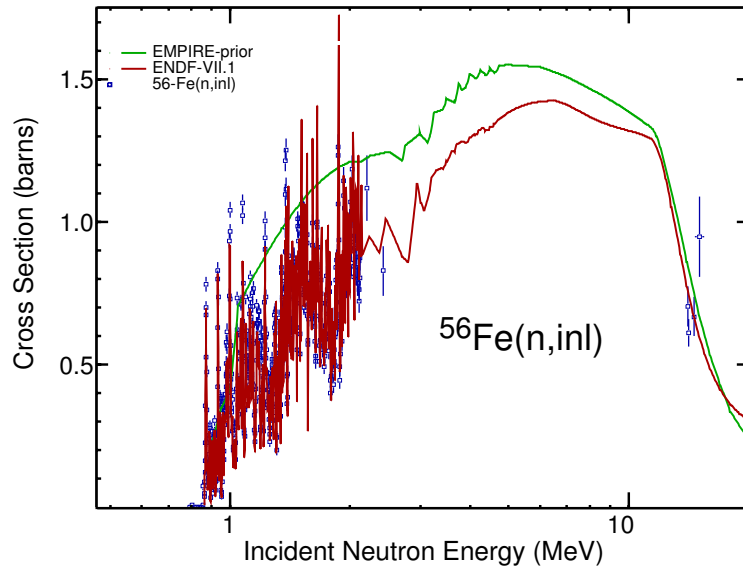
Figure 2.10: Inelastic cross sections for neutrons scattered from ^{56}Fe. EMPIRE calculations are compared with experimental data and ENDF/B-VII.1 evaluation.
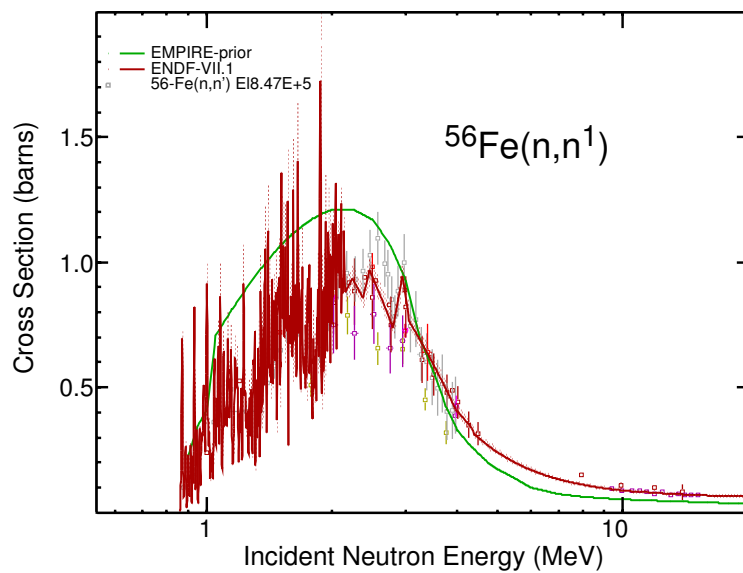
Figure 2.11: Cross sections for neutrons inelastically scattered to the first excited level in ^{56}Fe. EMPIRE calculations are compared with experimental data and ENDF/B-VII.1 evaluation.

Figure 2.12: Cross sections for the ^{56}Fe(n,p) reaction. EMPIRE calculations are compared with experimental data and ENDF/B-VII.1 evaluation.

Figure 2.13: Mu-bar for ^{56}Fe. EMPIRE calculations are compared with experimental data and ENDF/B-VII.1 evaluation

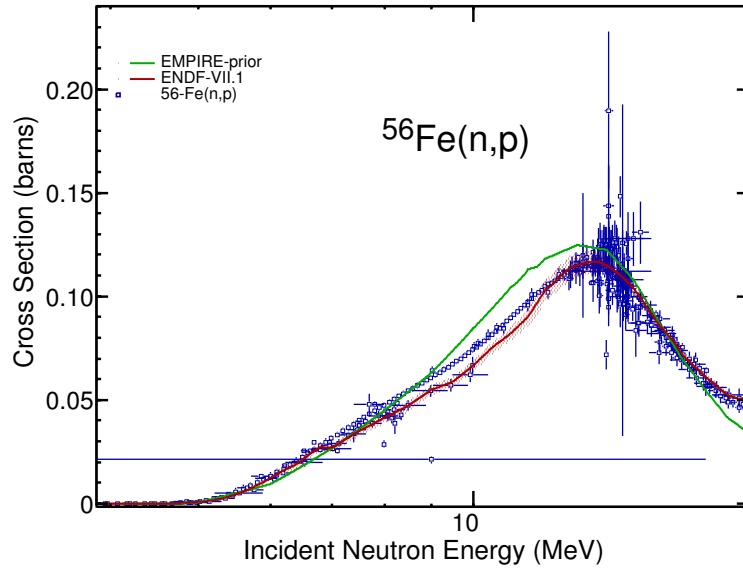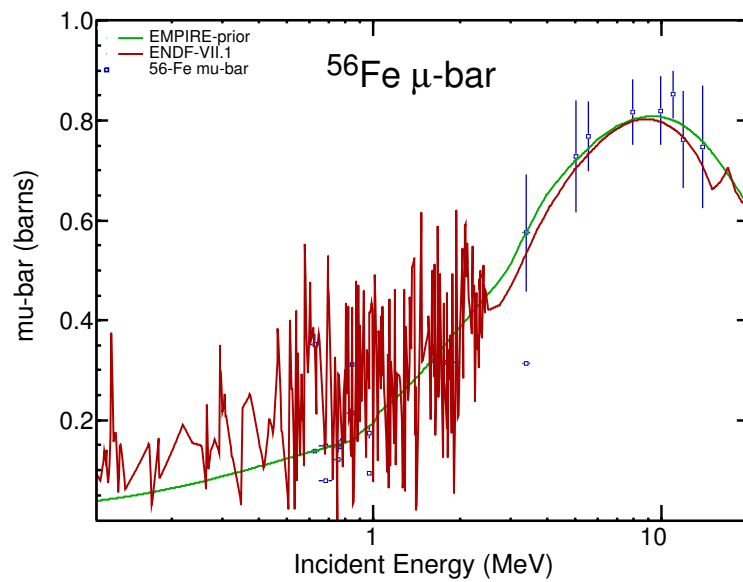relatively small cross section in this energy range, should not pose a problem in the assimilation. In Fig. 2.13 we compare our results for the average cosine of elastic scattering angle in the Lab system (known as $\bar{\mu}$) with ENDF/B-VII.1 and experimental results. Overall, predictions of the optical model are satisfactory above 3 MeV, but are obviously missing strong resonant structure below 3 MeV. In this region our results tend also to be somewhat below the average value of ENDF/B-VII.1. This deficiency might influence comparison with those integral experiments which are characterized by substantial leakage of neutrons.

Integral testing of the EMPIRE prior was carried out at INL and reported in Ref. [6]. It has been shown that based on the comparison with integral experiments, EMPIRE generated ^{56}Fe evaluation appears to be of lower quality when compared to the original ENDF/B-VII.0 data. This could be expected in view of discrepancies between the prior and ENDF/B-VII.0 shown in Figs. 2.8-2.11 and total neglect of the fluctuations in the cross sections and $\bar{\mu}$.

2.2.2 Sensitivities

Inelastic scattering is a channel of primary importance in applications. The sensitivity calculations prove that it depends only on the optical model parameters. Fig. 2.14 shows fractional change in the total inelastic scattering cross section due to the perturbation of the optical model parameters by 3%. Extremely high sensitivity to the volume real potential depth and radius is observed close to the threshold. This can be easily perceived since inelastic in this energy range consists of direct and compound nucleus decay contributions that both only depend on optical model parameters. In case of compound nucleus it is because residual level densities are not involved and and decay is determined directly through optical noel transmission coefficients. Therefore, proper optical model potential is absolutely critical for the correct description of the inelastic channel just above the threshold. More detailed study may even require modification of the Hauser-Feshbach formalism due to the presence of direct reactions, e.g., by employing the Engelbrecht-Weidenmueller [20] transformation. In case of ^{56}Fe the physical picture is additionally complicated by presence of strong fluctuations below 3 MeV, which will obscure any refined theory treatment.

2.2.3 Results of assimilation

The actual assimilation was performed at INL using ERANOS code and sensitivity matrices provided by the BNL. The latter ones were obtained by perturbing parameters for the selected resonances and parameters of nuclear reaction models in used the fast neutron range. The results were reported in the above mentioned report [6]. A total of 35 nuclear parameters were varied including the scattering radius, nine optical model parameters,
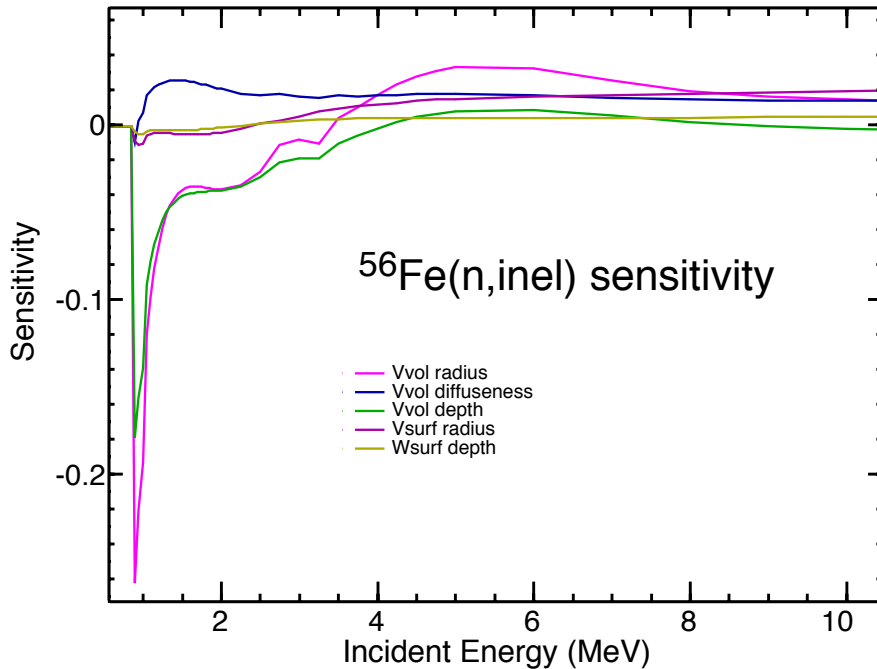
Figure 2.14: Sensitivity of inelastic scattering of neutrons on ^{56}Fe to perturbation of optical model parameters by 3%.

resonance energy, Γ_n and Γ_γ for the bound level, and Γ_n for 25 s-wave resonances that dominate the resonance region.

Results of assimilation are summarized in Tab. 2.4. In general, considerable improvement has been achieved. However, as shown in [6], this improvement is still insufficient to match performance of ENDF/B-VII.0. In particular, the last ZPR3-54 experiment is over calculated by 28% and two EURACOS experiments are under calculated by a factor of 2 - all far beyond experimental uncertainty.

A significant reduction in the final standard deviation was observed only for the scattering radius. However, as shown in Tab. 2.5, many parameters required modifications that were exceedingly large (more than 2σ) when compared with the initial standard deviations. Paramount are changes in the real volume depth of the optical potential and radii. This fact, combined with the previously observed inability to significantly improve some of the C/E's results and a value of the χ^2 test (more than 50 times the total degrees of freedom) make this exercise inconclusive.

2.2.4 Conclusions

The case of ^{56}Fe presents a number of challenges from the perspective of the assimilation procedure and was the most difficult case encountered during the project. The results

Table 2.4: Initial and new C/E before and after data assimilation.

Experiment		C/E ± σ (before)	C/E ± σ (after)
^{10}B(n,α) slope	ZPR3-54	0.853 ± 0.030	1.012 ± 0.022
^{235}U(n,f) slope	ZPR3-54	0.907 ± 0.030	1.015 ± 0.013
^{239}Pu(n,f) slope	ZPR3-54	0.889 ± 0.030	0.996 ± 0.013
^{238}U(n,f) slope	ZPR3-54	1.455 ± 0.030	1.284 ± 0.014
^{32}S(n,p) slope	EURACOS	0.879 ± 0.093	1.197 ± 0.055
^{197}Au(n,γ) slope	EURACOS	1.288 ± 0.098	1.054 ± 0.032
^{115}In(n,n') slope	EURACOS	0.327 ± 0.156	0.455 ± 0.042
^{103}Rh(n,n') slope	EURACOS	0.478 ± 0.071	0.511 ± 0.010

Table 2.5: Parameter variations and standard deviations obtained by data assimilation.

Parameter	Variation (%)	Init. Std. Dev. (%)	Final Std. Dev. (%)
Scat. Rad.[a]	-13.25	5.1	2.1
Γ_n Bound Level[b]	1.9	4.0	3.7
Γ_g Bound Level[b]	-2.1	5.0	4.8
Γ_n 277 keV[c]	-1.1	8.0	8.0
Γ_n 317 keV[c]	-2.2	8.0	8.0
Γ_n 361 keV[c]	-2.9	8.0	8.0
Γ_n 381 keV[c]	-3.0	8.0	8.0
Γ_n 665.6 keV[c]	1.3	8.0	8.0
Real well volume[d]	15.1	3.0	2.2
Nuclear radius Real Surf.[e]	10.5	3.0	2.9
Imag. & Real Surf.[f]	10.8	5.0	4.9
TOTRED[g]	-0.9	1.0	1.0
FUSRED[h]	-2.0	1.3	1.2

[a]Nuclear scattering radius.

[b]Bound Level resonance.

[c]Resonance peak energy.

[d]Optical model real well depth and real volume of target nucleus.

[e]Optical model nuclear radius and real surface of target nucleus.

[f]Optical model imaginary and real surface of target nucleus.

[g]Optical model scaling of total cross sections due to intrinsic model uncertainty.

[h]Optical model scaling of absorption cross sections due to intrinsic model uncertainty.

of the assimilation were below expectations. It is partially because iron is a very well measured material and due to its importance it has been carefully evaluated. Much more work should be invested to determine competitive prior able to reproduce differential data. Most likely, improvements are needed in the input to EMPIRE since our ^{56}Fe prior compares to differential cross sections significantly worse than the ENDF/B-VII.0 file. At the time of this exercise there was no good optical potential for iron in the RIPL-3 library, which resulted in the prior that does not match the quality of the existing evaluated libraries. A major improvement should be brought by a dispersive optical model potential.

Possibly, there may be inconsistencies among differential and integral measurements that have been used, or the adopted initial uncertainties for the nuclear parameters were not sufficiently large to cover the discrepancies between experimental and calculated values.

Persistent and very strong fluctuations producing resonance-like energy structure that extends up to 10 MeV cannot be predicted by theory, although it's not impossible that its lower energy part can be interpreted in terms of the resolved resonances. Lack of a suitable physical model in this application-important energy range makes applicability of the assimilation concept dubious. A way to circumvent this obstacle could be to accept numerical values of the fluctuating experimental cross sections and allow for a scaling factor to be applied to them. In this case, the sensitivity matrix would be calculated by perturbing a scaling factor that would just simulate uncertainty in the absolute normalization of the experimental data. This approach would, however, eliminate advantage of consistency when using physically sound nuclear reaction modeling.

2.2.5   Lesson learned

- A practical, necessarily approximative, method should be developed for treating fine energy fluctuations that can't be treated explicitly in terms of the reaction theory. This method should retain experimental shape of the fluctuations but allow for more or less flexible scaling of the energy average in such a way that cross sections are continuous on both extremes of the fluctuating range.

- Possible discrepancies between and among differential and integral experiments might make consistent assimilation difficult or impossible. This is a well known issue one has to face when fitting discrepant data.

- Integral experiments alone do not ensure restoring agreement with differential data if the prior is of poor quality. Using proper nuclear reaction modeling with parametrization capable of providing a prior reproducing differential data is a necessary prerequisite for a meaningful assimilation.

2.3 Assimilation of ^{105}Pd

2.3.1 EMPIRE calculations

The EMPIRE calculations and corresponding fitting were much simpler in the case of ^{105}Pd, since the newer version of EMPIRE code (revision 2869) was able to provide a very good agreement with experimental data by using the default input file with only minor modifications. The input file that best described data employed spherical optical model calculations, using the Zhang *et al.* [21] ^{105}Pd-specific spherical optical potential (indexed as 523 in RIPL-3 library). The standard EMPIRE-specific level densities were adopted. These level densities were adjusted to discrete levels and to the RIPL-3 experimental average s-wave neutron resonance spacings. Multi-step direct (MSD) calculations were enabled above 3.1 MeV using ORION+TRISTAN code. Heidelberg multi-step compound (MSC) calculations were also enabled. The exciton model with Iwamoto-Harada cluster emission (PCROSS) for the pre-equilibrium was enabled with mean free path multiplier set to 1.5. Also, the HRTW width fluctuation correction was enabled up to 3.0 MeV. Default γ-strength functions were adopted (MLO1 modified Lorentzian).

Figure 2.15: Total cross sections (assimilation prior) calculated by EMPIRE using input parameters obtained after fitting experimental data using Kalman filter (green curve). Evaluation from ENDF/B-VII.1 library (red curve) and experimental data from EXFOR (blue points) are plotted for comparison.

The cross sections obtained with this input file correspond to the assimilation prior and are shown in Figures 2.15, 2.16, 2.17 and 2.18, for total, capture, inelastic and (n,2n)
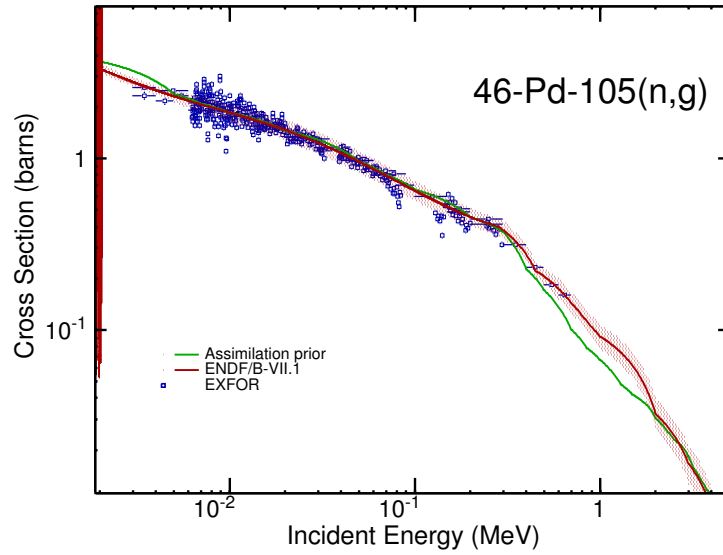
Figure 2.16: Capture cross sections (assimilation prior) calculated by EMPIRE using input parameters obtained after fitting using Kalman filter (green curve). Evaluation from ENDF/B-VII.1 library (red curve) and experimental data from EXFOR (blue points) are also plotted for comparison.

reactions, respectively.
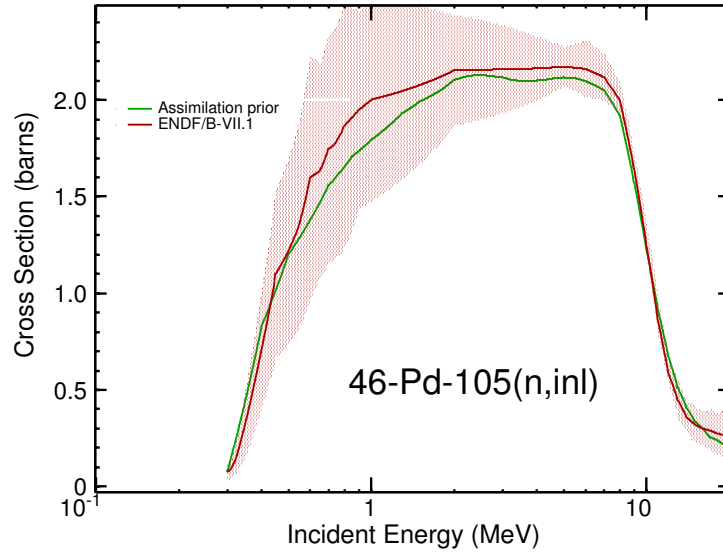
Figure 2.17: Inelastic cross sections (assimilation prior) calculated by EMPIRE using input parameters obtained after fitting using Kalman filter (green curve). Evaluation from ENDF/B-VII.1 library (red curve) is also plotted for comparison.
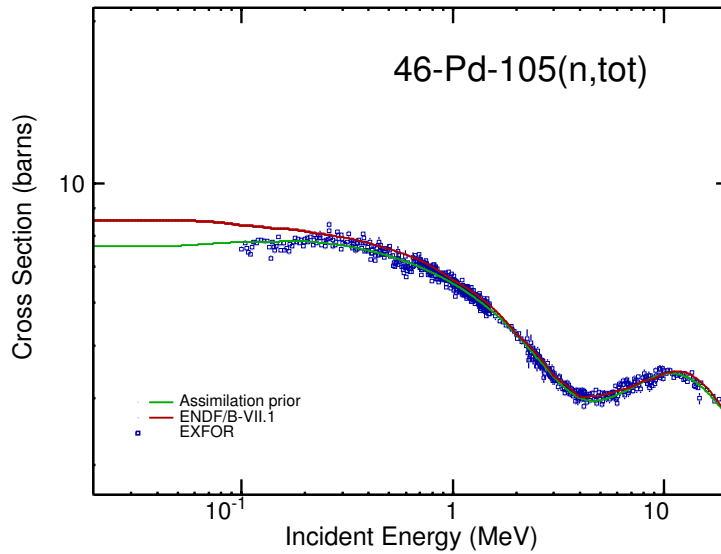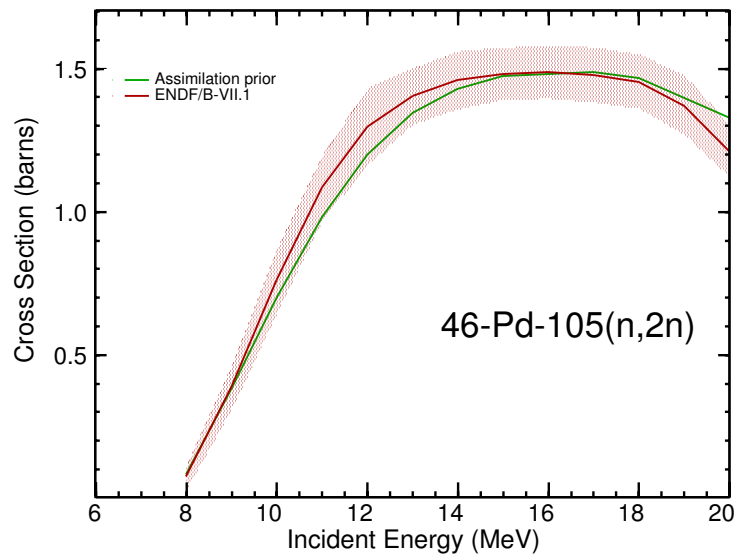

Figure 2.18: (n,2n) cross sections (assimilation prior) calculated by EMPIRE using input parameters obtained after fitting using Kalman filter (green curve). Evaluation from ENDF/B-VII.1 library (red curve) is also plotted for comparison.

2.3.2   Sensitivities

Before running KALMAN the sensitivities of the cross sections to perturbation of the input parameters were calculated. Figure 2.19 shows an example of such sensitivities in the case of capture reaction. All of the 24 parameters varied are displayed in Figure 2.19, allowing to pinpoint parameters to which capture cross sections are sensitive and assess energy regions and changes brought by variations of these parameters.
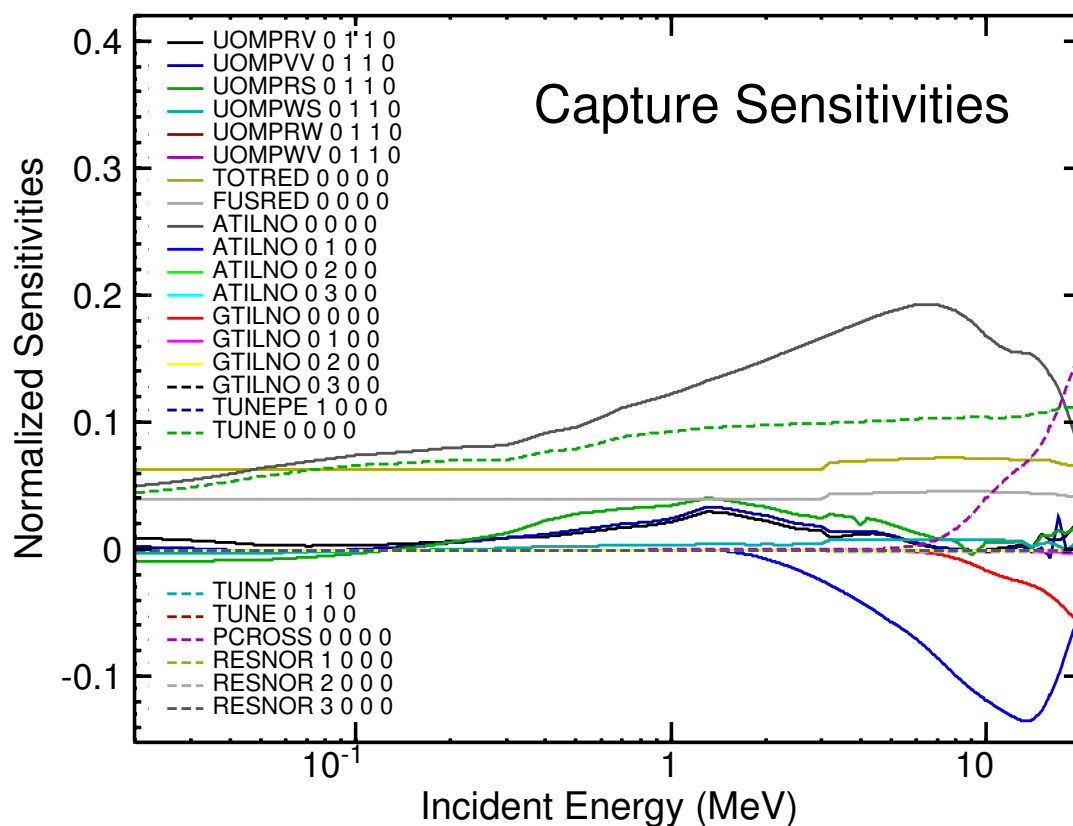
Figure 2.19: Sensitivities, for the capture reaction, of the parameters used to fit ^{105}Pd capture cross-section experimental data.

2.3.3   Covariances

A Kalman filter code (KALMAN) has been employed to fine tune EMPIRE calculations to the experimental data and to determine covariances for the model parameters. Since the default input was providing pretty good description of the differential data no major changes to the parameters were expected. This allowed us to use relatively generous
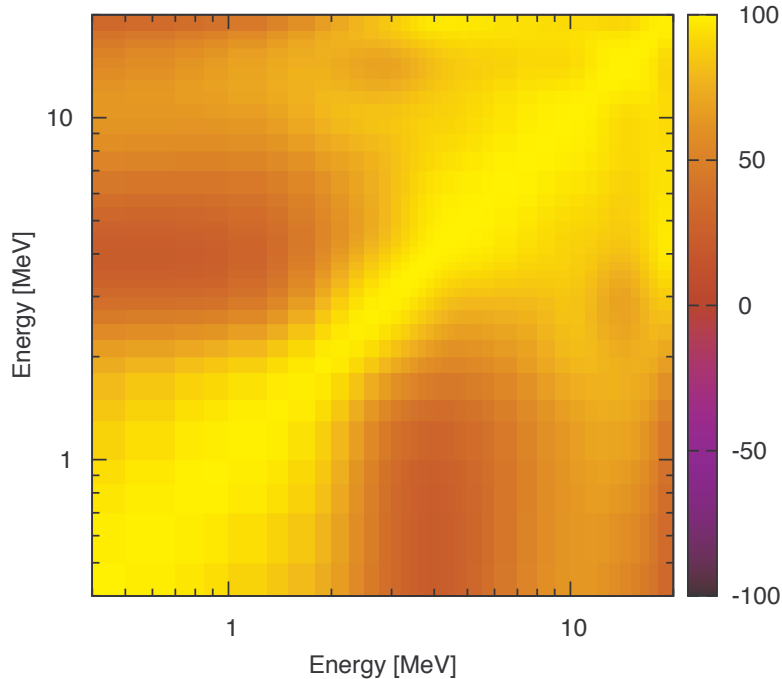
Figure 2.20: Correlation matrix for total cross section calculated using KALMAN.

initial uncertainties of the model parameters as non-linearity was not a major concern. Effectively, the final uncertainties were constrained mostly by the experimental data and estimates of the uncertainties of the global systematics. However, our calculations were affected by the PPP and to eliminate it we had to remove total cross section and absorption scaling factors from the fit. These two parameters take into account uncertainty in the absolute normalization and simulate model deficiencies. In the current exercise they were marginalized, i.e., they were assigned estimated uncertainties that were used in the calculation of the cross sections covariances but without being involved in the KALMAN fitting procedure. In other words, they were assumed to be uncorrelated with the other parameters.

The energy correlation matrices are shown in Figs. 2.20, 2.21, 2.22 and 2.23 for the total, inelastic, capture, and (n,2n) reactions, respectively. The correlations for total (Fig. 2.32) are experiment dominated with a slight reminiscence of the typical optical model pattern. The inelastic scattering correlation matrix (Fig. 2.21) reflects domination of the compound nucleus mechanism below 3 MeV and the pre-equilibrium emission above. Capture correlation matrix displays overwhelming contribution from γ-ray strength function which correlates nearly the whole energy range except energies above 15 MeV that are governed by the pre-equilibrium mechanism. Similar separation between compound and pre-equilibrium mechanisms is also evident in the (n,2n) correlation matrix.

The correlations among the model parameters varied during the fitting with Kalman
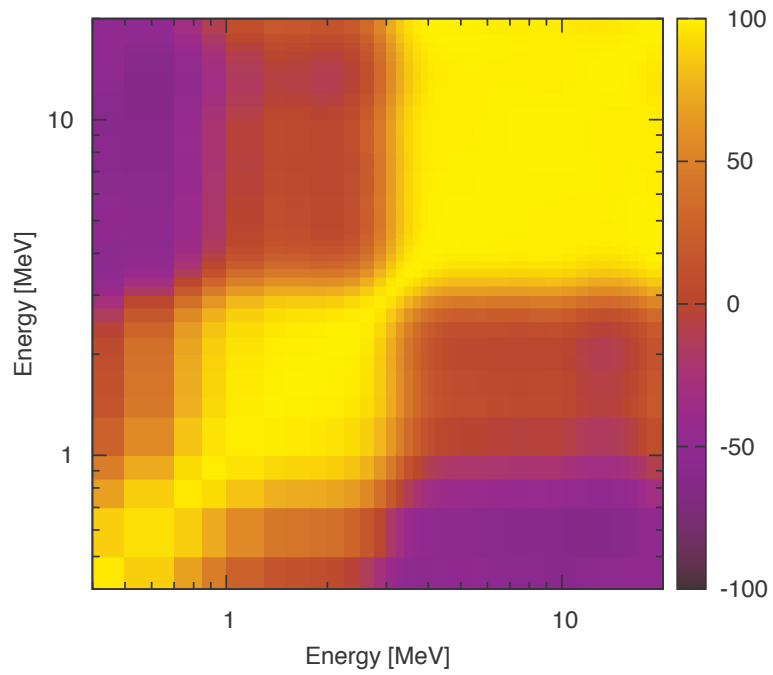
Figure 2.21: Correlation matrix for inelastic cross section calculated using KALMAN.
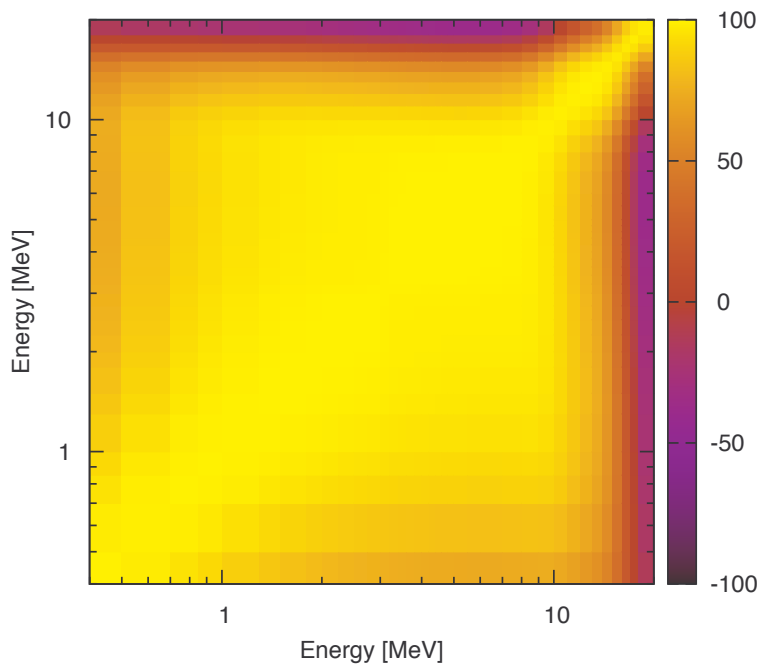
Figure 2.22: Correlation matrix for capture cross section calculated using KALMAN.
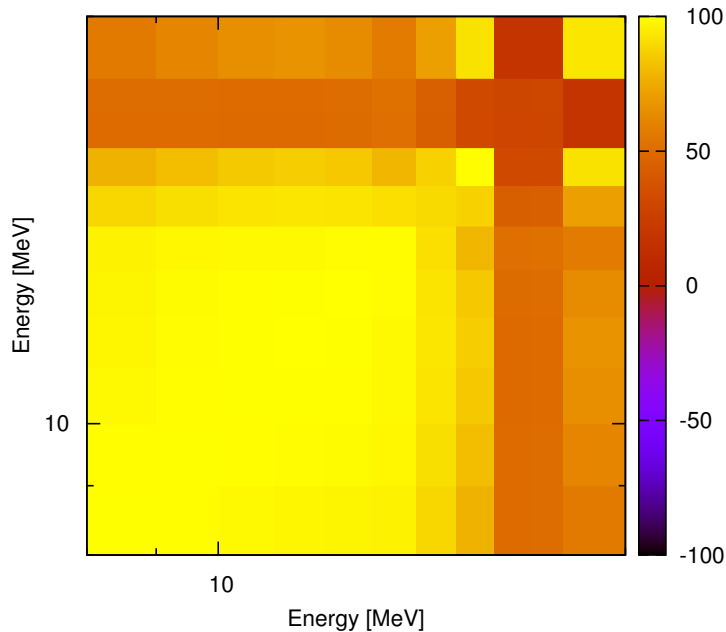
Figure 2.23: Correlation matrix for (n,2n) cross section calculated using KALMAN.

filter are reported in Table 2.6. We recall that these correlations are imposed by the experimental data. In other words, they ensure compensation needed to keep cross sections constant (optimal) under the change of each parameter. One notes that there are relatively few correlations that are different from zero. Apart from the strong correlations among optical model parameters, the prominent full anti-correlation is found between γ-ray strength function scaling parameter and asymptotic level density in the compound nucleus (parameters number 18 and 9 respectively). The latter will play an important, potentially destructive, role in the assimilation.

2.3.4 Results of assimilation

For the assimilation of ^{105}Pd, use was made of only single integral parameter - the ^{106}Pd build up in the ^{105}Pd sample of PROFIL-1. This parameter provides information on the ^{105}Pd capture cross the section. A total of 24 nuclear parameters were utilized in EMPIRE for characterizing the evaluation of the ^{105}Pd cross sections, among them optical model, level density, pre-equilibrium single-particle level density, response function, total and fusion cross-section and equilibrium decay width scaling parameters. The covariance matrix of these parameters was provided by the Kalman filter, while the group-wise cross section sensitivities were generated running EMPIRE with perturbed parameters and processing each evaluation with the NJOY code. Then the assimilation was performed at INL with the ERANOS code. The initial uncertainty of the parameters provided with the new evaluation

Table 2.6: Correlations among parameters (in units of %) in assimilation prior for ^{105}Pd. See text for discussion of the values presented below. Correlations above 50% and 25% are highlighted in red and yellow, respectively.

	Parameter	1	2	3	4	5	6	7	8	9	10	11	12	13	14	15	16	17	18	19	20	21	22	23	24
1	UOMPRV-011[a]	100																							
2	UOMPVV-011[a]	-99	100																						
3	UOMPRS-011[a]	-72	67	100																					
4	UOMPWS-011[a]	89	-89	-78	100																				
5	UOMPRW-011[a]	0	0	0	0	100																			
6	UOMPWV-011[a]	0	0	0	0	0	100																		
7	TOTRED-000[b]	0	0	0	0	0	0	100																	
8	FUSRED-000[b]	0	0	0	0	0	0	0	100																
9	ATILNO-000[c]	-4	4	2	-5	0	0	0	0	100															
10	ATILNO-010[c]	-40	40	26	-35	0	0	0	0	1	100														
11	ATILNO-020[c]	0	0	0	0	0	0	0	0	0	0	100													
12	ATILNO-030[c]	0	0	0	0	0	0	0	0	0	0	0	100												
13	GTILNO-000[d]	30	-30	-20	26	0	0	0	0	-1	-38	0	0	100											
14	GTILNO-010[d]	2	-2	-1	2	0	0	0	0	0	1	0	0	-5	100										
15	GTILNO-020[d]	0	0	0	0	0	0	0	0	0	0	0	0	0	0	100									
16	GTILNO-030[d]	0	0	0	0	0	0	0	0	0	0	0	0	0	0	0	100								
17	TUNEPE-100[e]	4	-4	-3	4	0	0	0	0	0	1	0	0	-10	-1	0	0	100							
18	TUNE-000[f]	6	-6	-4	7	0	0	0	0	-99	-2	0	0	2	0	0	0	0	100						
19	TUNE-011[f]	0	0	0	0	0	0	0	0	0	0	0	0	0	0	0	0	0	0	100					
20	TUNE-010[f]	0	0	0	0	0	0	0	0	0	0	0	0	0	0	0	0	0	0	0	100				
21	PCROSS-000[g]	-25	25	17	-23	0	0	0	0	1	68	0	0	36	2	0	0	5	-1	0	0	100			
22	RESNOR-100[h]	0	0	0	0	0	0	0	0	0	0	0	0	0	0	0	0	0	0	0	0	0	100		
23	RESNOR-200[h]	-1	1	1	-1	0	0	0	0	0	-24	0	0	5	0	0	0	1	0	0	0	0	0	100	
24	RESNOR-300[h]	0	0	0	0	0	0	0	0	0	-5	0	0	0	0	0	0	0	0	0	0	0	0	0	100

[a]Optical model parameters
[b]Scaling parameters
[c]Level density parameters
[d]Single particle level density parameters in PCROSS
[e]Preequilibrium decay width parameter
[f]Equilibrium decay width parameters
[g]Mean free path multiplier in PCROSS
[h]Response function parameters

Table 2.7: Old and new C/E before and after adjustment for ^{106}Pd build up in the ^{105}Pd sample of PROFIL-1

Experiment	old C/E $\pm\ \sigma$	new C/E $\pm\ \sigma$
PROFIL-1	0.835 ± 0.028	0.990 ± 0.027

Table 2.8: ^{105}Pd parameter variations and standard deviations obtained by data assimilation.

Parameter	Variation (%)	Init. % Std. Dev.	Final % Std. Dev.
TUNE000[a]	69.253	40.00	10.77
ATILNO000[b]	-2.573	1.49	0.43
FUSRED000[c]	0.353	2.00	1.99

[a]Scaling γ-strength function in ^{106}Pd (compound)
[b]Level density parameter for ^{106}Pd (compound)
[c]Scaling factor for fusion (reaction) cross section

were not large enough to allow for the effective assimilation. Reproducing build up of the ^{106}Pd in the PROFIL-1 experiment required higher capture cross sections that could be attained within the original covariances. An attempt to increase the uncertainties (while preserving correlations) resulted in the unphysically low level density parameter (parameter 9 in Tab. 2.6) compensated by the increase of the γ-strength in the compound nucleus (parameter 18 in Tab. 2.6) due to their complete anti-correlation. More plausible results were obtained by increasing uncertainty for the γ-strength function without increasing the level density counterpart.

The C/E results are presented in Table 2.7 before and after adjustment. A significant improvement was obtained with respect to the initial discrepancy; however, the normalized χ^2 after adjustment was 3.23, which still is quite a large value. Table 2.8 provides parameter variations and related standard deviations before and after the assimilation for the three most important parameters. As it can be seen, both TUNE000 and ATILNO000 required changes that significantly exceed their initial standard deviations, which explains the large value of χ^2.

Since the build up of ^{106}Pd is proportional to the integral of capture cross section weighted with the neutron flux the assimilation is changing capture cross section through modifying γ-ray strength function and level densities in the compound nucleus. Contributions of these parameters to the relative change of C/E are shown in Table 2.9. The first two quantities are, as shown in Tab. 2.6, strongly anti-correlated, which leaves a lot of room for compensation. Therefore, if at least one of the two parameters is not well

Table 2.9: Contribution of the parameter variation to the relative change of the C/E for ^{106}Pd build up in the ^{105}Pd sample of PROFIL-1.

Parameter	Contribution (%)
TUNE000[a]	20.46
ATILNO000[b]	-2.14
FUSRED000[c]	0.19
TOTAL	18.52

[a]Scaling γ-strength function in ^{106}Pd (compound)
[b]Level density parameter for ^{106}Pd (compound)
[c]Tuning (scaling factor) for fusion (reaction) cross section

pinned down by the differential experiment the assimilation may exploit anti-correlation to drive both of them out of the physically accepted values. This was actually the case when both uncertainties were doubled in one of the assimilation attempts.

The value of a reduced χ^2 well in excess of 1 and the fact that fitting the integral experiment required changes larger than initial standard deviations suggest that the differential and integral experiments are discrepant. This surmise was confirmed by the calculation of cross sections using in the EMPIRE input post-assimilation values of the parameters. As shown in Fig. 2.24, the post-assimilation capture adjusted to the integral data is considerably higher than the prior, which is in agreement with the differential data.

2.3.5 Conclusions

The case of ^{105}Pd is the one which should be relatively easy to assimilate. The integral experiment is a direct measurement of the capture cross section integrated over neutron spectrum and is not affected by other materials or cross sections. Reaction calculations on ^{105}Pd are straightforward, with the default EMPIRE calculations being very close to the differential data. Also, there are no measurements revealing fluctuations that complicate the assimilation, as in sodium and iron. In this circumstances, the assimilation, if necessary, should be carried out easily by a slight adjustment of the γ-ray strength function in the compound nucleus. The failure of doing so is most likely due to the discrepancy between differential and integral experiments. Encouragingly, the assimilation procedure proved to be solid in this case - the adjustment was not possible without 'ad hoc' modification of the covariance matrix for the prior (doubling of the uncertainty for the γ-ray strength function).
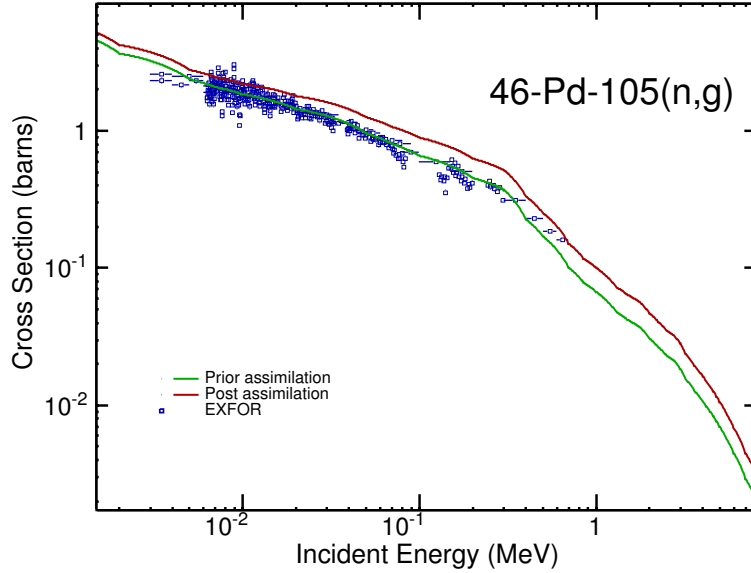
Figure 2.24: Comparison between *prior* (green) and *post* (red) capture cross sections obtained through the assimilation of ^{105}Pd.

2.3.6   Lesson learned

- In relatively simple cases, like build up of ^{106}Pd in PROFILE-1 that depends on a single reaction it is possible that all sensitivity is concentrated on a couple of model parameters. If these parameters happen to be anti-correlated assimilation may exploit this feature to drive both parameters out of the physical range. To ensure that assimilation is meaningful it is necessary that at least one of the parameters is well restrained by the differential data.

- If assimilation is not possible without increasing properly defined prior uncertainties it either means that the model is not adequate or flexible enough, or that differential and integral experiments are not consistent.

2.4   Assimilation of ^{235}U

We have performed two rounds of assimilation for the two major actinides (^{235}U and ^{239}Pu). The first round was completed in 2011 while the second is still in progress - new priors using the recently released version of the EMPIRE code have been prepared along with the sensitivity matrices and covariances for the model parameters. Actual assimilation will be done by INL in the near future (this round was not foreseen to be an INL milestone). Only for ^{239}Pu has direct assimilation been performed at BNL. In this section we summarize the first round of assimilation for ^{235}U and focus on EMPIRE results from the second round.

2.4.1   First Round of Assimilation

A first round of data assimilation for ^{235}U was performed in 2011, using the experimental data of the LANL sphere GODIVA as described in the FY11 Deliverable ARRA Consistent Assimilation report (Ref. [7]). A total of 52 nuclear parameters were used then in EMPIRE for characterizing the evaluation of the ^{235}U cross sections. The covariance matrix of these parameters were provided as well as the sensitivity of them in terms of multigroup cross sections, and a statistical adjustment was carried out. Table 2.10 shows the C/E before and after adjustment with related uncertainties, obtained at that time.

Table 2.10: C/E before and after adjustment for GODIVA experiments

Experiment	C/E $\pm$ σ (before)	C/E $\pm$ σ (after)
k_{eff}	0.9907 $\pm$ 0.002	1.0010 $\pm$ 0.002
^{238}U(n,f)/^{235}U(n,f)	1.0527 $\pm$ 0.013	1.0357 $\pm$ 0.004
^{239}Pu(n,f)/^{235}U(n,f)	0.9917 $\pm$ 0.018	0.9771 $\pm$ 0.003
^{237}Np(n,f)/^{235}U(n,f)	1.0703 $\pm$ 0.017	1.0536 $\pm$ 0.003
^{233}U(n,f)/^{235}U(n,f)	0.9964 $\pm$ 0.019	0.9820 $\pm$ 0.004

A significant improvement was obtained on the discrepancies on k_{eff} while for the fission spectral indices improvements (but still not good agreement with experimental values) are observed for the ^{238}U and ^{237}Np, while for ^{239}Pu and ^{233}U a certain degradation is observed. The χ^2 test after adjustment provided a normalized (to the number of degrees of freedom) value of 4.05; with major contributions coming from the ^{238}U (contribution of 2.01) and ^{237}Np (contribution of 2.36) spectral index integral parameters. Table 2.11 shows the obtained parameter variations before and after the first round of data assimilation for the parameters that mostly affect the assimilation.

Only the 'FUSRED000' parameter variation indicated by the data assimilation slightly exceeds the 1 σ initial uncertainty, while the other variations stay within that range. Table

Table 2.11: ^{235}U parameter variations and standard deviations obtained by data assimilation.

Parameter	Variation (%)	Init. Std. Dev. (%)	Final Std. Dev. (%)
FUSRED000[a]	1.402	1.257	0.878
TOTRED000[b]	0.461	0.966	0.917
ATILNO000[c]	-0.236	0.950	0.946
DELTAF000[d]	-0.025	0.649	0.621
VB000[e]	-0.006	0.133	0.118
UOMPVV011[f]	0.033	0.116	0.116
UOMPRS011[g]	0.072	0.834	0.834
UOMPWS011[h]	-0.110	2.023	2.022
TUNE000[i]	-0.099	1.908	1.908

[a]Factor multiplying the reaction (fusion, absorption, compound nucleus formation) cross section.
[b]Factor multiplying total cross section.
[c]Asymptotic level density parameter in Compound Nucleus.
[d]Pairing energy in the level dens. at saddle point in compound nucleus (first chance fission).
[e]Height of the second hump in the fission barrier in Compound Nucleus.
[f]Real depth of the Optical model potential for n + target.
[g]Surface imaginary Optical model potential radius for n + target.
[h]Surface imaginary Optical Model potential depth for n + target.
[i]Factor on the gamma emission width in Compound Nucleus (scales capture).

2.12 reports the contribution of the parameter variations of Table 2.11 to the relative change of the C/E of the GODIVA k_{eff}. The largest, dominating, contribution is provided by the 'FUSRED000' parameter.

The new standard deviations obtained by the first round of data assimilation were applied to reevaluate the uncertainty of the GODIVA k_{eff}. A reduction of 13.8% was observed, mostly coming from the fission cross section contribution.

After applying to the EMPIRE prior input the parameter changes obtained in the first-round assimilation, new post-assimilation cross sections were calculated. Figure 2.25 compares both prior and post fission cross sections for this first round of ^{235}U assimilation.

2.4.2 Second Round of Assimilation

2.4.2.1 EMPIRE calculations

For the second round of assimilation of ^{235}U, a much newer and much more powerful version (revision 3094) of EMPIRE code was employed. This new version of EMPIRE is able to furnish reasonable cross-section results, when compared to experimental data, for most reactions and for most materials, with hardly any modifications to the input file. This gives the possibility of obtaining a much better prior calculation for the assimilation.

Table 2.12: Contribution of the parameter variation to the relative change of the C/E of the GODIVA k_{eff}.

Parameter	Variation (pcm)
FUSRED000	867
TOTRED000	66
ATILNO000	43
DELTAF000	31
VB000	29
UOMPVV011	-18
UOMPRS011	6
UOMPWS011	-6
TUNE000	6
Total	1038

In the case of ^{235}U, however, the default EMPIRE input file provided a poor description of experimental data, in particular for fission reaction. Therefore, many manual modifications of input parameters, especially to those parameters related to fission barriers, were necessary before an automated fitting process could be initiated. In this process, the standard EMPIRE-specific level densities were adopted. Those level densities are adjusted to discrete levels and to the RIPL-3 experimental average s-wave neutron resonance spacings. Multi-step direct (MSD) calculations were enabled above 5.6 MeV, including the MSD contribution to discrete levels. This gives the vibrational component of the direct cross section. Multi-step compound (MSC) calculations were also enabled. Coupling constants of multi-polarity $\lambda = 2, 3$ and 4 and response function were manually fitted, as well as the energy window for neutron- and proton-pairing calculations. The exciton model with Iwamoto-Harada cluster emission (PCROSS) for the pre-equilibrium was enabled with mean free path multiplier set to 1.5 and coefficient defining the equilibrium exciton number set to 0.2. Also, the HRTW width fluctuation correction was enabled up to 2.0 MeV. Default γ strength functions were adopted (MLO1 modified Lorentzian). The equilibrium decay width of γ ejectile from the compound nucleus and the scaling of fusion (reaction) cross section were also manually fitted. The coupled-channels (CC) method was employed for the calculation of inelastic scattering to collective levels in the incident channel, and also for the calculation of elastic and reaction cross sections. For the incident, outgoing-neutron and outgoing-protons channels, the CC optical potentials of R. Capote *et al.* [22], indexed as 2408 and 5408 by EMPIRE, were used. The original fission barrier data were taken from RIPL-3 empirical fission barriers library and the level densities at saddle points were calculated using the low K limit version of the EGSM. Discrete transitional states above fission barrier and sub-barrier effects were considered.

Such manual fits provided a much more reasonable description of data, allowing to use
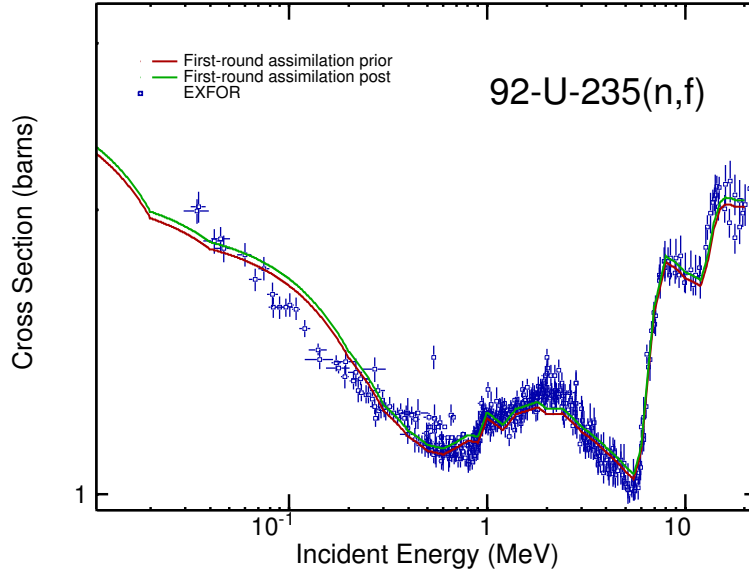
Figure 2.25: Comparison between prior and post fission cross sections obtained through the first round of assimilation of ^{235}U.

this new input file as a starting point for employing the Kalman fitting routine KALMAN to optimize the agreement with experimental data and to calculate covariances. A total of 81 parameters were selected for variation with KALMAN. Those parameters modify different features of the physical models, such as those related to optical model, level density, equilibrium decay width scaling, excitation energy shift, response functions, giant dipole resonance, fission level density, fission vibrational enhancement, fission level density at saddle point, fission barrier heights and widths. After fitting, an "optimal" set of EMPIRE parameters was obtained, generating input files that, after an EMPIRE run, could best describe experimental data. The cross sections obtained from this calculation correspond to the prior-assimilation curves and are shown in Figures 2.26, 2.27, 2.28 and 2.29, for total, elastic, fission and capture reactions, respectively.

Figure 2.30 compares the fission cross section obtained from the EMPIRE input used to provide the prior-assimilation curves for the second round of assimilation to that of the first round of assimilation. As it may be seen in Figure 2.30, the starting point for the assimilation of ^{235}U in this second round is in a much better agreement with experimental data than the one used in the first round. Considering that the first round already produced encouraging results, it is reasonable to assume that even better results may be expected from this second-round assimilation. The final step of assimilation (obtaining new uncertainties and post parameters and cross sections) is still pending for this second round.
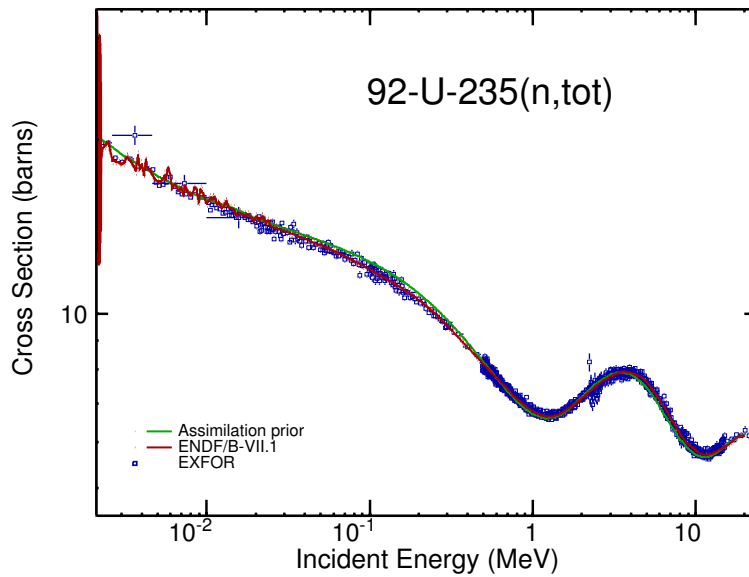
Figure 2.26: Total cross sections calculated by EMPIRE using input parameters obtained after fitting using KALMAN, which will be used as Assimilation prior calculation (green curve). Evaluation from ENDF/B-VII.1 library (red curve) and experimental data from EXFOR (blue points) are also plotted, for comparison purposes.
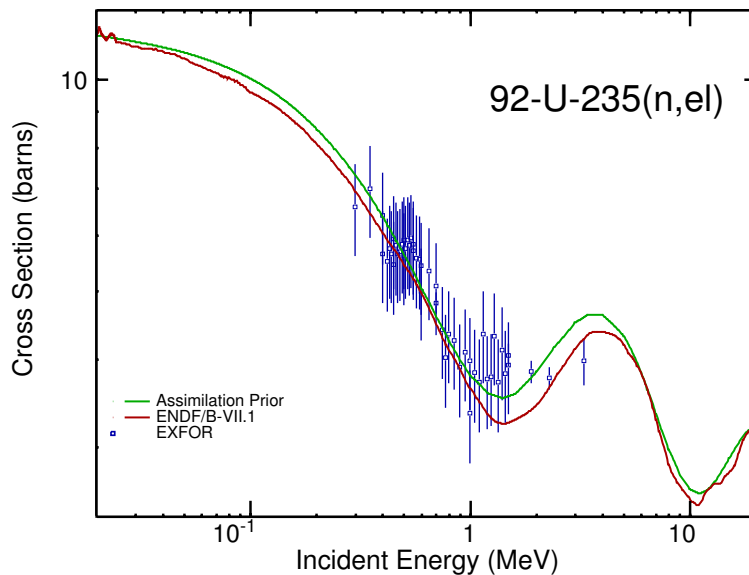
Figure 2.27: Elastic cross sections calculated by EMPIRE using input parameters obtained after fitting using KALMAN, which will be used as Assimilation prior calculation (green curve). Evaluation from ENDF/B-VII.1 library (red curve) and experimental data from EXFOR (blue points) are also plotted, for comparison purposes.

Figure 2.28: Fission cross section prior (green curve) as calculated by EMPIRE using parameters obtained from KALMAN fit. ENDF/B-VII.1 evaluation (red curve) and EXFOR experimental data (blue points) are shown for comparison.

Figure 2.29: Capture cross section prior (green curve) as calculated by EMPIRE using parameters obtained from KALMAN fit. ENDF/B-VII.1 evaluation (red curve) and EXFOR experimental data (blue points) are shown for comparison.

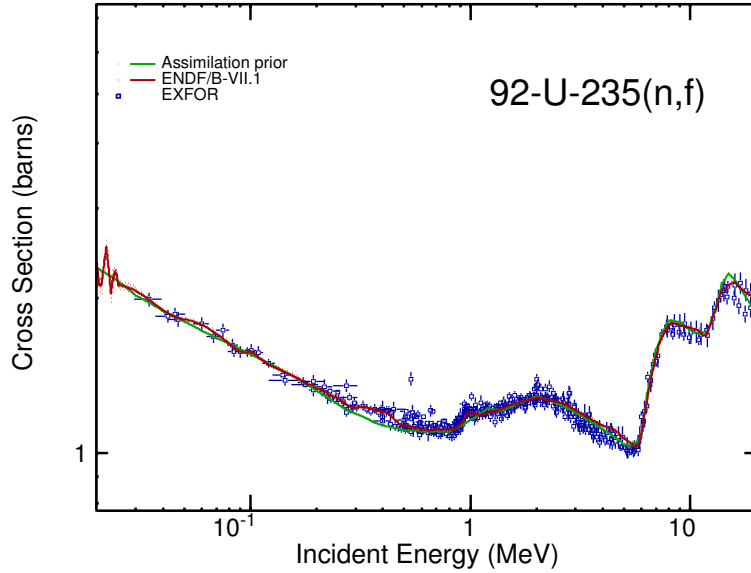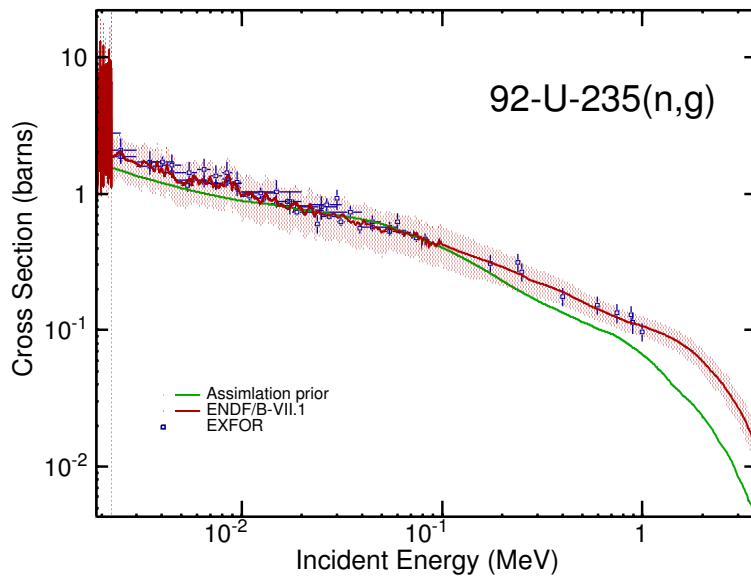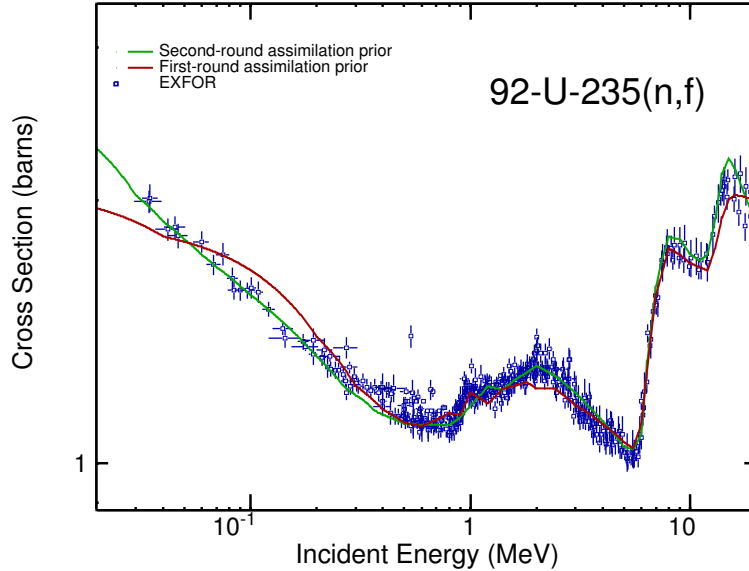Figure 2.30: Comparison between the fission cross sections used as prior calculations for the first and second round of assimilation of ^{235}U.

2.4.2.2 Sensitivities

In preparation for fitting the EMPIRE results to experimental data, the sensitivities of the cross sections to each varied EMPIRE parameter are calculated. These sensitivities were calculated using the NNDC cluster to vary each parameter up and down by an amount small enough to limit the effects of non-linearities. They were then used as input to KALMAN to adjust to parameters to fit the differential data. Figure 2.31 shows an example of such sensitivities in the case of fission reaction. Even though more than 80 parameters were used in this fit, only the 28 most important for fission fitting are displayed in Figure 2.31 in order to make it more easily-readable. Of these parameters, the uncertainty in the real optical model volume, UOMPVV, and the width of the giant dipole resonance, GGDR1, were especially sensitive at lower energies, while the level density scaling parameter ATILNO and height of the second fission barrier, FISVF2 are more important at higher energy.

2.4.2.3 Covariances

The energy correlation matrices are shown in Figures 2.32, 2.33, 2.34 and 2.35 for the total, elastic, fission and capture reactions, respectively. The correlation for total reaction (Figure 2.32) tends to full correlation due to the dominance of total cross section scaling parameter, while the elastic correlation matrix (Figure 2.33) exhibits the usual optical model pattern. The fission correlation (Figure 2.34) shows that the cross section follows
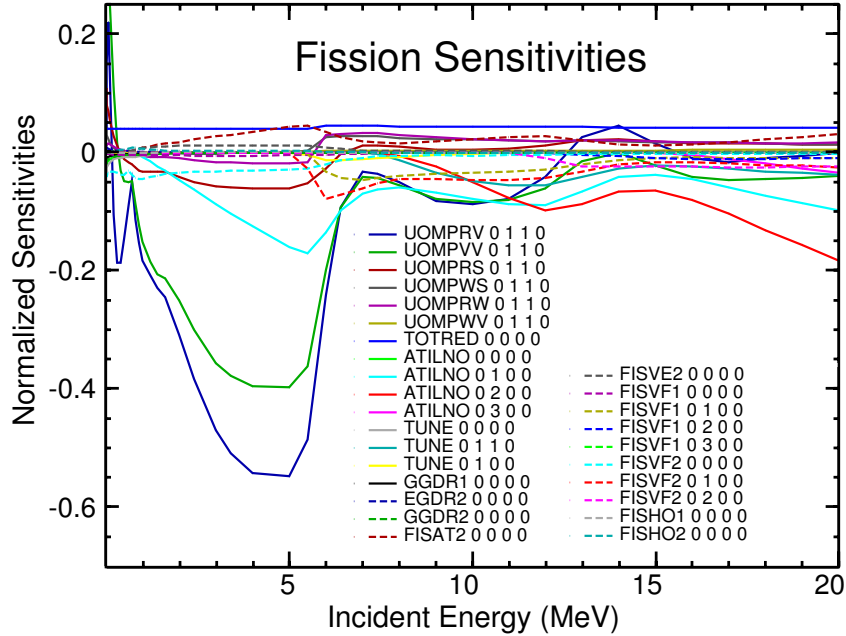
Figure 2.31: Sensitivities, for the fission reaction, of some of the most relevant parameters necessary to fit fission cross-section experimental data.

experimental data, and the correlation matrix for capture (Figure 2.35) displays the effect of pre-equilibrium.

Table 2.13 shows the prior correlation matrix for the 24 parameters, among the 81 parameters varied, which have a correlation of 10% of higher with any other parameter. Strong correlations above 50% are highlighted in red while correlations between 25% and 50% are highlighted in yellow, for easy visualization. It may be seen that in this case of ^{235}U there are three pairs of parameters with strong correlations. One of them is between the parameters indexed as 17 and 14, displaying the clear anti-correlation between the level-density parameter in the (n,2n) channel and the scaling of the equilibrium decay width for neutron emission for the target nucleus. The strongest correlation, of 85%, is observed between the level-density parameter for the target nucleus, indexed with the number 13, and the fission level density at the saddle point for the compound nucleus, with index 46. The other pair of parameters with strong correlation (62%) is formed by the parameter controlling the height of the second fission barrier for target nucleus (index 71) and the one controlling the height of the first fission barrier, again for target nucleus (index 67).

Figure 2.32: Correlation matrix for total cross section calculated using KALMAN.

Figure 2.33: Correlation matrix for elastic cross section calculated using KALMAN.

Figure 2.34: Correlation matrix for fission cross section calculated using KALMAN.

Figure 2.35: Correlation matrix for capture cross section calculated using KALMAN.

Table 2.13: Correlations among parameters (in units of %) in assimilation prior for ^{235}U. See text for discussion of the 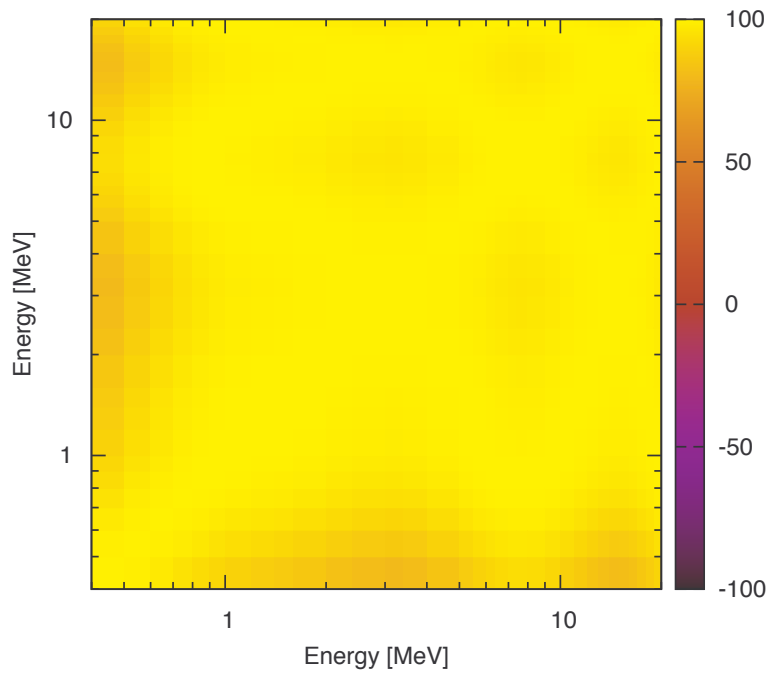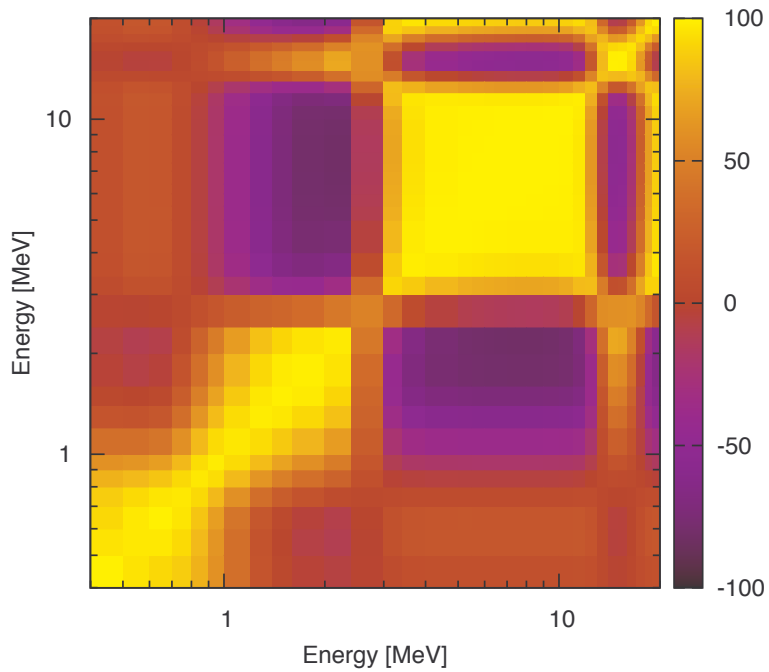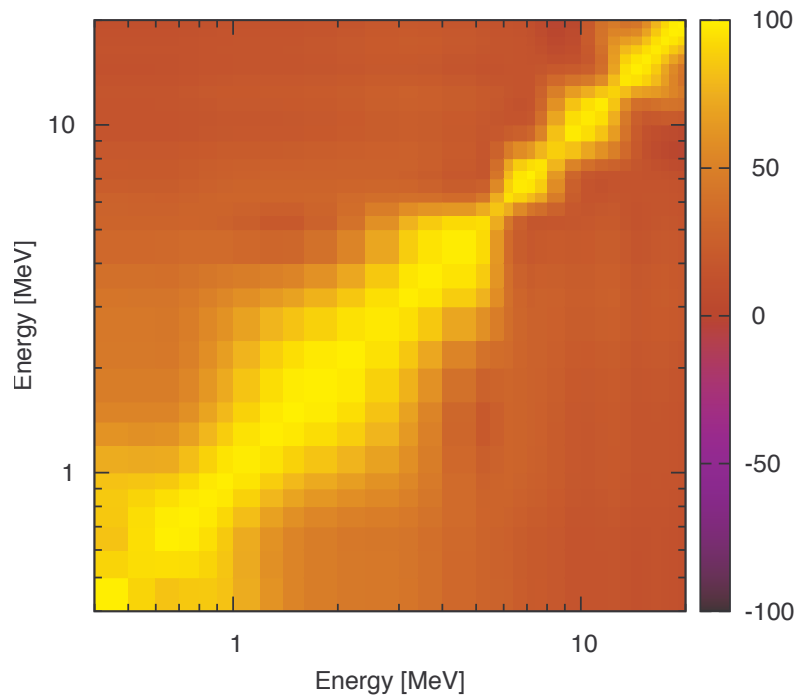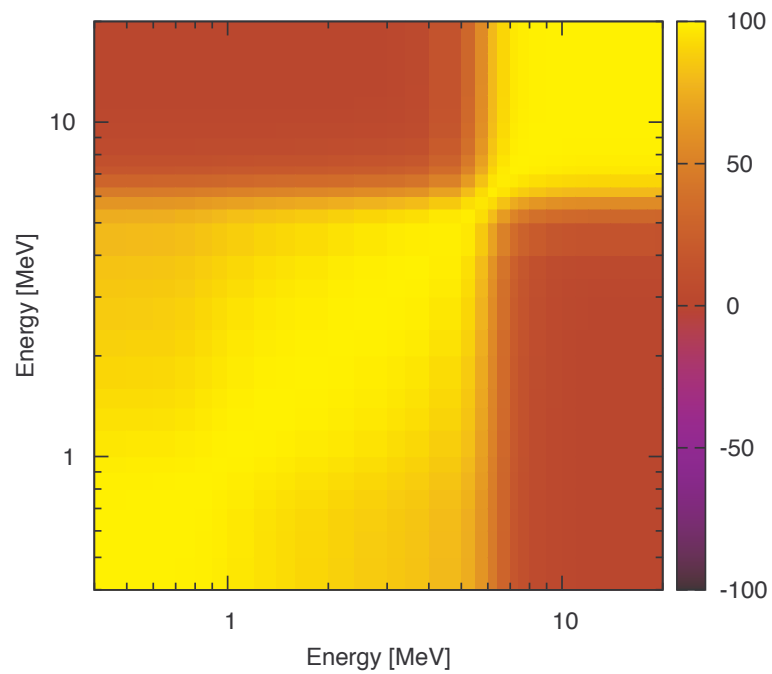values presented below. Columns and rows corresponding to parameters that have only off-diagonal correlations below 10% were omitted in order to fit the page. Correlations above 50% and 25% are highlighted in red and yellow, respectively.

Parameter	12	13	14	15	16	17	18	22	23	30	31	32	33	37	43	46	47	54	62	67	70	71	72	78
12 ATILNO-000[a]	100																							
13 ATILNO-010[a]	-2	100																						
14 ATILNO-020[a]	0	2	100																					
15 ATILNO-030[a]	0	0	-22	100																				
16 TUNE-000[b]	-13	-1	0	0	100																			
17 TUNE-011[b]	0	1	-62	15	0	100																		
18 TUNE-010[b]	0	-2	0	0	0	9	100																	
22 LDSHIF-010[c]	-2	-12	-2	0	-1	-1	-2	100																
23 LDSHIF-020[c]	0	0	-3	0	0	13	0	0	100															
30 EGDR1-000[d]	16	2	0	0	8	0	0	1	0	100														
31 GGDR1-000[e]	-8	-1	0	0	-4	0	0	0	0	5	100													
32 EGDR2-000[f]	30	4	1	0	16	0	0	3	0	-20	10	100												
33 GGDR2-000[g]	-14	-1	0	0	-7	7	0	-1	0	9	-4	17	100											
37 GGDR2-010[g]	0	-1	0	0	0	12	-11	-2	0	0	0	0	0	100										
43 FISAT1-010[h]	0	0	10	0	0	12	0	-22	0	2	-1	4	-2	0	100									
46 FISAT2-000[h]	-3	85	5	0	-2	3	0	-22	0	2	-1	4	-2	0	0	100								
47 FISAT2-010[h]	0	0	33	5	0	4	0	0	0	0	0	0	0	-1	0	0	100							
54 FISVE2-000[i]	-3	4	-2	0	-1	-1	0	-29	0	2	-1	4	-2	0	0	-12	0	100						
62 FISDL2-000[j]	-3	-2	-1	0	-2	-1	0	-32	0	2	-1	5	-2	0	0	-12	0	-12	100					
67 FISVF1-010[k]	-1	1	13	0	0	-25	-15	0	2	0	0	1	0	-11	3	0	1	-1	0	100				
70 FISVF2-000[k]	-27	11	3	0	-14	0	0	10	0	18	-9	33	-16	0	0	13	0	12	14	4	100			
71 FISVF2-010[k]	0	-9	-5	0	0	1	-19	-11	0	0	0	0	0	-13	0	1	0	0	0	-62	0	100		
72 FISVF2-020[k]	0	1	-48	4	0	14	0	0	-1	0	0	0	0	0	0	1	1	0	0	3	0	-1	100	
78 FISHO2-000[l]	-12	-18	0	0	-7	0	0	22	0	8	-4	14	-7	0	0	-9	0	-8	-9	-1	48	0	0	100

[a]Level density parameters
[b]Equilibrium decay width parameters
[c]Shifts of excitation energy
[d]Energy of first peak of Giant Dipole Resonance
[e]Width of first peak of Giant Dipole Resonance
[f]Energy of second peak of Giant Dipole Resonance
[g]Widths of second peak of Giant Dipole Resonance
[h]Fission level density at saddle point
[i]Vibrational enhancement of fission level density at saddle point
[j]Shift for fission level density at saddle point
[k]Heights of fission barriers
[l]Width of fission barriers

2.4.2.4 PFNS

The capabilities of calculating and fitting prompt fission neutron spectra (PFNS) were recently implemented in EMPIRE and KALMAN. It was thus possible to include the four new PFNS parameters of EMPIRE in the new (second) round of ^{235}U assimilation. Two models were used: the Los Alamos [23] and Kornilov [24] models. KALMAN was used to find an optimal set of values for the four PFNS parameters that best describes the ^{235}U thermal PFNS experimental data. The values obtained after fitting the two models are shown in Table 2.14

Table 2.14: Values obtained for PFNS parameters after fitting, using two different PFNS models implemented in EMPIRE, the Los Alamos and Kornilov models.

Parameter	Los Alamos model	Kornilov model
PFNTKE	1.0084E+0	1.1315E+0
PFNALP	9.3971E-1	8.9950E-1
PFNRAT	8.5436E-1	9.4934E-1
PFNERE	1.0157E+0	1.1129E+0

Figure 2.36 compares the thermal PFNS that resulted from the fits, which correspond to prior-assimilation calculations, to the original calculation (default input), for both Los Alamos and Kornilov models. PFNS evaluation from ENDF/B-VII.1 library and experimental data from EXFOR are also plotted, for comparison purposes.

We note that current PFNS calculations in the EMPIRE code are independent from the cross section calculations and, therefore, there are no correlations between respective parameters. Such correlations might be introduced by the integral data during the assimilation. When EMPIRE is extended to allow PFNS computation for multiple chance fission, the PFNS parameters will naturally be correlated with the reaction model parameters involved in the modeling of higher fission chances.

2.4.3 Conclusions

Two ^{235}U priors have been prepared with different versions of the EMPIRE code. The first was successfully assimilated by INL. The k_{eff} for GODIVA has been brought to 1.0 within the uncertainty and two of the four spectral indices were ameliorated while the remaining two indices suffered some degradation. These results were obtained in spite of the relatively poor prior, which was apparently inferior to the ENDF/B-VII.1 evaluation. The assimilation resulted in slightly increased a fission cross section below 6 MeV. This change was obtained with tiny modifications of a few model parameters. The only parameter that changed more significantly (1.4%) was the factor scaling absorption
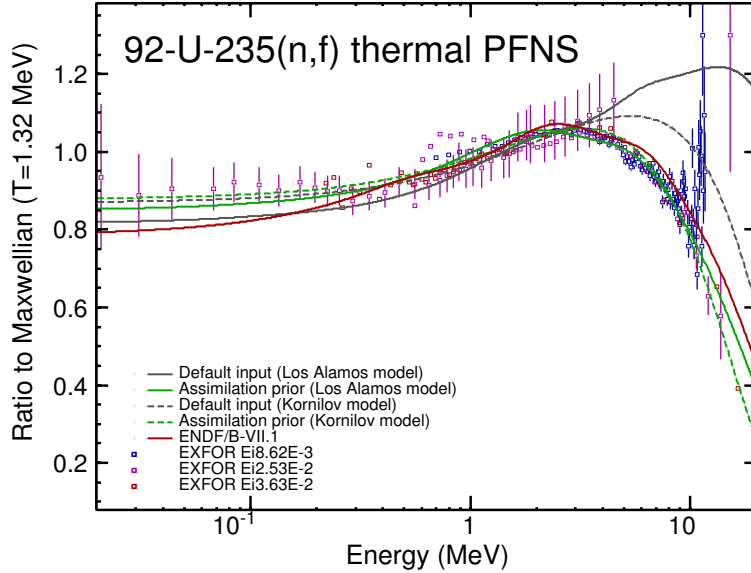
Figure 2.36: Prompt fission neutron spectra (PFNS) for thermal neutrons calculated by EMPIREusing a default input (grey curves) and input files containing PFNS parameters fitted with KALMAN (green curves), for both Los Alamos (solid lines) and Kornilov (dashed lines) PFNS models. Evaluation from ENDF/B-VII.1 library (red curve) and experimental data from EXFOR (blue points) are plotted for comparison.

cross section, which is consistent with the change of the fission cross section. Post-assimilation fission cross sections appear closer to the experiment between 0.6 and 3 MeV but overestimate measurements between 50 and 200 keV even more than the prior.

The new prior, obtained with the more recent version of the EMPIRE code is much closer to the ENDF/B-VII.1 evaluation and comes with the EMPIRE calculated PFNS and adjustable ν-bar. In view of the previous experience we expect that the assimilation of this latter evaluation should provide very good agreement with both differential and integral experiments.

2.4.4 Lesson learned

- A single integral experiment can be successfully assimilated even when starting with a poor prior. For example, a perfect $k_{eff}=1$ may be obtained by scaling the fission cross section regardless of how well it reproduces differential data. Adding more integral experiments with diverse characteristics should reduce such ambiguities.

2.5   Assimilation prior for ^{238}U

The major actinide ^{238}U was not initially included in the assimilation project since there are not clean integral experiments that are sensitive primarily to ^{238}U; however, it is a major component of many critical assemblies and neglecting it might distort the assimilation by forcing changes to other isotopes in order compensate potential deficiencies of ^{238}U. Therefore, we have decided to start working on ^{238}U so that it is available when actually needed. In addition, it was important to test whether our modeling is capable of describing all three major actinides. At the time this report was written BNL had completed calculations of the prior cross sections, parameter covariances, and sensitivity matrices for ^{238}U. The assimilation had not yet been performed but all the ingredients were in place.

2.5.1   EMPIRE calculations

When modeling ^{238}U one cannot disregard the fact that ^{238}U(n,f) is the standard at and above 2 MeV [25]. This poses a particularly tough requirement for the prior cross sections: as a matter of principle they should agree with the standard within its stated uncertainty.

The ^{238}U prior was prepared using a new, unpublished optical model potential developed by Capote, Soukhovitskii, Quesada, and Chiba (RIPL catalog no. 2412). This Lane consistent, dispersive potential is valid for neutrons incident on actinides in the energy range between 1 keV and 200 MeV. An essential innovative feature of this potential is the coupling of 15 collective levels (usually it is four or five). It has been recently shown by Dietrich *et al* [26] that such a high number of levels is needed to ensure convergence of Coupled-Channels (CC) calculations on statically deformed nuclei. The new potential assumes rigid rotor ground state and accounts for dynamical deformations of the excited states. These new features require use of the OPTMAN code, implemented in the latest version of EMPIRE instead of the standard ECIS code. A CC formalism is used not only for the incident channel and inelastic scattering to the collective levels but also for the computation of transmission coefficients for outgoing neutrons. The complexity of the potential and the fact that OPTMAN is slower than ECIS make for quite CPU-intensive calculations.

The CC calculations were supplemented with the DWBA computation of inelastic scattering to 14 levels. Tab. 2.15 lists the levels used in both calculations. These direct reaction components were followed by multi-step direct (MSD) and multi-step compound (MSC) calculations accounting for the pre-equilibrium emission of neutrons. Classical exciton model (PCROSS) was employed for the pre-equilibrium emission of protons and gammas, while Iwamoto-Harada formalism was used for α-particles.

The decay of the compound nucleus was treated in terms of HRTW model up to 1 MeV at which we changed over to the statistical Hauser-Fesbach formalism. The full γ-cascade was accounted for in both models. The pre-equilibrium γ-emission was also followed by

the compound nucleus γ-cascade down to the ground state. In these calculations E1 γ-strength function was computed using modified Lorentzian model (MLO1) with GDR parameters taken from RIPL-3. EMPIRE-specific level densities (EGSM) in "low-K" approximation were employed for statistical decay as well as in the fission channel.

The optical model for fission concept was used to account for the fission mechanisms associated to the different degrees of damping of the vibrational states within the minima of the fission path and allow for reproduction of the resonant structure of the fission cross section in the sub-threshold region due to the coupling among these vibrational states.

The default parameters were adjusted by Mihaela Sin and the fission input file was modified at BNL to reproduce experimental data in all reaction channels (and a particular emphasis on reproducing the 1.5 - 1.6 MeV region while improving the agreement to the Slovacek data [27]). When doing so ENDF/B-VII.1 cross sections were interpreted as the average of the experimental data. The adjustment concerned field strength for different multipolarity transfer in the multi-step direct, mean-free path in the exciton model, and parameters of the GDR in ^{238}U in addition to fine tuning of the fission barriers and level densities at saddles.

Overall, agreement with the ENDF/B-VII.1 evaluation is excellent as can be seen in Figs. 2.37 - 2.41. Above 2 MeV our fission agrees with ENDF/B-VII.1 standard cross sections within 2%, i.e., nearly within the standards' uncertainty (see Fig. 2.38). Some discrepancies are observed only for the (n,2n) reaction (Fig. 2.42), which is outside the energy range where assimilated integral experiments are sensitive. Although a number of fertile nuclei exhibit damped vibrational resonance structure [28], ^{238}U shows such behavior from 1.2 - 1.3 MeV (Fig. 2.37).

Table 2.15: Collective levels used in the CC and DWBA calculations of ^{238}U. The ground state deformations were $\beta_2 = 0.23$, $\beta_4 = 0.06$, and $\beta_6 = -0.0064$.

N	E (MeV)	J^π	Model
1	0.0000	0^+	CC
2	0.0449	2^+	CC
3	0.1484	4^+	CC
4	0.3072	6^+	CC
5	0.5181	8^+	CC
6	0.6801	1^-	CC
7	0.7319	3^-	CC
9	0.8266	5^-	CC
10	0.9272	0^+	CC
13	0.9661	2^+	CC
15	0.9972	0^+	CC
18	1.0373	2^+	CC
22	1.0603	2^+	CC
24	1.1057	3^+	CC
38	0.7759	10^+	DWBA
41	0.9305	1^-	DWBA
42	0.9501	2^-	DWBA
46	0.9976	3^-	DWBA
47	1.0280	4^-	DWBA
49	1.0564	4^+	DWBA
50	1.0577	3^+	DWBA
51	1.0597	3^+	DWBA
55	1.1288	2^-	DWBA
56	1.1307	4^+	DWBA
57	1.1357	1^+	DWBA
60	1.1630	4^+	DWBA
61	1.1680	4^+	DWBA
62	1.1689	3^-	DWBA

Figure 2.37: The prior fission cross section for ^{238}U, shown with ENDF/B-VII.1 and experimental data for comparison.
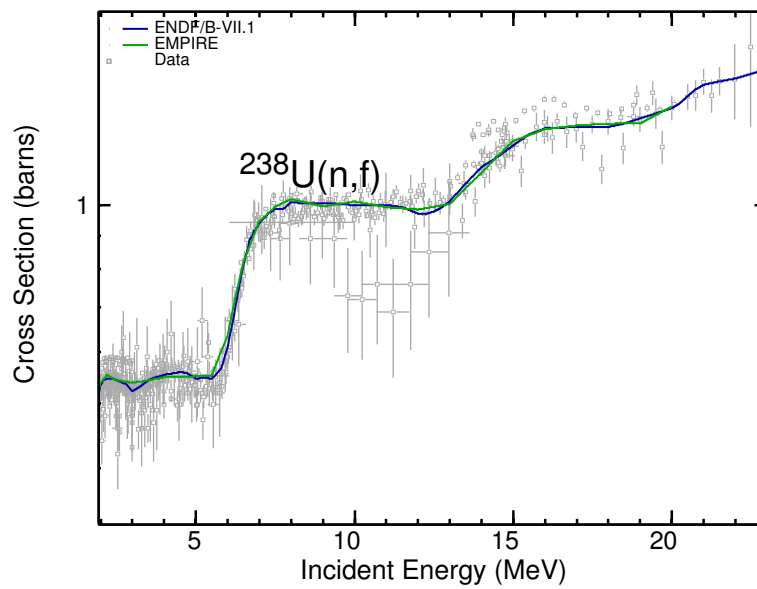
Figure 2.38: The prior fission cross section for ^{238}U, compared with ENDF/B-VII.1 between 2 and 20 MeV where ENDF/B-VII.1 is a standard.

Figure 2.39: The prior capture cross section for ^{238}U, shown with ENDF/B-VII.1 and experimental data for comparison.

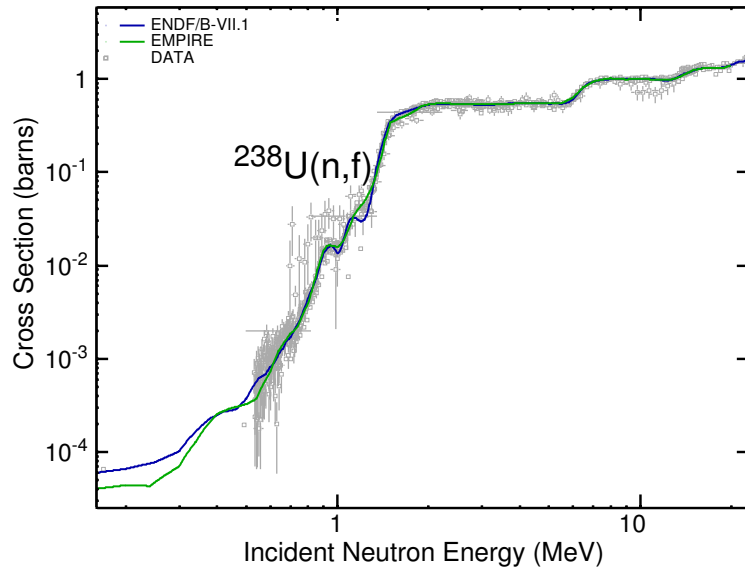
Figure 2.40: The prior total cross section for ^{238}U, shown with ENDF/B-VII.1 and experimental data for comparison.

Figure 2.41: The prior elastic cross section for ^{238}U, shown with ENDF/B-VII.1 and experimental data for comparison.

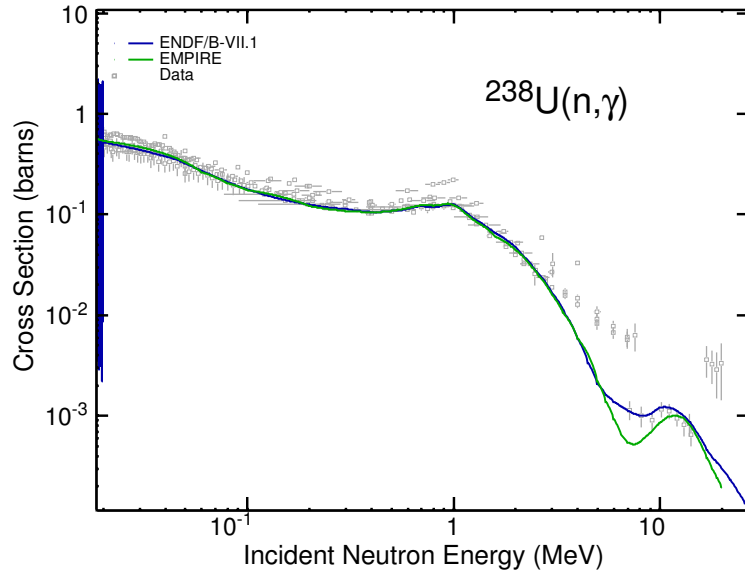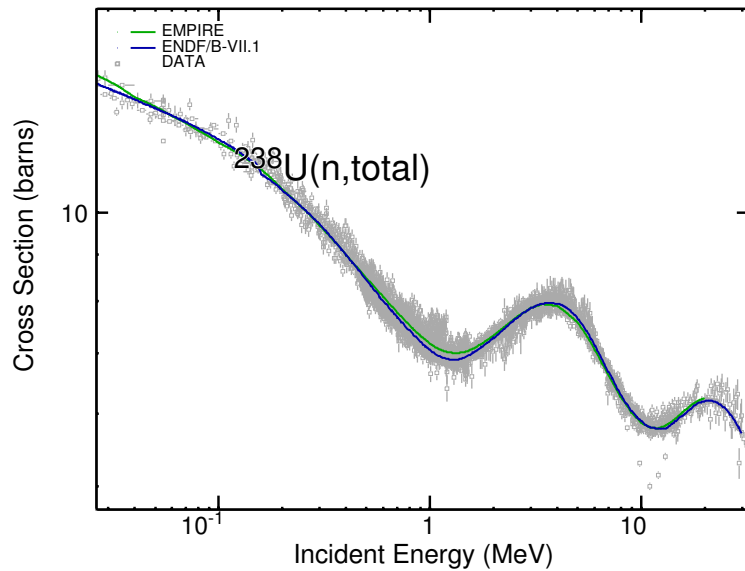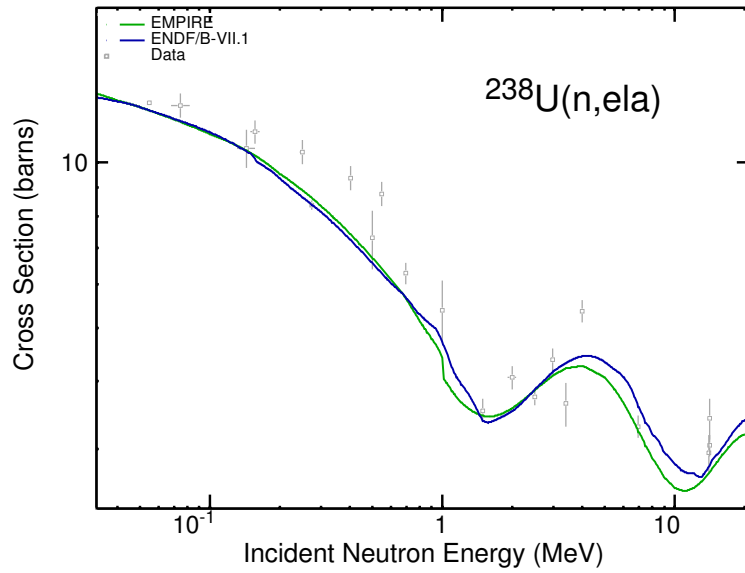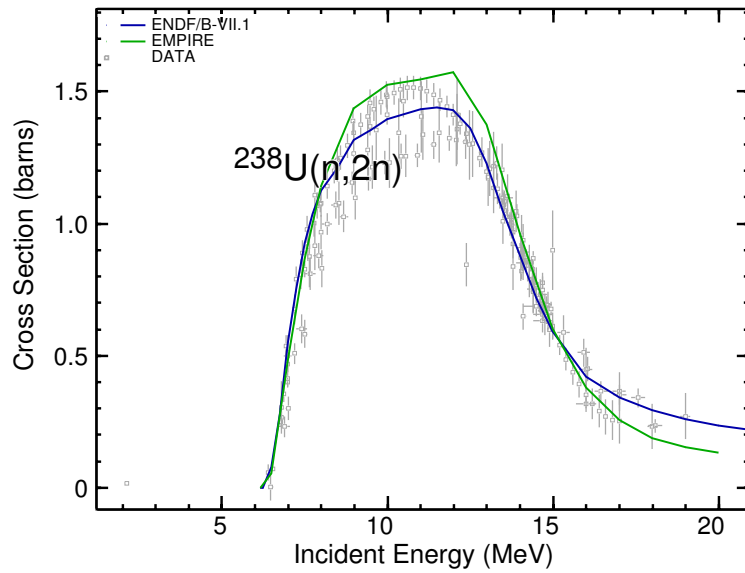Figure 2.42: The prior (n,2n) cross section for ^{238}U, shown with ENDF/B-VII.1 and experimental data for comparison.

2.5.2   Sensitivities

In Fig. 2.43 we present sensitivities of ^{238}U fission to the reaction model parameters, which, if perturbed by an amount considered reasonable for a given parameter, produce largest changes in the fission cross section. We stress that since perturbations are chosen 'reasonable for a given parameter' they differ from parameter to parameter. Therefore, the sensitivities plotted in Fig. 2.43 represent maximum change of the cross section that can be achieved by physically reasonable perturbation of the parameter rather than the derivative of the cross section with respect to the parameter.

We notice extremely negative sensitivity to the first fission barrier hump in ^{239}U for under barrier fission, i.e., for incident neutron energies below 2 MeV. As expected, major sensitivity is observed for fission barrier parameters and level densities corresponding to subsequent fission chances.
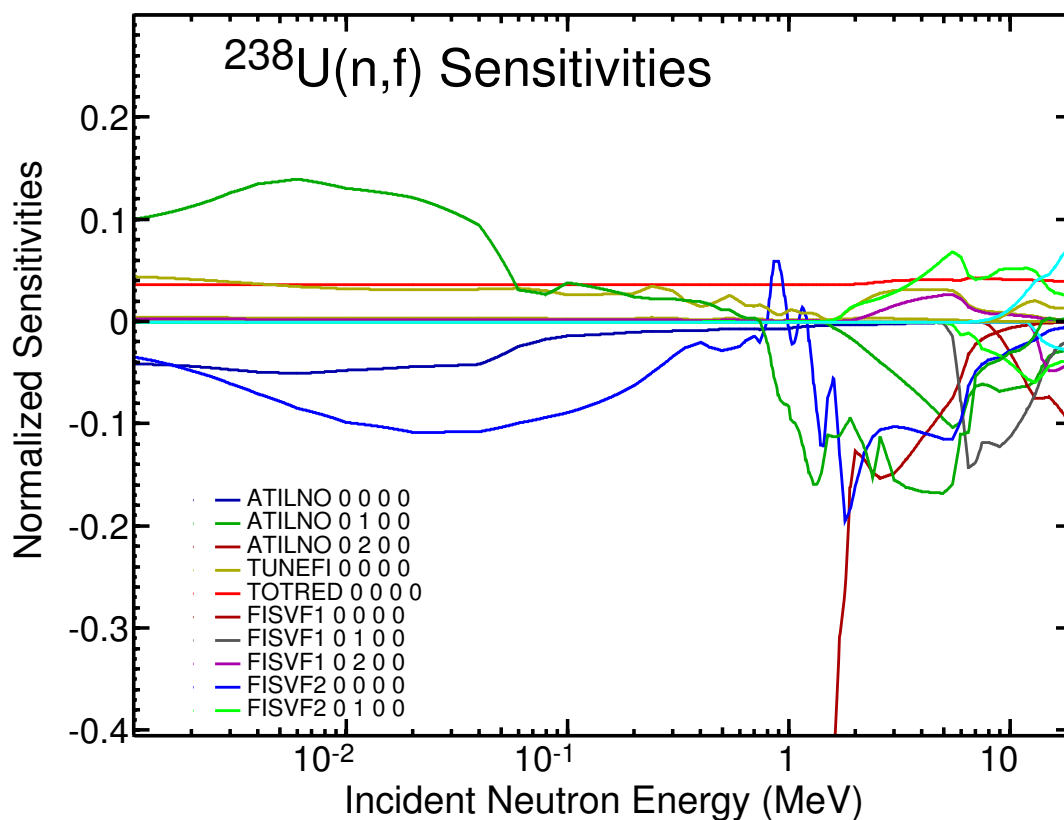
Figure 2.43: Sensitivities of the ^{238}U(n,f) to the most effective model parameters. See Eq. 1.1 for the convention used when calculating the sensitivities. Note that sensitivity to the height of the first fission barrier hump (FISVF1) in ^{239}U is so strong that below 2 MeV it exceeds plotted range of sensitivities and reaches -1.2.

63

2.5.3 PFNS

Prompt fission neutron spectra (PFNS) were calculated using both Kornilov and Los Alamos models implemented in the Rivoli version of the EMPIRE code. The default parameters were adjusted using KALMAN to the experimental data of Kornilov at incident neutron energy of 6.01 MeV. Table 2.16 and 2.17 show the parameter variations resulting from KALMAN fit for both models. Figure 2.44 shows the PFNS of ^{238}U normalized to the Maxwellian spectrum. For both models, the calculations match the data at the lowest energy points. Below 100 keV the Los Alamos model tends to produce lower values than the Kornilov model. Our calculations in this energy range are consistently above ENDF/B-VII.1. One notes that each of the major libraries suggest different shape of the spectra. In this comparison both our calculations are closer to ENDF/B-VII.1 than to JENDL-4.0 or JEFF-3.1.

Table 2.16: Variation of the default EMPIRE parameters of the Kornilov PFNS model in case of ^{238}U obtained after KALMAN adjustment to experimental data

Parameter	Factor
PFNALP	0.987
PFNRAT	0.971
PFNERE	0.998
PFNTKE	1.001

Table 2.17: Variation of the default EMPIRE parameters of the Los Alamos PFNS model in case of ^{238}U obtained after KALMAN adjustment to experimental data

Parameter	Factor
PFNALP	1.020
PFNRAT	0.984
PFNERE	1.001
PFNTKE	1.008

2.5.4 Conclusions

The ^{238}U prior with respective sensitivity matrices and covariance for the model parameters have been prepared for assimilation of integral experiments. The prior is entirely based on EMPIRE calculations without any manual modification of cross sections and

without any energy dependent tuning of model parameters. In spite of these strict conditions, EMPIRE calculations reproduce ENDF/B-VII.1 very closely, including the fission cross section above 2 MeV, which is the standard. The new prior includes PFNS for the first chance fission that were calculated internally by EMPIRE with parameters of the Kornilov and Los Alamos models adjusted to reproduce experimental data. Covariances provided for the PFNS are obtained in the independent fit and are not correlated with the remaining EMPIRE parameters.

2.5.5   Lesson learned

Work on ^{238}U proved essential prerequisite for the assimilation:

- Modern reaction modeling has reached a level of sophistication that allows for reproducing standard cross sections with a precision comparable to the standard uncertainties.
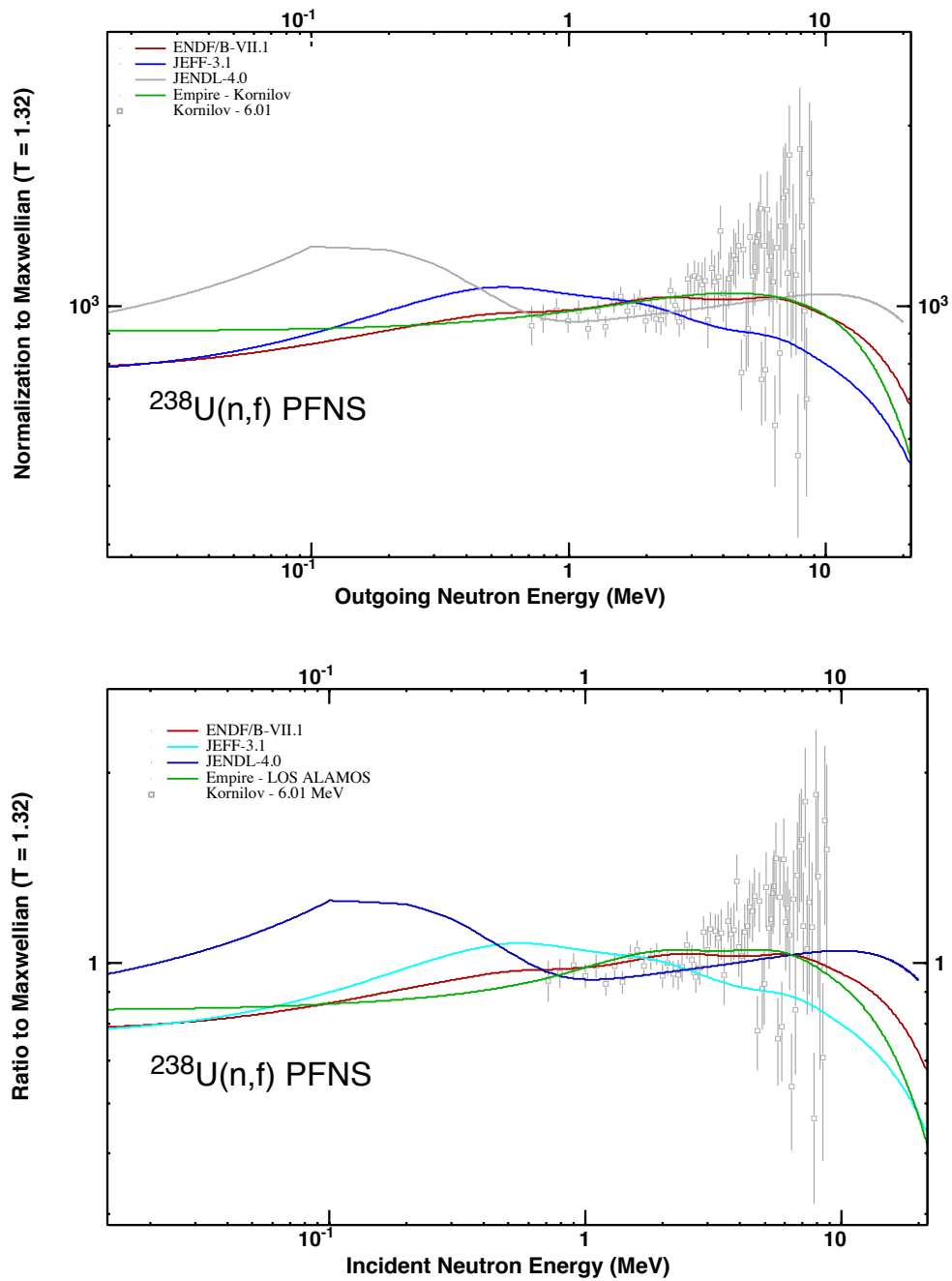
Figure 2.44: Ration of the prompt fission neutron spectra (PFNS) of ^{238}U to the Maxwellian at T=1.32 MeV. EMPIRE calculations using the Kornilov (upper panel) and Los Alamos (lower panel) models are compared with Kornilov data at 6.01 MeV and evaluated results from ENDF/B-VII.1, JENDL-4.0 and JEFF-3.1.

2.6 Assimilation of ^{239}Pu

^{239}Pu is a major actinide and is produced in a light water reactor through neutron capture on ^{238}U, followed by two successive β^- decays. Fast reactor sensitivity studies have shown the need for decreasing the uncertainties associated with ^{239}Pu fission cross section in the fast region. ^{239}Pu has been chosen for the present assimilation exercise due to its paramount importance and availability of a clean and relatively simple to model integral experiment (JEZEBEL).

Similarly to ^{235}U, two rounds of assimilation have been scheduled for ^{239}Pu. The first one was completed in 2011 and reported in the INL Report [7]. The second round has advanced to the point of producing an improved prior, model parameter covariances, and group-wise sensitivity matrices, but the actual assimilation has not yet been completed.

2.6.1 First round of assimilation

2.6.1.1 EMPIRE calculations

The subversion of EMPIRE-3 used in this calculations was ARCOLE, rev: 1978. The nuclear reaction models and major options used to prepare the prior are summarized below:

- Coupled Channels (ECIS code) used for direct inelastic scattering and absorption calculations

- Spherical optical model transmission coefficients used in compound nucleus decay

- Optical model parameters used

  - direct inelastic scattering RIPL-3 no. 2408
  - neutrons RIPL-3 no. 2408
  - protons RIPL-3 no. 5408

- Exciton model used for pre equilibrium emission of neutrons, protons and gammas

- Iwamoto-Harada model used for cluster emission

- HRTW width fluctuation correction was used for compound nucleus decay for incident neutrons energies below 3.00 MeV

- Hauser-Feshbach model with full γ-cascade used for compound nucleus decay

- Optical model for fission used for fission calculations

- Internal EMPIRE library used for fission barrier parameterization

- Discrete levels above fission barriers taken into account

- EMPIRE-specific EGSM level densities used in Hauser-Fashbach model and fission calculations

- E1 γ-strength function set to modified Lorentzian (RIPL-3 MLO1 option)

The default EMPIRE input was adjusted by modifying several parameters, especially level densities, fission barriers, and transitional states above fission barriers, to reproduce experimental data in all reaction channels. In doing so we used the ENDF/B-VII.0 evaluation as a guidance. Some energy dependent tuning of the parameters was invoked to bring calculations closer to the ENDF/B-VII.0 cross sections. In this initial attempt PFNS and $\bar{\nu}$ were taken over from the ENDF/B-VII.0 evaluation and were not subject to assimilation. Also the resonance parameters were imported from ENDF/B-VII.0. BNL provided the multigroup cross sections, covariance matrix for the model parameters and the sensitivities in terms of the multigroup cross sections to INL.

2.6.1.2 Results of assimilation

The assimilation was performed at INL using the JEZEBEL integral experiment. Detailed description of this work was reported in Ref. [7] and we only summarize its final results. The integral parameters considered were k_{eff}, and the fission spectral indices. The prior cross sections from EMPIRE calculations resulted in a k_{eff} of 0.9857 ± 8 pcm. The results from the assimilated cross sections resulted in $k_{\mathrm{eff}} = 0.99980 \pm 8$ pcm. For comparison, the ENDF/B-VII.0 yields k_{eff} of 0.99986 ± 9 pcm. Fig. 2.45 shows the assimilated fission cross section compared to the prior and ENDF/B-VII.0, which are equal to ENDF/B-VII.1. The assimilation increased fission of ^{239}Pu below 6 MeV bringing it closer to ENDF/B-VII.0 between 1 and 6 MeV and worsening the agreement below 1 MeV. The agreement with ENDF/B-VII.1 has slightly improved but overall ENDF/B-VII.1 is still in much better agreement with the differential data than our post-assimilation evaluation. This happens in spite of the fact that both files show perfectly equivalent performance with JEZEBEL k_{eff}.

The results of the assimilation for the full set of integral parameters are summarized in Tab. 2.18. A significant improvement was obtained on the discrepancies of k_{eff}, as mentioned above, and the fission spectral index of ^{239}Pu, while that of the fission spectral index of ^{238}U stays essential the same after adjustment. The remaining two fission spectral indices were already in good agreement and do not change significantly. The two improved integral parameters are directly related to the ^{239}Pu fission cross sections, and, therefore, one should expect such amelioration. For the ^{238}U spectral index it is likely that an improvement would be obtained when we take into account the dependence from the ^{238}U fission cross section.
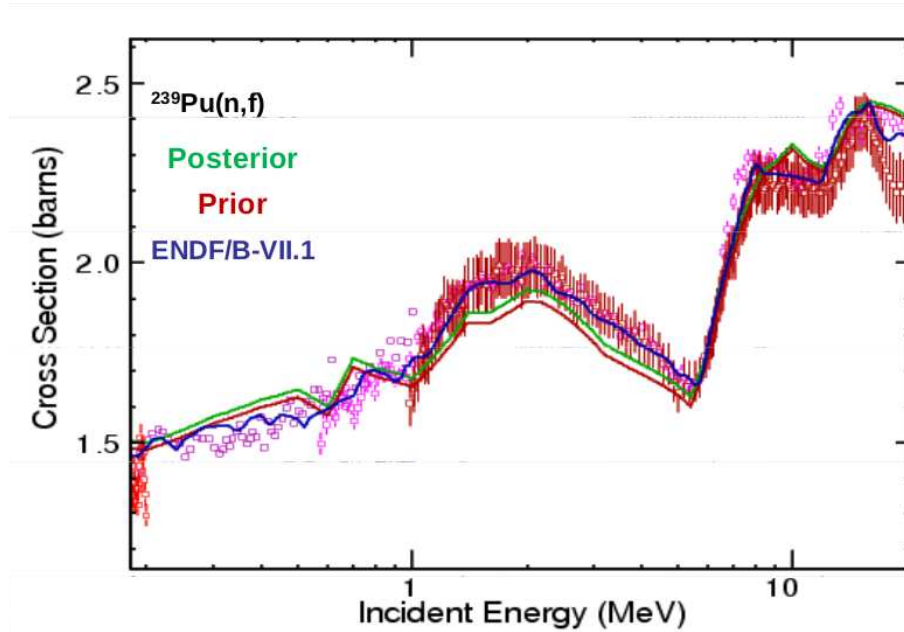
Figure 2.45: Comparison of the post-assimilation fission cross sections for ^{239}Pu compared with the respective prior, ENDF/B-VII.1 (equal to ENDF/B-VII.0) and selected experimental data.

Table 2.19 shows the parameter variations and standard deviations obtained by the data assimilation (using a prior obtained with an older version of EMPIRE). One can notice that only the VA000 parameter variation slightly exceeds the initial uncertainty, while the other variations stay within that range.

It is interesting to note that the new standard deviations of Tab. 2.19 obtained after the data assimilation produce a reduction of the evaluated uncertainty of the JEZEBEL k_{eff} of 18.7% mostly coming from the fission cross section contribution. This is already an indication of the potential gain, in terms of uncertainty reduction, that the data assimilation can produce. One should expect more reductions when other integral experiments are included in the data assimilation process.

Table 2.18: Calculation to experiment ratios (C/E) before and after adjustment to JEZEBEL experiments in the first round of the ^{239}Pu assimilation

Experiment	prior C/E $\pm \sigma$	post C/E $\pm \sigma$
k_{eff}	0.9857 $\pm$ 0.002	0..9998 $\pm$ 0.002
Fis.238U/Fis.235U	0.9561 $\pm$ 0.009	0.9598 $\pm$ 0.002
Fis.239Pu/Fis.235U	0.9708 $\pm$ 0.020	0.9917 $\pm$ 0.003
Fis.237Np/Fis.235U	0.9988 $\pm$ 0.017	1.0010 $\pm$ 0.001
Fis.233U/Fis.235U	1.0003 $\pm$ 0.017	1.0002 $\pm$ 0.001

Table 2.19: EMPIRE parameters varied during the assimilation of ^{239}Pu with Jezebel. Each parameter varied is listed along with the % variation from the assimilation and the initial and final % uncertainties. All parameter energies in units of MeV.

Parameter	Variation (%)	Prior Std. Dev. (%)	Posterior Std. Dev. (%)
VA000[a]	-0.141	0.134	0.121
FUSRED000[b]	0.432	0.951	0.612
LDSHIF010[c]	0.299	0.705	0.692
DELTAF000[d]	-0.120	0.671	0.668
ATILNO010[e]	-0.076	0.965	0.958
VB000[f]	-0.079	0.480	0.479
ATLATF000[g]	0.128	1.240	1.239
TOTRED000[h]	-0.0831	0.918	0.815
HA000[i]	-0.155	0.474	0.471

[a]Height of first fission barrier hump in ^{240}Pu.
[b]Factor multiplying reaction (fusion, absorption, compound nucleus formation) cross sections.
[c]Shift (LDSHIFT-1) of the level densities in target at the point of discrete levels.
[d]Pairing energy used in the level densities at the saddle point in ^{240}Pu.
[e]Factor multiplying asymptotic level density parameter in the target.
[f]Height of the second fission barrier hump in ^{240}Pu.
[g]Factor multiplying asymptotic level density parameter at the saddle point in ^{240}Pu.
[h]Factor multiplying total cross section.
[i]Width of the first fission barrier hump in ^{239}Pu.

2.6.2 Second round of assimilation

The second round of ^{239}Pu assimilation was undertaken to take advantage of the new version of the EMPIRE code (version 2893) , which allows for a much better description of the differential data without, or with minimal use of, the energy-dependent scaling of model parameters. In addition, the second round of assimilation will also take into account PFNS and $\bar{\nu}$. Extending the methodology by including these two new quantities along with a better prior should lead to more sound evaluation that is consistent with the differential and integral experiments. It should also shed light on the correlations between cross sections and PFNS and possible cancellation effects in the previous evaluations.

2.6.2.1 EMPIRE calculations

The EMPIRE modeling of ^{239}Pu employed coupled-channels calculations for the inelastic scattering to the first five levels in ^{239}Pu using the optical model potential by Capote *at al* (RIPL no. 2408 [22, 29].

Multistep preequilibrium emission of neutrons was calculated with the MSD model starting at 5.7 MeV, including contribution to discrete levels, and supplemented by the Heidelberg MSC calculations. Preeqilibrium emission of protons and γs was treated within the classical exciton model using the code PCROSS. Cluster emission was computed in terms of the Iwamoto-Harada model. Kalbach systematics was used for angular distributions of preequilibrium nucleons.

Decay of the compound nucleus for incident energies up to 2.00 MeV was calculated using HRTW model to account for the width fluctuation correction. At higher incident energies standard Hauser-Feshbach model including full γ-cascade was employed. For the E1 γ-ray strength function the RIPL-3 MLO1 option was adopted.

The fission channel was calculated within the simplified, full damping, approach although discrete transitional states above the fission barrier were taken into account. The level densities at the saddle points were provided by the low-K approximation EGSM model. The experimental fission barriers of RIPL-3 were taken as a starting point.

The default input was manually modified to improve agreement with experimental data. In particular, additional discrete transition states above fission barriers were added. Then, repeated iterations with KALMAN were performed to fine tune model parameters to the experimental data in all reaction channels and produce covariances for the model parameters.

Finally, EMPIRE calculations were completed with the ^{239}Pu resonance region taken from the ENDF/B-VII.1 file. The resolved resonance region extends from 0 up to 2.5 keV and is followed by the unresolved range that ends at 30 keV. Taking into account that integral experiment JEZEBEL is not sensitive to the resonance region, this range was not subject to adjustment during the assimilation.

2.6.2.2 Sensitivities

Fig. 2.46 shows nuclear reaction models parameters that are most effective in changing ^{239}Pu fission cross sections. In the low energy range below the threshold for the first chance fission the most important parameters are (in this order): (i) the height of the first hump in the fission barrier in the compound nucleus (CN) (FISVF100), (ii) the height of the second hump in the fission barrier in CN (FISVF2000), (iii) CN asymptotic level density parameter (ATILNO000), (iv) the width of the first hump in the fission barrier in CN (FISHO100). The global parameters TOTRED and FUSRED that scale total and fusion cross sections respectively have a constant impact in the whole energy range although a small kink is observed at the threshold for the second chance fission.
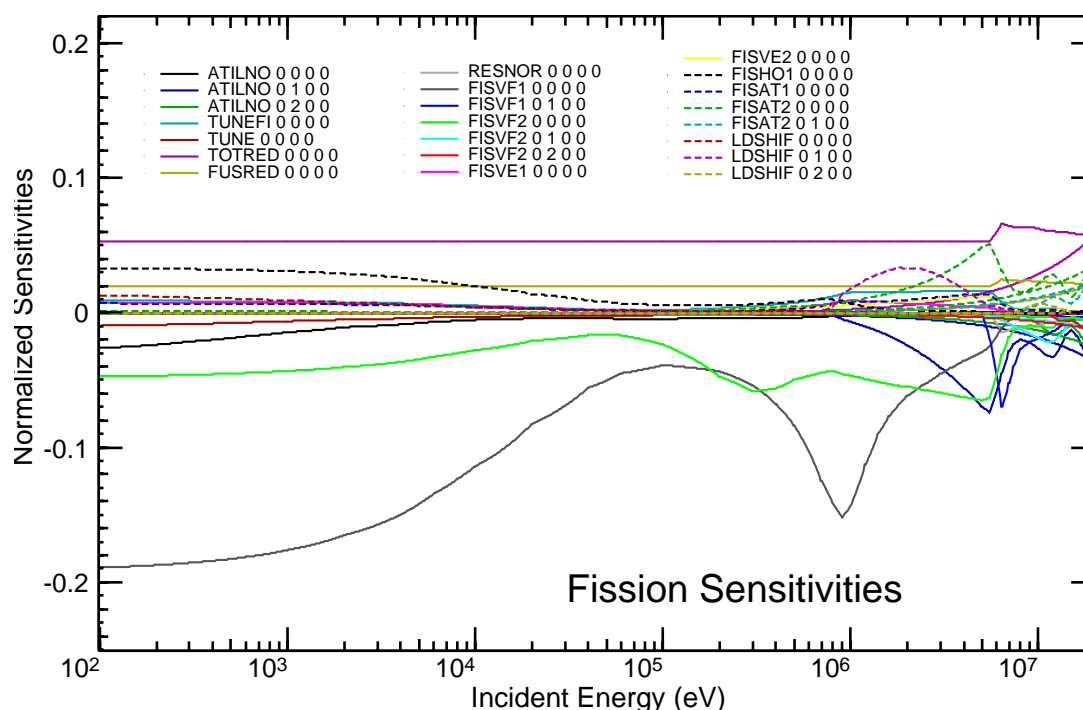
Figure 2.46: Sensitivities, for the fission reaction, of some of the most relevant parameters necessary to fit fission cross-section experimental data.

Once the first chance fission opens the situation becomes more complicated with more parameters affecting the cross sections. The most important added parameters are (i) the level density parameter in the target (ATILNO0100), level density shift in the target (LDSHIF0100), and level density parameter at the second hump of the CN fission barrier. (FISAT20000). Thus, while fission barrier parameters are determining the under-barrier fission, target level densities add to this list above the threshold for the first chance fission. It is worth noting, that another factor that strongly influences fission above the barrier are level densities above the second hump (not the first hump!) of the fission barrier in

the CN.

When the second chance fission opens many additional parameters enter the game and the picture becomes quite complicated but it is still possible to identify parameters that are most important; there are just many more of them.

2.6.3 PFNS

Prompt fission neutron spectra (PFNS) were fit to ^{239}Pu thermal data sets of Boytsov [30] and Starostov [31]. Fig. 2.47 shows EMPIRE calculations for ^{239}Pu PFNS using both the Los Alamos and Kornilov models. The Kornilov data was normalzied with a Maxwellian at temperature 1.32 MeV while the Los Alamos model was normalized at a temperature 1.42 MeV. For both plots the initial EMPIRE calculation is shown in green. KALMAN was then used to fit the default Kornilov parameters. The fitted adjustments for the Kornilov model are listed in Table 2.20 and for the Los Alamos model in Table 2.21. For the Kornilov model this fit (blue curve) resulted in better agreement with the data at lower energy. No signfcant improvement was achieved with the the Los Alamos model. At an incident energy of 2.5 MeV, the average PFNS total energy for the Los Alamos model is 2.163 MeV and for the Kornilov model is 2.154 MeV.

Table 2.20: Variation of the default EMPIRE parameters of the Kornilov PFNS model in case of ^{239}Pu obtained after KALMAN adjustment to experimental data.

Parameter	Factor
PFNALP	0.926
PFNRAT	0.999
PFNERE	0.990
PFNTKE	0.975

Table 2.21: Variation of the default EMPIRE parameters of the Los Alamos PFNS model in case of ^{239}Pu obtained after KALMAN adjustment to experimental data.

Parameter	Factor
PFNALP	1.000
PFNRAT	0.990
PFNERE	1.002
PFNTKE	0.999

Tables 2.20 and 2.21 show the parameter final KALMAN values for both models. One sees the strong sensitivity of the Kornilov model to the kinetic energy of the fragment due to neutron emission. In contrast, the Los Alamos model parameter values showed a markedly decreased variation. For both models, ENDF/B-VII.1 fails to reproduce the data at the lowest energy range (up to about 500 keV).
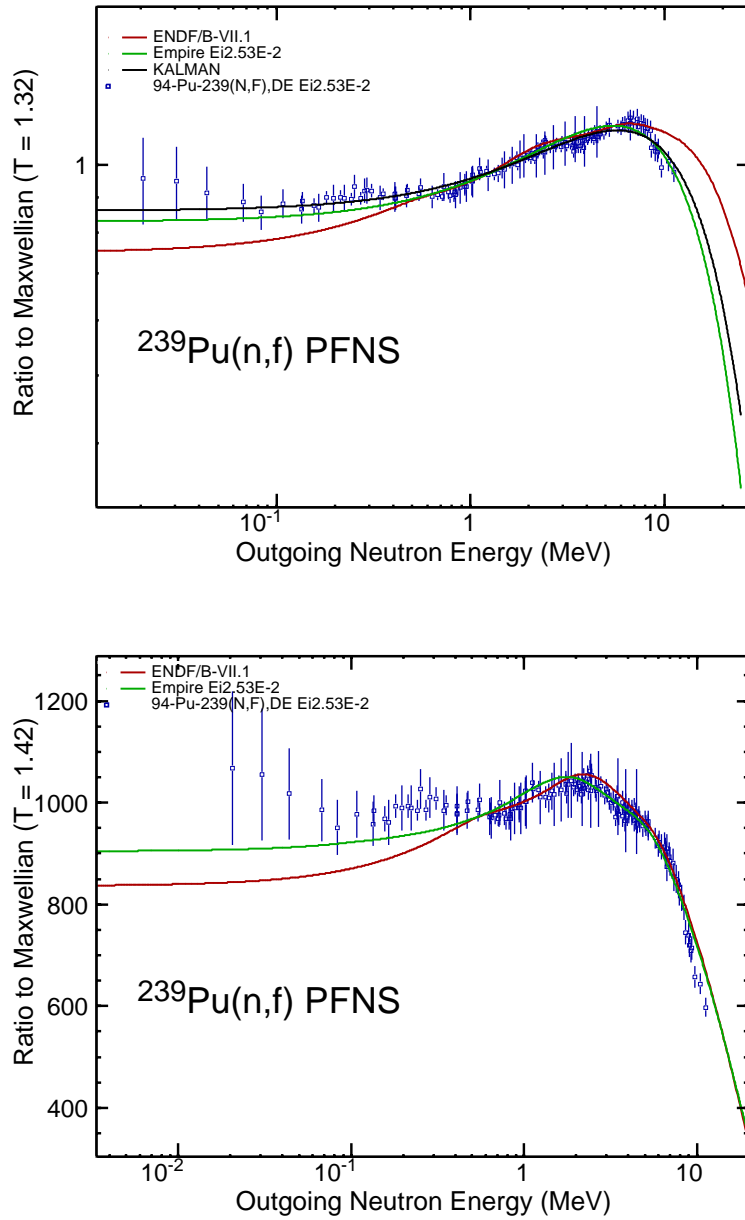
Figure 2.47: The Empire calculations for PFNS of ^{239}Pu using the Kornilov (top) and Los Alamos (bottom) models as fit to experimental data shown in blue. For comparison, the ENDF/B-VII.1 evaluation is shown in red.

2.6.4 Results of direct assimilation

The direct assimilation method described in section 1.4 was tested for ^{239}Pu. For this material the integral experiment modeled was JEZEBEL, a solid sphere of ^{239}Pu [32]. The simulation also required ACE cross section tables for trace amounts of ^{240,241}Pu and Gallium, which were not varied and taken from ENDF/B-VII.1. Using the ACE file for ^{239}Pu (using the central values from the KALMAN fit to differential data), generated a value of k_{eff} = 1.00516 ± 0.00008. After fitting k_{eff} with the KALMAN code and then running EMPIRE with the fitted parameters (to account for any non-linearities) we obtained a final value of $k_{\mathrm{eff}} = 0.99959 \pm 0.00008$. As this value was within the quoted uncertainty for k_{eff} another iteration of assimilation was not required. The changes to the EMPIRE parameters were minor, as shown in Table 2.6.4, and well within the uncertainty of the parameters when fitted to differential data, and the resulting differences in the differential cross sections calculated by EMPIRE are small compared to the uncertainties in the differential cross sections, as shown for fission in Fig. 2.48, where the changes in the EMPIRE calculations pre- and post-assimilation are shown with a small sample of available differential data. The change required for assimilation is very small in comparison to the uncertainties of the experimental data sets. Integral experiments serve as global constraints on the cross sections which can help guide the fitting of the EMPIRE parameters, and these constraints are sensitive to minor modifications to the differential cross sections which are far smaller than the uncertainties currently available for most differential data sets. The fitting of integral experiments is an important additional tool to help determine a consistent set of values for the differential cross sections.

Figs. 2.48 and 2.49 show the fission and capture cross sections of ^{239}Pu. Figs. 2.50, 2.51, 2.52 and 2.53 show the total, elastic, inelastic, and the n,2n calculations of ^{239}Pu thus illustrating the goodness of the capture and fission calculated cross sections. The capture and fission cross sections are compared to ENDF/B-VII.1.

Table 2.23 shows the posterior (post-assimilation) correlation matrix for the 29 parameters, out of the total of 53 parameters varied, which have a correlation of 10% or higher with any other parameter. Strong correlations above 50% are highlighted in red while correlations between 25% and 50% are highlighted in yellow, for easy visualization. It may be seen that there are seven pairs of parameters with strong correlations. Three of those pairs correspond to PFNS parameters (indices 50 through 53). PFNS parameters are very strongly correlated among themselves, but weakly with cross-section parameters. Excluding the PFNS correlations, the one with highest value (anticorrelation of 98%) is the one connecting the parameters indexed 9 and 10, which correspond to scaling parameters of the total and reaction cross sections. This is expected since implementation of these parameters in EMPIRE is such that changing total or reaction cross sections by a certain amount results in changing the other cross section by the same amount, thus preserving value of the elastic channel. There are three more correlation values highlighted in red in Table 2.23. One of them is between the parameters indexed as 12 and

Table 2.22: Results of direct assimilation of ^{239}Pu. EMPIRE parameters varied are listed with values before and after assimilation of integral experiment JEZABEL. Parameters which had the default value of 1.0 and were not varied during assimilation are not listed.

Parameter Name	pre-assimilation	post-assimilation
ATILNO-000	1.083	1.0851
ATILNO-001	0.907	0.9034
ATILNO-020	0.938	0.9380
ATILNO-030	0.988	0.9880
TUNEFI-010	0.833	0.8327
TUNE-000	2.228	2.2230
FUSRED-000	0.970	0.9700
RESNOR-000	1.320	1.3200
FISVF1-000	1.000	0.9995
FISVF1-010	1.000	1.0005
FISVF2-000	1.000	1.0042
FISVE1-000	1.000	0.9985
FISVE2-000	1.000	0.9995
FISHO1-000	1.000	0.9992
FISHO2-000	1.000	0.9992
FISAT1-000	0.917	0.9157
FISAT2-000	0.971	0.9717
FISAT2-010	0.981	0.9810
FISDL1-000	1.000	0.9999
FISDL2-000	1.000	0.9999
LDSHIF-000	1.100	1.0990
LDSHIF-010	1.063	1.0647
LDSHIF-020	0.917	0.9170
PFNALP-000	0.963	0.9613
PFNRAT-000	0.928	0.9279
PFNERE-000	0.999	1.0002
PFNTKE-000	0.984	0.9853

16, displaying the obvious anticorrelation between the parameters controlling the heights of the first and second, respectively, fission barrier of the compound nucleus. Another strong correlation is observed between the fission level density at the saddle point for the compound nucleus, with index 37, and the level-density parameter for the target nucleus, indexed with the number 2. Finally, the last pair of parameters with strong correlation (50%) is formed by the fission-barrier-height parameter for the compound nucleus (index

Table 2.23: Correlations among reaction model parameters (in %) resulting from the direct assimilation post for ^{239}Pu. See text for discussion of the values presented below. Columns and rows with all off-diagonal correlations below 10% were omitted in order to fit the page. Correlations above 50% and 25% are highlighted in red and yellow, respectively.

#	Parameter	1	2	3	5	6	7	9	10	11	12	13	14	16	17	18	20	23	24	26	34	37	38	46	47	48	50	51	52	53
1	ATILNO-000[a]	100																												
2	ATILNO-010[a]	4	100																											
3	ATILNO-020[a]	-2	0	100																										
5	TUNEFI-010[b]	0	1	4	100																									
6	TUNEFI-000[b]	-1	2	-1	0	100																								
7	TUNE-000[c]	-19	-2	1	0	-1	100																							
9	TOTRED-000[d]	0	0	0	0	0	0	100																						
10	FUSRED-000[d]	0	0	0	0	0	0	-98	100																					
11	RESNOR-000[e]	-5	15	-7	1	0	2	1	0	100																				
12	FISVF1-000[f]	-3	47	-12	2	8	-3	0	0	17	100																			
13	FISVF1-010[f]	-2	-13	22	-2	0	1	0	0	-47	-7	100																		
14	FISVF1-020[f]	2	6	-21	-1	0	-1	0	0	0	0	-5	100																	
16	FISVF2-000[f]	-13	-38	17	-3	12	4	0	0	-19	-67	6	3	100																
17	FISVF2-010[f]	-2	-5	-21	19	-1	0	0	0	-2	-16	-26	2	22	100															
18	FISVF2-020[f]	0	3	-24	-1	0	0	0	0	0	-2	1	-29	4	6	100														
20	FISVE1-000[g]	-1	-2	0	0	-1	-1	0	0	0	17	0	0	9	0	0	100													
23	FISVE2-000[g]	-2	7	-2	0	-1	-1	0	0	0	0	0	0	18	-2	0	-1	100												
24	FISVE2-010[g]	0	0	5	-2	-1	-1	0	0	0	2	-1	0	-3	12	0	0	2	100											
26	FISHO1-000[h]	4	3	1	0	2	1	-1	0	6	34	0	-2	3	3	0	1	-2	0	100										
34	FISAT1-000[i]	-1	10	-3	1	-1	-1	0	0	1	3	-3	1	20	-4	8	-1	-4	-3	-1	100									
37	FISAT2-000[i]	-2	67	21	-3	-2	0	0	0	-4	-2	10	7	20	20	17	0	1	-3	3	-3	100								
38	FISAT2-010[i]	2	-1	37	-3	0	-1	0	0	4	7	-12	12	-10	17	17	0	1	0	-1	2	-14	100							
46	LDSHIF-000[j]	21	-18	0	0	0	4	0	0	2	3	-1	-1	2	0	3	0	1	-1	-4	0	1	0	100						
47	LDSHIF-010[j]	-9	1	5	-1	-7	-1	1	0	-17	-13	-15	7	50	7	3	-10	-6	-1	11	-6	8	-2	-1	100					
48	LDSHIF-020[j]	0	1	1	-6	0	0	0	0	1	3	-5	-4	-3	30	-8	0	0	-3	0	0	-2	-1	0	0	100				
50	PFNALP-000[k]	0	-1	0	0	0	0	0	0	2	-1	1	-1	3	0	0	0	0	0	0	0	0	-1	0	-1	0	100			
51	PFNRAT-000[k]	0	0	0	0	0	0	0	0	0	0	0	0	0	0	0	0	0	0	0	0	0	0	0	0	0	65	100		
52	PFNERE-000[k]	-1	2	-1	0	0	1	1	0	-2	1	-1	1	-4	0	0	0	0	0	0	0	0	1	0	-1	0	-65	-1	100	
53	PFNTKE-000[k]	-1	1	0	0	0	0	0	0	-2	1	-1	1	-4	0	0	0	0	0	0	0	0	1	0	-1	0	-24	44	88	100

[a]Level density parameters
[b]Fission decay width parameters
[c]Equilibrium decay width parameter
[d]Scaling parameters
[e]Response function parameter
[f]Heights of fission barriers
[g]Vibrational enhancements of fission level density at saddle point
[h]Width of fission barriers
[i]Fission level densities at saddle point
[j]Shifts of excitation energy
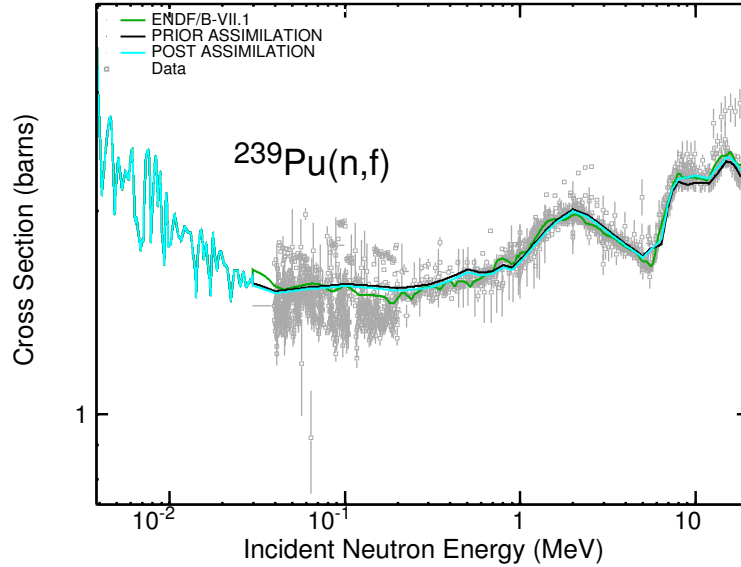[k]Prompt fission neutron spectra parameters

Figure 2.48: The pre-assimilation fit to differential fission data for ^{239}Pu data shown in solid black with the post-assimilation shown in cyan. Also shown are a sample of the experimental data fitted with EMPIRE (grey points) and the ENDF/B-VII.1 evaluation (green line). Note the small difference between the prior and post-assimilation curves compared to the uncertainties and scatter of the differential data. These small differences introduced by the assimilation are enough to bring calculated k_{eff} into agreement with the experiment.

16) the parameter that shifts the excitation energy in level densities in the target nucleus (index 47).

2.6.5   Conclusions

The first round of assimilation for ^{239}Pu has been successful, showing the potential of the method to improve integral performance of the file and reduce associated uncertainties on the calculated integral through reduction of uncertainties for the reaction model parameters. We note, however, that this improvement in the integral performance was obtained with a file which is visibly inferior to ENDF/B-VII.0 when compared to differential data. It illustrates a long standing issue of error compensation when "good agreement is obtained for bad reasons".
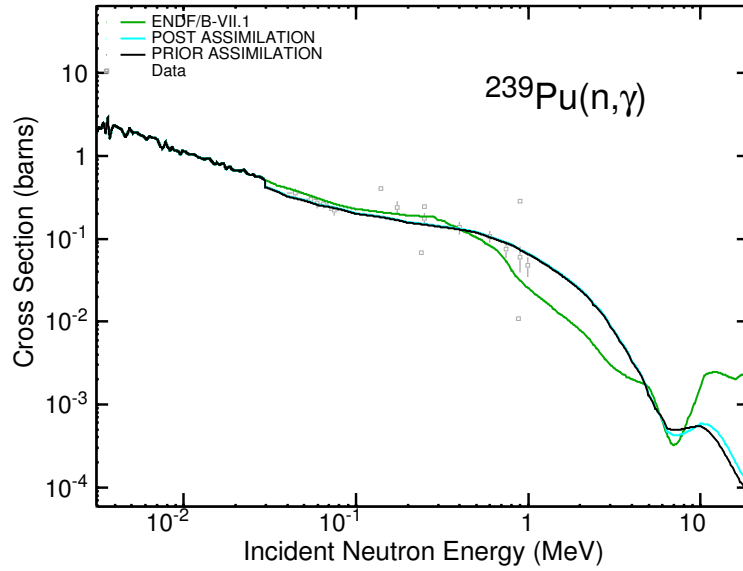
Figure 2.49: The capture of ^{239}Pu

2.6.6 Lesson learned

- Previously learned lessons are confirmed - perfect agreement with an integral parameter can be obtained without satisfactorily reproducing the differential data. There is no substitute for a good prior.

- Successful assimilations lead to the reduction of uncertainties in the reaction model parameters and consequently also in the calculated integral result.
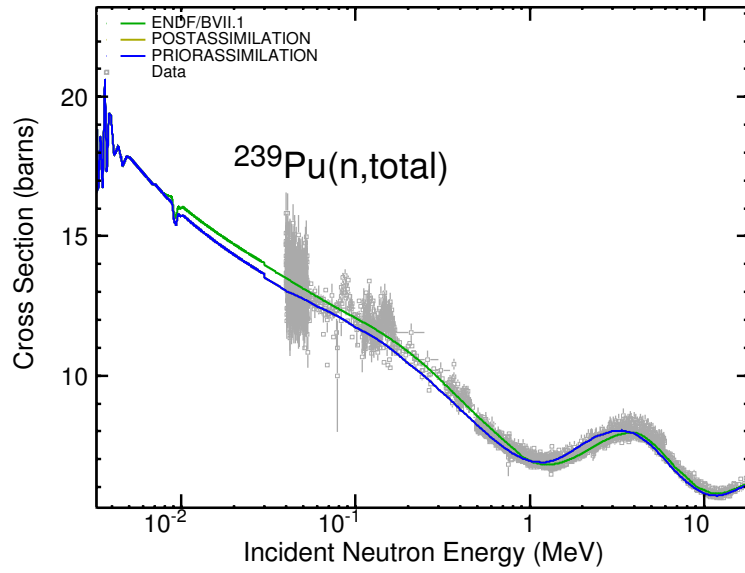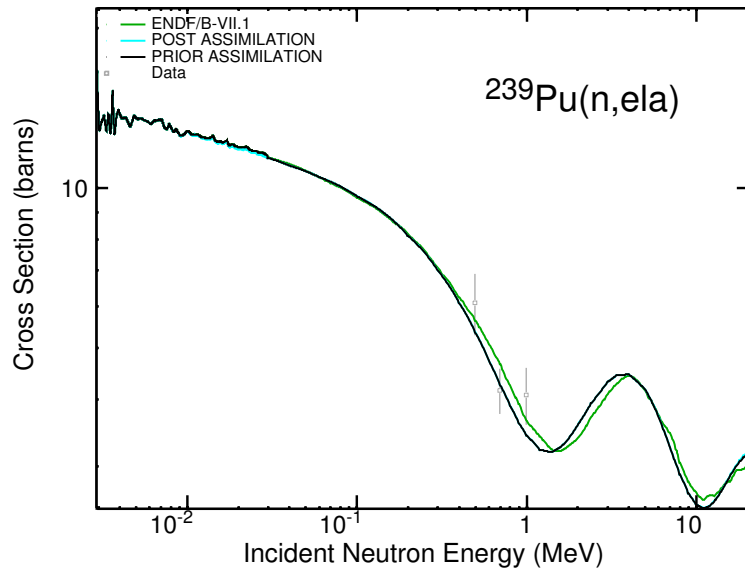
Figure 2.50: The total cross section of ^{239}Pu
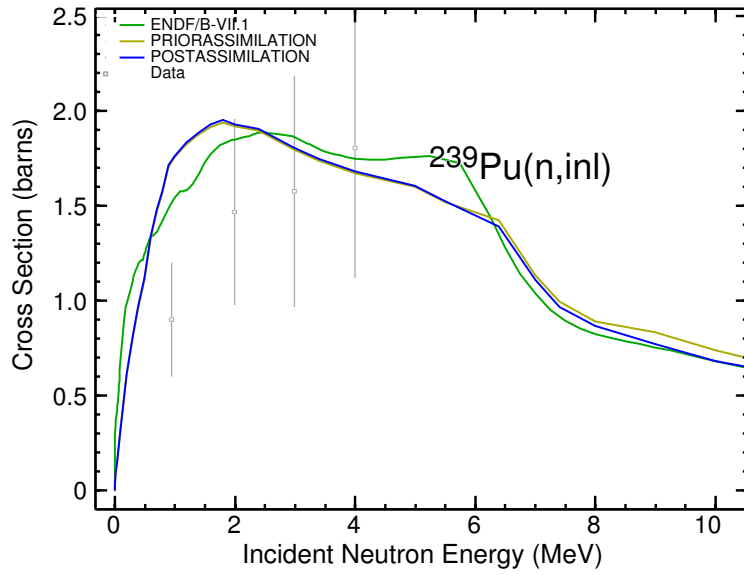

Figure 2.51: The elastic cross section of ^{239}Pu
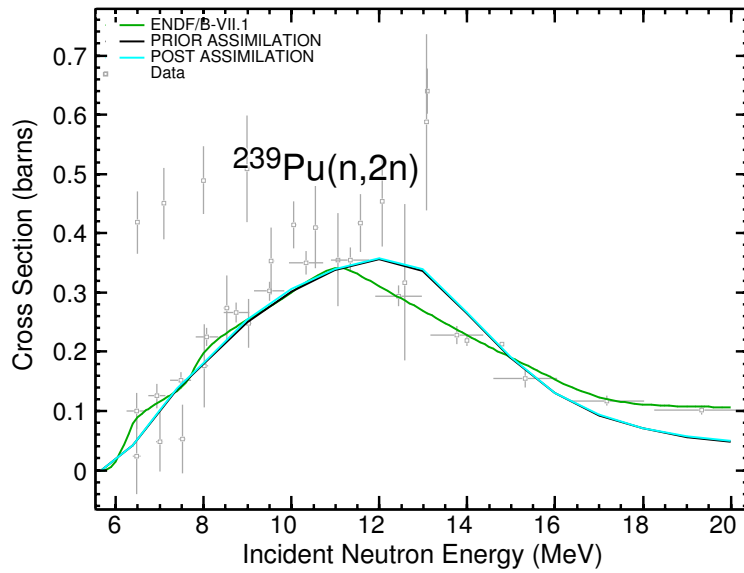
Figure 2.52: The inelastic cross section of ^{239}Pu

Figure 2.53: (^{239}Pu (n,2n)

2.7 Assimilation of ^{242}Pu

The ^{242}Pu was chosen for assimilation as an example of a minor actinide for which there are clean irradiation experiments, PROFIL-1, PROFIL-2 [33, 34], and COSMO. The irradiation experiments are relatively clean when compared to k_{eff} experiments, which imply transport calculations and often involve various materials. On the contrary, irradiation experiments essentially probe a single reaction on a given material and, in this sense, resemble measurements of Maxwellian averaged cross sections. The major source of uncertainty is the determination of the neutron energy spectrum.

2.7.1 EMPIRE calculations

The analysis of ^{242}Pu cross sections was performed using a new version of the reaction model code EMPIRE [15] with improved treatment of fission and modified level densities. A dispersive isospin-dependent coupled-channels potential by R. Capote *et al.* [22, 29] (RIPL-3, no. 2408) was used. This regional potential, tested on 30 actinides and valid in the energy range from 0.001 to 200 MeV, was also used in our analysis of ^{239}Pu. The ^{242}Pu was treated as a well-deformed rigid rotor and the first five levels of the ground state rotational band were coupled. Furthermore, DWBA calculations to 12 discrete levels (9 of them embedded in the continuum) were performed to account for the direct strength not included in the CC calculations. Tab. 2.24 list all the levels used in these calculations.

The vibrational multi-step contribution was taken into account above 0.5 MeV using the Tamura-Udagawa-Lenske model implemented in EMPIRE. This contribution was complemented with the Heidelberg MSC model to cover all mechanisms relevant to the pre-equilibrium emission of neutrons. The classical exciton model was used for the pre-equilibrium emission of protons and gammas. Thus, altogether two direct (CC and DWBA) and three pre-equilibrium models (MSD, MSC, and exciton) were employed to describe neutron interaction with ^{242}Pu before the statistical regime was attained. At incident energies below 3 MeV the statistical decay of compound nucleus was treated in terms of the HRTW model accounting for the width fluctuations, while Hauser-Feshbach model was utilized at incident energies above 3 MeV. Both formulations provided for modeling of the full gamma cascade. The EGSM formalism with the recently introduced low-K approximation was used for level density determination in all nuclei including fission saddle points. The Enhanced Generalized Lorentzian (EGLO) was employed for modeling the γ-ray strength function. Optical model for fission with partial damping was selected for the fission calculations and RIPL-3 empirical fission barriers were used for all nuclei along with Maslov transition states (RIPL-3).

Manual adjustment of the default parameters was carried out to improve reproduction of differential experimental data. When doing this no effort was spared to achieve the best possible agreement within available reaction models and with physically sound values of the parameters. No manual changes of the cross sections were permitted, and energy

Table 2.24: Collective levels in ^{242}Pu considered in the CC and DWBA calculations. The levels indicated as "DWBA-cont" are actually embedded in the continuum.

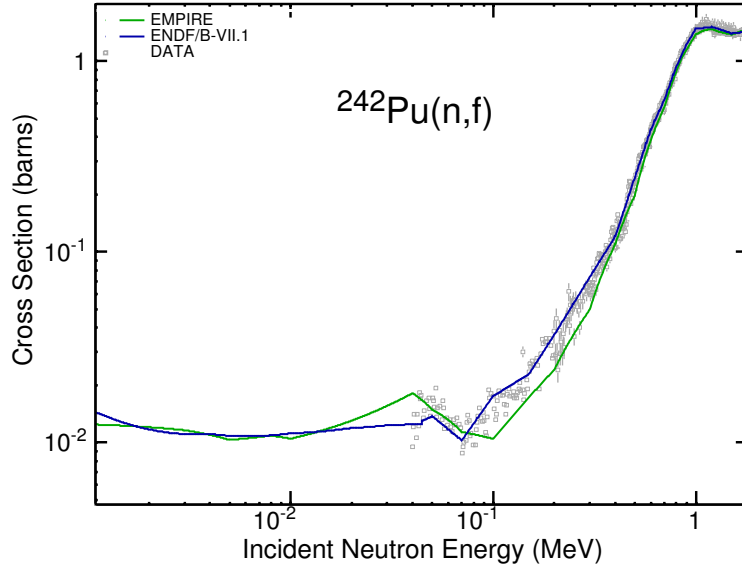| N	E [MeV]	J^π	Model
1	0.0000	0^+	CC
2	0.0445	2^+	CC
3	0.1473	4^+	CC
4	0.3064	6^+	CC
5	0.5181	8^+	CC
6	0.7786	10^+	DWBA
7	0.7804	1^-	DWBA
8	0.8323	3^-	DWBA
10	0.9270	5^-	DWBA-cont
11	0.9560	0^+	DWBA-cont
12	0.9925	2^+	DWBA-cont
13	1.0195	3^-	DWBA-cont
14	1.0392	2^+	DWBA-cont
15	1.0640	4^-	DWBA-cont
18	1.1020	2^+	DWBA-cont
20	1.1510	3^-	DWBA-cont
21	1.1545	3^-	DWBA-cont

Figure 2.54: The fission cross section of ^{242}Pu. The EMPIRE prior (green line) is compared with ENDF/B-VII.1 librar (red line) and selected experimental data.

dependent tuning of model parameters, which is allowed in EMPIRE, was limited to the absolute minimum. The adjustment resulted in all MSD response functions being scaled by a factor of 1.3, the γ-emission widths in ^{242}Pu and ^{243}Pu being multiplied by 2.5, and some modifications being applied to level density parameters to fit fission cross sections. In particular, 10% change was applied to the level density parameter above the first fission barrier in the compound nucleus. As an exceptional measure, the energy dependent tuning of the fission width was invoked between 1 and 3 MeV in order to improve description of the fission channel. This should not affect assimilation since the integral experiments involved are only sensitive to cross sections below 1 MeV [35], i.e., to the energy range which was calculated without any energy-dependent tuning.

The EMPIRE calculations were extended down to the upper end of the resonance region to maintain sensitivity of the cross sections to the variation of model parameters. Therefore, the unresolved resonance parameters, taken from ENDF/B-VII.1, were used for Doppler-broadening only.

The EMPIRE priors for fission and capture are compared to ENDF/B-VII.1 and experimental data in Figs. 2.54 and 2.55. Both evaluations agree above 1 MeV, while EMPIRE prior is slightly lower below this energy. Below 100 keV EMPIRE prior an ENDF/B-VII.1 agree well within ENDF/B-VII.1 uncertainties.
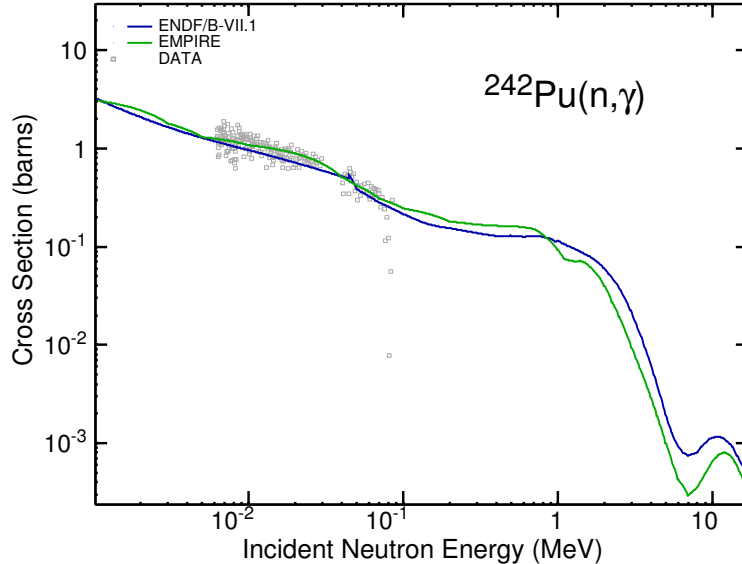
Figure 2.55: The capture cross section of ^{242}Pu.

2.7.2 Results of assimilation

The assimilation performed at INL made use of six experimental results for the associated integral parameters: the ^{243}Am build up in the irradiation experiments of PROFIL1, PROFIL2, TRAPU1, TRAPU2, and TRAPU3 and the fission spectral index of ^{242}Pu in COSMO. The first 5 experiments provide information on the capture cross section of ^{242}Pu, while the last one provides information on the fission cross section.

A total of 50 reaction model parameters were used in EMPIRE for characterizing the ^{242}Pu evaluation. BNL provided the covariance matrix for these parameters as well as the sensitivities of 33 energy-group cross sections to the parameter variations. The ERANOS code was used to calculate the multigroup sensitivity coefficients to the six integral experiments. Subsequently, this set of sensitivity coefficients was used together with the calculated C/E for performing a statistical adjustment. Table 2.25 shows the C/E before and after adjustment with related uncertainties.

In general C/E's are better for the PROFIL experiments while for the TRAPU experiments only TRAPU3 show a definite amelioration. The COSMO C/E shows a spectacular improvement; however, the uncertainty after adjustment stays about the same, which is an indication of the presence of some problem.

Table 2.26 shows the obtained parameter variations and the related standard deviations before and after the data assimilation for the parameters that mostly affect the assimilation. One can notice that only the FISVF100 parameter variation indicated by the data assimilation exceeds the 1σ initial uncertainty, while the other variations stay

Table 2.25: Ratio of Calculation to Experiment (C/E) before and after adjustment for JEZEBEL experiments.

Experiment	before C/E ± uncert.	after C/E ± uncert.
^{243}Am buildup PROFIL1	1.107 ± 0.035	1.047 ± 0.018
^{243}Am buildup PROFIL2	1.116 ± 0.046	1.057 ± 0.017
^{243}Am buildup TRAPU1	1.020 ± 0.045	0.962 ± 0.018
^{243}Am buildup TRAPU2	0.998 ± 0.048	0.942 ± 0.018
^{243}Am buildup TRAPU3	1.047 ± 0.036	0.987 ± 0.018
^{242}Pu(n,f)/^{235}U(n,f) COSMO	0.890 ± 0.023	0.988 ± 0.022

within that range. In Tab. 2.27 we report the contribution of the parameter variations of Tab. 2.26 to the relative change of the C/E's of the PROFIL1, TRAPU2, and COSMO. The χ^2 test after adjustment provided a normalized (to the number of degrees of freedom) value of 1.40; however, most of the contributions to this value are coming from the two PROFIL experiments and the COSMO one as shown in Tab. 2.28. This is mainly due to the fact that two PROFIL experiments and the three TRAPU ones have very similar sensitivities but their C/Es are contradictory (large discrepancies for PROFIL and acceptable ones for TRAPU). For COSMO the large contribution is due to the fact that in order to achieve a reasonable C/E the variation on the FISVF10000 (by large the main contributor) has to exceed in a significant amount the 1σ uncertainty. An attempt was done using only the two PROFIL and the COSMO experiments. The χ^2 stay essentially the same with the major contribution now coming from the COSMO experiment (0.999), but for the PROFIL experiments the new C/E after adjustment are very close to (1.01).

Table 2.26: Parameter variations and standard deviations obtained by data assimilation.

Parameter	Variation (%)	Prior stand. dev. (%)	Posterior stand. dev. (%)
TUNE000[a]	4.841	12.875	8.077
FUSRED000[b]	0.432	2.500	2.310
FISVF100[c]	-1.601	1.000	0.430
TOTRED000[d]	-0.898	1.000	0.849
LDSHIF000[e]	-0.883	3.067	2.951
FISVF2000[f]	-0.869	1.000	0.878
FISVE2000[g]	2.208	5.537	5.407
ATILNO010[h]	0.513	1.755	1.732

[a]Scaling of the gammas - compound.
[b]Scaling of the fusion cross section
[c]Height of the 1st barrier - compound.
[d]Scaling of the total cross section.
[e]Level density shift - compound.
[f]Height of the 2nd barrier - compound.
[g]Level Vibrational enhancement (saddle) of 2nd barrier - compound.
[h]Scaling of the level density (parameter 'a') - target.

Table 2.27: Contribution of the parameter variation to the relative change of the C/E of selected experiments.

Parameter	% ^{243}Am buildup PROFIL1	% ^{243}Am buildup TRAPU2	% ^{242}Pu(n,f)/^{235}U(n,f) COSMO
TUNE000[a]	-2.53	-2.55	0.20
FUSRED000[b]	-1.33	-1.42	-1.62
FISVF1000[c]	-1.15	-1.28	12.15
TOTRED000[d]	-0.79	-0.76	-0.95
LDSHIF000[e]	0.48	0.48	-0.03
FISVF2000[f]	-	-	1.02
FISVE2000[g]	-	-	0.23
ATILNO010[h]	-	-	-0.18
TOTAL	-5.38	-5.64	10.99

---

[a]Scaling of the gammas - compound.
[b]Scaling of the fusion cross section.
[c]Height of the 1st barrier - compound.
[d]Scaling of the total cross section.
[e]Level density shift - compound.
[f]Height of the 2nd barrier - compound.
[g]Level Vibrational enhancement (saddle) of 2nd barrier - compound.
[h]Scaling of the level density (parameter 'a') - target.

Table 2.28: Contribution by experiment to χ^2.

Experiment		Contribution to χ^2
^{243}Am buildup	PROFIL1	0.573
^{243}Am buildup	PROFIL2	0.419
^{243}Am buildup	TRAPU1	-0.060
^{243}Am buildup	TRAPU2	0.008
^{243}Am buildup	TRAPU3	-0.069
^{242}Pu(n,f)/^{235}U(n,f)	COSMO	0.529
Total		1.402

2.7.3 Conclusions

The assimilation of ^{242}Pu was finally successful but required the increase of prior uncertainties. The C/E ratios for four out of six experiments were improved (COSMO showed a remarkable 10% improvement), while the remaining two got somewhat worse. The post-assimilation uncertainties for C/E were reduced to one-half or less with the exception of COSMO for which the uncertainty has remained practically unchanged in spite of the spectacular improvement of the C/E ratio. These might be due to the contradictory trends for two PROFILE and three TRAPU experiments.

2.7.4 Lesson learned

- An assimilation may be held back by possible inconsistencies among integral experiments.

Section 3

Conclusions

The assimilation of integral and differential experimental data to produce a unified set of reaction cross sections that describe all experimental data is a lofty goal. Once achieved, the evaluated cross sections should be in good agreement with the experimental differential data while at the same time be able reproduce results of integral experiments, without requiring adjustments tailored to each application. This work describes the first attempt by the BNL-INL collaboration towards this goal. The methodology is built upon the reaction modeling code EMPIRE, long in use at BNL, and the wide array of integral experiments and modeling available at INL and arranged around the ERANOS code. The interface of these two packages is a set of cross sections for the most important reactions studied in an energy-grouped structure. BNL would perform an evaluation for a given material, calculate the group-wise cross sections for each reaction, the sensitivity of each cross section to the varied EMPIRE parameters, and the covariance matrix of the parameters when fitting the cross sections to differential experimental data sets. These results from the EMPIRE fits would then be used to determine the sensitivity of the integral experimental results to the reaction parameters, through a 'folding' process using the sensitivity of the integral experiments to the group-wise cross sections. The covariance matrix of EMPIRE parameters would be translated to a covariance of group-wise reaction cross sections used as inputs to the integral modeling. The use of the covariances is easy to overlook, but it is important - the covariances from fits to differential data 'tell' the integral fitting how to modify the parameters in such a way as to minimize the effect on the differential cross sections. If the differential and integral data sets are consistent, then a successful assimilation should reproduce both types of data from the same set of basic reaction cross sections.

We have used this procedure on a group of materials that served as a test of the feasibility of this method. The first were a couple of important structural materials, ^{23}Na and ^{56}Fe. While the method produced reasonable results, it became clear that the linear extrapolation inherent in this method can lead to unphysical results when non-linear terms are too large. This was the case in ^{23}Na, where an apparently good fit to the integral models were not reproduced when the resulting set of parameters were re-

calculated with EMPIRE. It became clear that this would become an iterative method, where small steps should be taken towards a global fit, with each step iterated through EMPIRE with re-calculation of the sensitivities and covariances. Also, both materials exhibit large fluctuations to rather high energy, which cannot be modeled with theory. For this reason, the resonance description should be extended as high as possible along with a practical way of reproducing the fluctuations at higher energy. Also, a new CC and dispersive potential is available for ^{56}Fe that deserves further study.

The assimilation of ^{105}Pd, a fission product with rather clean integral measurements, was also undertaken. Here, in spite of a rather simple fit with sensitivities mostly in capture, a good fit to the differential data was not possible without ad hoc modifications to the uncertainties of a few EMPIRE parameters. As the cross sections do not fluctuate at higher energy, as in ^{23}Na, the problem likely lies with an inconsistency between the differential and integral methods. This itself is valuable information which perhaps indicates a need for a re-evaluation of either or both differential and integral data.

The actinide ^{235}U was studied. The first prior cross sections were prepared with an older version of EMPIRE, but in spite of the rather poor fits to the differential cross sections, a good fit to k_{eff} was obtained for the integral experiment by rather minor scaling of the fission cross section. What became clear with this material was the need for a good prior calculation that fits the differential data well. This was achieved with an updated EMPIRE and also the ability to fit PFNS. The results of this second round awaits assimilation.

The Pu actinides ^{239}Pu and ^{242}Pu were also studied. For ^{239}Pu, a first assimilation was completed and showed promising results, but some parameters required variations beyond 1σ variation. A new EMPIRE evaluation has been completed that includes PFNS parameters, but has not yet been assimilated. For ^{242}Pu a number of integral experiments were available, with improvements for some, while other remained the same or were worse. This could have been due to possible inconsistencies between the integral experiments.

Finally, an assimilation of ^{238}U was started using a new version of EMPIRE with an improved optical potential. This has produced very good prior cross sections for many reactions, including fission, which was able to reproduce the standards cross section above 2 MeV within the standards' uncertainty. The resulting cross sections have not yet been assimilated.

It should always be kept in mind that the reaction modeling in EMPIRE is not perfect. Scaling parameters are in place to account for deficiencies in the calculated cross sections, but not for angular distributions, which can have a significant impact on integral modeling. This may explain some of the discrepancies between the calculated and experimental data using assimilated model parameters: the cross sections may have been adjusted to compensate for model defects (or deficiencies) in the angular distributions. Also, both KALMAN and the assimilation use a linear extrapolation of the model predictions based on the sensitivities. To mitigate non-linear effects, the changes in the model parameters should be limited, as was done for most of the materials tested. Some cross sections may also depend (strongly) on the cutoff of discrete levels, which affects level densities. This

effect has not been taken into account in the present work.

In addition to the above method where cross sections, sensitivities and covariances are prepared at BNL and assimilated at INL, a method was also developed at BNL where the results of the EMPIRE calculations are used to perform MCNP Monte-Carlo simulations of integral experiments directly from the calculated EMPIRE cross sections without first passing through energy grouping, hence a 'direct' assimilation. This method was tested for ^{239}Pu with the JEZEBEL experiment, with promising results. The value for k_{eff} was brought to within experimental uncertainties with one iteration of assimilation. It is striking what small differences in the cross sections are needed to reproduce the result of an integral experiment, in this case for $k_{\text{eff}} = 1.0$. It is unlikely that differential data alone will be able to reproduce this accuracy in the near future. But used together with assimilation, the differential and integral data can hopefully be used to produce evaluations that reproduce simultaneously the differential and integral data as well as satisfy physics constraints by nuclear reaction theory.

Bibliography

[1] G. Aliberti et al. Nuclear Data Sensitivity, Uncertainty and Target Accuracy Assessment for Future Nuclear Systems. *Annals of Nuclear Energy*, 33:700–733, 2006.

[2] M. Salvatores, G. Aliberti, and G. Palmiotti. Nuclear Data Needs for Advanced Reactor Systems. A NEA Nuclear Science Committee Initiative. In *ND 2007: International Conference on Nuclear Data for Science and Technology*, Nice, France, April 22-27 2007.

[3] M. B. Chadwick, M. Herman, P. Obložinský, M. E. Dunn, Y. Danon, A. C. Kahler, D. L. Smith, B. Pritychenko, G. Arbanas, R. Arcilla, R. Brewer, D. A. Brown, R. Capote, A. D. Carlson, Y. S. Cho, H. Derrien, K. Guber, G. M. Hale, S. Hoblit, S. Holloway, T. D. Johnson, T. Kawano, B. C. Kiedrowski, H. Kim, S. Kunieda, N. M. Larson, L. Leal, J. P. Lestone, R. C. Little, E. A. McCutchan, R. E. MacFarlane, M. MacInnes, C. M. Mattoon, R. D. McKnight, S. F. Mughabghab, G. P. A. Nobre, G. Palmiotti, A. Palumbo, M. T. Pigni, V. G. Pronyaev, R. O. Sayer, A. A. Sonzogni, N. C. Summers, P. Talou, I. J. Thompson, A. Trkov, R. L. Vogt, S. C. van der Marck, A. Wallner, M. C. White, D. Wiarda, and P. G. Young. ENDF/B-VII.1 Nuclear Data for Science and Technology: Cross Sections, Covariances, Fission Product Yields and Decay Data. *Nuclear Data Sheets*, 112(12):2887–2996, 12 2011.

[4] G. Palmiotti et al. Requirements for Advanced Simulation of Nuclear Reactor and Chemical Separation Plants. Technical Report ANL-AFCI-168, Argonne National Lab, 2006.

[5] M. Salvatores et al. Uncertainty and Target Accuracy Assessment for Innovative Systems Using Recent Covariance Data Evaluations. Technical Report NEA/WPEC-26, NEA, 2008.

[6] G. Palmiotti, H. Hiruta, and M. Salvatores. Consistent Data Assimilation of Actinide Isotopes: ^{23}Na and ^{56}Fe. Technical Report INL/EXT-10-20094, Idaho National Lab, 2010.

[7] G. Palmiotti, H. Hiruta, and M. Salvatores. Consistent Data Assimilation of Actinide Isotopes: ^{235}U and ^{239}Pu. Technical Report INL/EXT-11-23501, Idaho National Lab, 2011.

[8] G. Palmiotti, H. Hiruta, and M. Salvatores. Consistent Data Assimilation of Isotopes: ^{242}Pu and ^{105}Pd. Technical Report INL/EXT-12-27127, Idaho National Lab, 2011.

[9] A. Gandini and M. Petilli. Amara: A code using the lagrange multipliers methods of nuclear data adjustment. Technical Report RT/FI(73)39, Comitato Nazionale per l'Energia Nucleare, Italy, 1973.

[10] A. Gandini. *Uncertainty Analysis and Experimental Data Transposition Methods in Uncertainty Analysis.* CRC Press, New York, 1988.

[11] M. Salvatores, G. Aliberti, and G. Palmiotti. Nuclear Data Validation and Fast Reactor Design Performances Uncertainty Reduction. In *ANS Meeting 96*, page 519, Boston, Massachusetts, June 22-26 2007.

[12] A. D. D'Angelo, A. Oliva, G. Palmiotti, M. Salvatores, and S. Zero. Consistent Utilization of Shielding Benchmark Experiments. *Nuclear Science Engineering*, 65:477, 1978.

[13] M. Salvatores, G. Palmiotti, et al. Resonance Parameter Data Uncertainty Effects on Integral Characteristics of Fast Reactors. In *IAEA Specialist's Meeting on Resonance Parameters*, Vienna, Austria, Sept 28 - Oct 2 1981.

[14] G. Rimpault. The ERANOS Code and Data System for Fast Reactor Neutronic Analyses. In *Proc. Physor 2002 Conference*, Seoul, Korea, Oct 2002.

[15] M. Herman, R. Capote, B.V. Carlson, P. Oblozinský, M. Sin, A. Trkov, H. Wienke, and V. Zerkin. Empire: Nuclear reaction model code system for data evaluation. *Nuclear Data Sheets*, 108(12):2655 – 2715, 2007. Special Issue on Evaluations of Neutron Cross Sections.

[16] M.B. Chadwick, P. Obložinský, M. Herman, N.M. Greene, R.D. McKnight, D.L. Smith, P.G. Young, R.E. MacFarlane, G.M. Hale, S.C. Frankle, A.C. Kahler, T. Kawano, R.C. Little, D.G. Madland, P. Moller, R.D. Mosteller, P.R. Page, P. Talou, H. Trellue, M.C. White, W.B. Wilson, R. Arcilla, C.L. Dunford, S.F. Mughabghab, B. Pritychenko, D. Rochman, A.A. Sonzogni, C.R. Lubitz, T.H. Trumbull, J.P. Weinman, D.A. Brown, D.E. Cullen, D.P. Heinrichs, D.P. McNabb, H. Derrien, M.E. Dunn, N.M. Larson, L.C. Leal, A.D. Carlson, R.C. Block, J.B. Briggs, E.T. Cheng, H.C. Huria, M.L. Zerkle, K.S. Kozier, A. Courcelle, V. Pronyaev, and S.C. van der Marck. ENDF/B-VII.0: Next generation evaluated nuclear data library for nuclear science and technology. *Nuclear Data Sheets*, 107(12):2931–3118, 2006.

[17] S. F. Mughabghab. *Atlas of Neutron Resonances: Thermal Cross Sections and Resonance Parameters.* Elsevier, Amsterdam, 2006.

[18] A. J. Koning and J. P. Delaroche. Local and global nucleon optical models from 1 keV to 200 MeV. *Nucl.Phys.*, A713:231, 2003.

[19] J. P. Delaroche, S. M. El-Kadi, P. P. Guss, C. E. Floyd, and R. L. Walter. *Nucl. Phys.*, A390:541, 1982.

[20] C. A. Engelbrecht and Hans A. Weidenmüller. Hauser-feshbach theory and ericson fluctuations in the presence of direct reactions. *Phys. Rev. C*, 8:859–862, Sep 1973.

[21] Zhang Zhengjun *et al.* Unpublished.

[22] R. Capote, E. Chiba, J. M. Soukhovitskii, E. Quesada, and E. Bauge. A Global Dispersive Coupled-Chanel Optical Model Potential for Actinides. *J. Nuc. Sci. Tech.*, 45:333–340, 2008.

[23] D. G. Madland and J. R. Nix. New calculation of prompt fission neutron-spectra and average prompt neutron multiplicities. *Nucl. Sci. and Eng.*, 81:213–271, 1982.

[24] N. V. Kornilov, A. B. Kagalenko, and F.-J. Hambsch. Computing the spectra of prompt fission neutrons on the basis of a new systematics of experimental data. *Physics of Atomic Nuclei*, 62:173, 1999.

[25] A.D. Carlson, V.G. Pronyaev, D.L. Smith, N.M. Larson, Chen Zhenpeng, G.M. Hale, F.-J. Hambsch, E.V. Gai, Soo-Youl Oh, S.A. Badikov, T. Kawano, H.M. Hofmann, H. Vonach, and S. Tagesen. ^{238}U(n,f) section of the endf/b-vii standards sub-library. *International Evaluation of Neutron Cross Section Standards*, 110:3215–3324, 2009.

[26] F. S. Dietrich, I. J. Thompson, and T. Kawano. Target-state dependence of cross sections for reactions on statically deformed nuclei. *Phys. Rev. C*, 85:044611, Apr 2012.

[27] R. E. Slovacek, D. S. Cramer, E. B. Bean, J. R. Valentine, R. W. Hockenbury, and R. C. Block. ^{238}U Measurements Below 100 keV. *Nuclear Science and Engineering*, 62:455–462, 1977.

[28] S. Bjørnholm and J. E. Lynn. The double-humped fission barrier. *Rev. Mod. Phys.*, 52:725, 1980.

[29] R. Capote, E. Soukhovitskii, J. M. Quesada, and S. Chiba. In *Proc. of the Inter. Conf. on Nuclear Data for Science and Technology*, page 07765, Nice, France, 2007. ND2007.

[30] A. A. Boytsov, A. F. Semenov, and B. I. Starostov. Relative measurements of the spectra of prompt fission neutrons for thermal neutron fission of the nuclei ^{233}U, ^{235}U, ^{239}Pu in the energy range 0.01 - 5 MeV. In *Conf.: 6.All-Union Conf.on Neutron Physics*, volume 2, page 294, Seoul, Korea, Oct 2-6 1983.

[31] B. I. Starostov, V. N. Nefedov, and A. A. Boykov. Prompt neutrons spectra from the thermal neutron fission of ^{233}U, ^{235}U, ^{239}Pu and spontaneous fission of ^{252}Cf in the secondary neutron energy range 0.01 - 12 MeV. *Vop. At.Nauki i Tekhn.,Ser.Yadernye Konstanty*, 3:16, 1985.

[32] R. D. Mosteller. Validation suite for mcnp. In *12th Biennial RPSD Topical Meeting*, Sante Fe, NM, April 2002.

[33] J. Tommasi, E. Dupont, and P. Marimbeau. Analysis of Sample Irradiation Experiments in Phénix for JEFF-3.0 Nuclear Data Validation. *Nuclear Science and Engineering*, 154(2):119–133, Oct 2006.

[34] J. Tommasi and Noguére. Analysis of the PROFIL and PROFIL-2 Sample Irradiation Experiments in Phènix for JEFF-3.1 Nuclear Data Validation. *Nuclear Science and Engineering*, 160:232–241, 2008.

[35] G. Palmiotti. Private Communication, 2012.